NTNU

Norwegian University of
Science and Technology

Establishing Characterization and Methodology for Analyzing Performance of Commercial Particulate Silver Catalyst for Formalin Production

Vegard Naustdal

Chemical Engineering and Biotechnology
Submission date: June 2016
Supervisor: Hilde Johnsen Venvik, IKP
Co-supervisor: Rune Lødeng, SINTEF
Jia Yang, SINTEF
Kristin Bingen, DYNEA AS

Norwegian University of Science and Technology
Department of Chemical Engineering

Vegard Andreas Naustdal

Establishing characterization and methodology for analyzing performance of commercial particulate silver catalyst for formalin production

Master's thesis
for the degree of Master of Technology

Trondheim, June 2016

Norwegian University of Science and Technology
Faculty of Natural Science and Technology
Department of Chemical Engineering

NTNU
Det skapende universitet

NTNU

Norwegian University of Science and Technology

Master's thesis
for the degree of Master of Technology

Faculty of Natural Science and Technology
Department of Chemical Engineering

ISBN N/A (printed version)
ISBN N/A (electronic version)
ISSN 1503-8181

Master's theses at NTNU, 2016:N/A

Printed by NTNU-trykk

Preface

This master thesis is a continuation of the specialization course TKP 4510 in Catalysis and Petro chemistry. Both this thesis and the specialization course was written for the Department of Chemical engineering at the Norwegian University of Science and Technology.

The project is affiliated with iCSI, a Center for research based innovation (SFI) awarded by the Research Council of Norway to NTNU, with SINTEF and the University of Oslo (UiO) as research partners, and YARA, K.A. Rasmussen, Dynea, INEOS and Haldor Topsøe AS as industrial partners. During this work professor Hilde J. Venvik was the main supervisor, and senior scientist Rune Lødeng and research scientist Jia Yang from Sintef were co-supervisors.

I would like to thank my supervisor professor Hilde J. Venvik and co-advisor senior scientist Rune Lødeng and research scientist Jia Yang for academic guidance throughout the project. An extra thank to Jia for all the practical help at the lab. An especially thanks to fellow student Stine Lervold for her high spirits and discussions during the long hours at the lab.

Finally I would thank Marita Helene Gustavsen, for her support and patience during the long hours at the office during the last semester.

Declarence of compliance
I declare that this is an independent
work according to the exam regulations
of the Norwegian University of Science
and Technology (NTNU).

Vegard Andreas Naustdal
June 17, 2016

Abstract

Formaldehyde is the simplest aldehyde and is an active organic compound in many reactions making it a versatile building block for the chemical industry. Formaldehyde can be produced by partial oxidative dehydrogenation of methanol over a silver catalyst. The silver catalyzed process is the preferred technology in terms of operation cost and energy consumption, however the process has some challenges in product yield. This giving the silver processes the highest potential for increasing its yield and thus making the process more profitability.

This thesis have two focus areas. First to establishing a suitable characterization methodology for Ag based catalysts, this to identify factors critical to selectivity and stability of the process. Samples from fresh and plant exposed catalyst are investigated using techniques as scanning electron microscope (SEM), X-ray diffraction (XRD), X-Ray fluorescence (XRF), Thermo gravimetric analysis (TGA), Nitrogen adsorption and oxygen chemisorption.

And second, to establish methodology where one can study the silver catalyst in conditions of industrial interest. This by to converting an already existing DME rig to be suitable to run methanol to formaldehyde (MTF) synthesis and try to achieve conversions and selectivity close to what is achieved in the industry.

SEM reveals a massive change in the morphology in the plant exposed catalyst compared to the fresh catalyst. Pinholes in the plant exposed catalyst is observed. From the literature it is proposed that pinholes is due to formation of water in the bulk, indicating that there is bulk diffusion of both hydrogen and oxygen under industrial plant conditions. There are also seen structures similar to carbon structures.

The XRD analysis shows a growth in crystallite size for the plant exposed

catalyst, which is expected from metal exposed to high temperatures. The quantitative calculations for XRF analysis gave 100 % silver for both the fresh and the plant exposed catalyst.

Temperature programmed analysis in TGA, did not show any apparent weight change. Oxygen is a low molecular weight specie compared to silver, as the oxide layer is at the surface raises the question if the weight change is detectable. To support this silver oxide was reduced in a TGA and no weight change was observed after the analysis.

The nitrogen adsorption did not yield any results for the surface area. This is believed to be due to low surface area of the silver catalyst and therefore not possible to measure it with nitrogen adsorption. However, by using a gas with lower vapor pressure like krypton it should be able to yield results for measuring surface area. The oxygen chemisorption did not give any reliable results.

Creating a rig suitable for MTF synthesis is not a trivial, an ideal setup is not necessary a practically one so compromises were made. Several aspect as calibration of MFC, LFC and CG, stabilized vaporization, avoiding condensation in pipelines, accurate temperature and control, and suppressing gas phase reactions have been taken into consideration.

The significance of temperature and flow is seen in both selectivity and conversion. The methanol conversion was highly dependent on oxygen concentration.

The reactor oven had a large temperature gradient and a large heated area, the reactor had a large heated void volume. This promotes gas phase reactions. By reducing the void space in the reactor with SiC the conversion and selectivities is approaching industrially performance. The conversion reached was 90 % with 84 % formaldehyde selectivity 7.5 % selectivity to CO and CO and 1 % selectivity towards CH_4. This was achieved using a feed composition of 8 % methanol 11 % water 3 % oxygen and 78 % nitrogen with 250 NmL/ min and 600 °C oven set point temperature. Both reactor design and oven design should be reconsidered combined with reducing the pipelines in the rig.

From the experiment testing for external mass transfer it is hard to determine if there are any external mass transfer limitations. The temperature effect on reaction rate is exponential resulting in deviation from isotherm conditions have effect on kinetic data. The decrease in reaction rate from 500 to 863 NmL/ min might be due to the temperature decrease. The increase in reaction from 250 NmL/ min to 500 NmL/ min might indicate that there are mass transfer limitations in that area, or can be a concentration effect due to lower conversion at 500 NmL/ min.

Sammendrag

Formaldehyd er det enkleste av aldehydene og er en aktiv organisk forbindlese i mange reaksjoner. Detter gjør den til en allsidig byggestein i den kjemiske industrien. Formaldehyd kanfremstilles ved partiell oksidativ dehydrogenering av metanol over en sølvkatalysator. Den sølvkatalyserte prosessen er den foretrukne teknologien for produksjon av formaldehyd, når man tar hensyn til energibruk og driftkostnader. Prosessen har fortsatt noen utfordringer når man tenker på utbytte. Dette gjør at der finnes et potensial for å øke utbyttet og dermed gjøre prosessen mer lønnsom.

Denne masteroppgaven har to hovedfous. Først å etablere en passende metode for karakterisering av sølvkatalysatoren, dette for å identifisere faktorer som er kritiske for selektivitet og sabilitet for prosessen. Dette ble gjort ved å analysere ubrukt katalysator og sammenligne prøver som har vært brukt og utsatt for industrielle betingelser. De forskjellige analyse metodene som ble brukt er; "Scanning" elektron-mikroskopi (SEM), røntgen diffraksjon (XRD), røntgen fluorisens (XRF), nitrogenadsorpsjon, termo gravimetriske metoder (TGA) og oksygen kjemisorpsjon.

Og andre, for å etablere en metodikk hvor man kan studere sølvkatalysator i forhold til industriell interesse. Dette ved å omdanne en allerede eksisterende DME rigg ftil å være egnet til å kjøre metanol til formaldehyd (MTF) syntese og prøve å oppnå omdanning og selektivitet nær det som er oppnådd i industrien.

SEM viser en forandring i morfologien i katalysatoren som er utsatt for industrielle betingelser sammenlignet med ubrukt katalysator. Overskridelse av Tammann temperatur gir sintering og vil skape overflater med lavest energi konfigurasjon. Det er observert "Nålehull" i den brukte katalysatoren. "Nålehullene"er på grunn av dannelse av vann i massen, noe som indikerer at

det er bulk diffusjon av både hydrogen og oksygen under industrielle drift. Det og sett strukturer som ligner på karbonstrukturer.

XRD-analyse viser en vekst i krystallittstørrelse for den brukte, noe som er forventet fra metallet utsettes for høye temperaturer. De kvantitative beregninger for XRF-analyse ga 100 % sølv for både den brukte og ubrukte katalysatoren.

TGA analysene viste ingen vektendring for katalysatoren. Oksygen har lav molekylvekt sammenlignet med sølv. Dette gjør at vektendring er vanskelig å oppdage når ett oksidlag vil være på overflaten. Nitrogenadsorpsjon gav ingen resultat på overflateareal. Siden sølv har relativt lav overflate er ikke nitrogenadsorpsjon egnet til å måle denne. Oksygen kjemisorpsjon gav heller ingen resultat også på grunn av lavt overflateareal.

Å etablere en rig som passer for syntese av formaledehyd er ikke trivielt. Her må det inngå kompromiss mellom hva som er praktisk og hva som er ideelt. Flere aspekt som kalibrering av masse og væske kontrollere, fordamping av væske, å ungå kondensasjon, nøyaktige målinger av temperatur og å undertrykke gassfasereaksjoner har blitt tatt hensyn til.

Betydning av temperatur og strøming er sett i både selektivitet og omsetting. Metanolomsettningen var også avhengig av oksygenkonsentrasjonen.

Reaktorovnen hadde en stor temperaturgradient og et stort oppvarmet område og reaktoren hadde et stort oppvarmet dødvolum. Dette vil fremme gassfasereaksjoner, ved å redusere dødvolumet i reaktoren med SiC ble omsentningen og selektivitetene nært industrielle ytelser. Den nådde omsettningen var 90 % med 84 % formaldehyd selektivitet 7.5 % selektivitet til CO og CO og 1 % selektivitet mot CH_4. Dette ble oppnådd ved hjelp av en fødesammensetning av 8 % metanol 11 % vann 3 % oksygen og 78 % nitrogen med 250 NmL/ min og en temperature i reaktorovnen på 600 °C.

Både reaktordesign og ovndesign bør revurderes sammen med å redusere lengden av rørledninger i riggen.

Det er vanskelig å avgjøre om det er eksterne masseoverføringsbegrensninger fra forsøket. Temperaturens effekt på reaksjonshastigheten er eksponentiell noe som resulterer i at avvik fra isoterme betingelser vil ha stor virkning på kinetiske data. Reduksjonen i reaksjonshastigheten 500-863 NmL/ min kan være på grunn av temperaturfallet, det ble prøvd å estimere innvirkningen av temperatur men den beregnede observerte hastighet ble forsatt for lav. Økningen i reaksjonen fra 250 NmL/ min 500 NmL/ min kan indikere at det er masseoverføringsbegrensninger i dette området, eller kan være en konsentrasjon effekt på grunn av lavere omdannelse ved 500 NmL/ min.

Contents

Abbreviations

BET	Isotherm of Brunauer, Emmet and Teller
BSE	Back scattered electrons
CEM	Controlled evaporation and mixing
DME	Dimethyl ether
EDX	Energy dispersive X-Ray
EDXRF	Energy dispersive X-Ray Fluorescence
FWHM	Full width at half maximum
GC	Gas chromatography
LFC	Liquid flow controller
MeOH	Methanol
MFC	Mass flow controller
MTF	Methanol to formaldehyde
PFD	Process flow diagram
SE	Secondary electrons
SEM	Scanning electron microscope
TCD	Thermal conductive detector
TGA	Thermal gravimetric analysis
TOS	Time on stream
TPO	Temperature programmed oxidation
TPR	Temperature programmed reduction
WDXRF	Wave dispersive X-ray fluorescence
XPS	X-ray photoelectron spectroscopy
XRD	X-ray diffraction
XRF	X-ray fluorescence

List of Figures

List of Tables

Chapter 1

Introduction

Methanal, also known by the trivial name formaldehyde, is the simplest aldehyde and have the chemical formula CH_2O. Formaldehyde is a very reactive organic compound making it active in many reactions such as polymerization, addition reactions and condensation reactions [1]. Formaldehydes reactivity makes it quite a versatile building block for the chemical industry and is in use from medical industry to textile and glue.

Butlerov was the first to synthesize formaldehyde in 1859 by hydrolysis of methylene acetate. Hofferman conclusively identified formaldehyde in 1867 by passing methanol vapor and air over a heated platinum spiral. The main principles of the method are still used in the industrial production of formaldehyde, but with changes in the catalysts [1].

The predominantly industrial processes to produce formaldehyde today are the silver catalyst process and a transition metal based process. The silver catalyst process is either a complete or an incomplete partial oxidation over a silver catalyst while the iron oxide based process uses iron oxide mixture catalyst to oxidate methanol. These processes have different advantages over each other; the iron oxide based process having higher yield however is more expensive, while the silver catalyzed reaction have lower yield but is cheaper.

The silver catalyzed process is the preferred technology in terms of operation cost and energy consumption, however the process has some challenges in product yield. This gives the partial oxidation silver processes the highest potential for increasing its yield and thus making the process more profitable.

1.1 Purpose of the thesis

This thesis have two focus areas. First part aims at establishing a suitable characterization methodology for silver (Ag) based catalysts, this to identify factors critical to selectivity and stability of the process. Samples from fresh and plant exposed catalysts are investigated using techniques as scanning electron microscope (SEM), X-ray diffraction (XRD), X-Ray fluorescence (XRF), Thermo gravimetric analysis (TGA), Nitrogen adsorption and oxygen Chemisorption.

And second, to establish methodology where one can study the silver catalyst in conditions of industrial interest. This by to converting an already existing DME rig to be suitable to run methanol to formaldehyde (MTF) synthesis and try to achieve conversions and selectivity close to what is achieved in the industry.

Downscaling a process from industrial conditions is not without challenges. Temperature control, gas phase reactions and residence time are key points for what is difficult to imitate. Industrially, controlling gas phase reactions is done by increasing the linear gas flow velocity. At lab scale different action must be done.

First objective is to achieve conversion and formaldehyde selectivities close to whats obtainable industrially, then determine what may be manipulated to increase the selectivity towards formaldehyde.

Converting and testing of the MTF rig was done with fellow graduate student Stine Lervold. Data presented from the tests are therefore a collaboration with her.

Chapter 2

Theory

2.1 Oxidative dehydrogenation of methanol over silver

There are several methods used to produce formaldehyde, one method is oxidative dehydrogenation of methanol over a silver catalyst. The process is conducted by passing excess methanol combined with air and steam over a 10-50 mm thin silver catalyst bed. The main reactions that occur during production of formaldehyde from methanol are given in the following equations (2.1) [1].

$$CH_3OH \rightarrow CH_2O + H_2 \qquad \Delta H = +85 kJ/mol \tag{2.1a}$$

$$H_2 + 1/2O_2 \rightarrow H_2O \qquad \Delta H = -243 kJ/mol \tag{2.1b}$$

$$CH_3OH + 1/2O_2 \rightarrow CH_2O + H_2O \qquad \Delta H = -159 kJ/mol \tag{2.1c}$$

There are also formed byproducts in secondary reactions. The secondary reactions given by the following Equations (2.2).

$$CH_3OH + 3/2O_2 \rightarrow CO_2 + 2H_2O \qquad \Delta H = -674 kJ/mol \tag{2.2a}$$

$$CH_2O \rightarrow H_2 + CO \qquad \Delta H = +12.5 kJ/mol \tag{2.2b}$$

$$CH_2O + O_2 \rightarrow CO_2 + H_2O \qquad \Delta H = -519 kJ/mol \tag{2.2c}$$

Formation of methane, formic acid and methylformate is also possible side reactions [1].

The complete reaction mechanism for the conversion of methanol to formaldehyde over a silver catalyst is not proposed yet, however spectroscopic investigation shows the influence of different adsorbed oxygen species

on selectivity and reaction pathways [2, 1]. The exothermic reaction (2.1b) and to some extent reactions, equation (2.2a) and (2.2c) share the oxygen in the process air. The amount of process air will therefore control the reaction temperature and the rate of the endothermic reactions, equations 2.1a and 2.2b [1].

Waterhouse et. al [3, 2] has presented a study on the different oxygen species adsorbed on silver planes. Under industrial conditions atomic silver were present as two different species; bridging Ag-O-Ag O_α) and the strong chemisorbed Ag=O (O_γ). While O_α promoted all oxidation of methanol were O_γ more selective towards the partial oxidation, equation 2.1c. Figure 2.1 illustrates the reaction scheme of the different oxygen species. The selectivity towards formaldehyde was related to the relative amount of the different adsorbed oxygen species.

The O_α chemisorb weakly to (111) and (110) facets through dissociative chemisorption. At high surface coverages O_α may diffuse into the bulk.

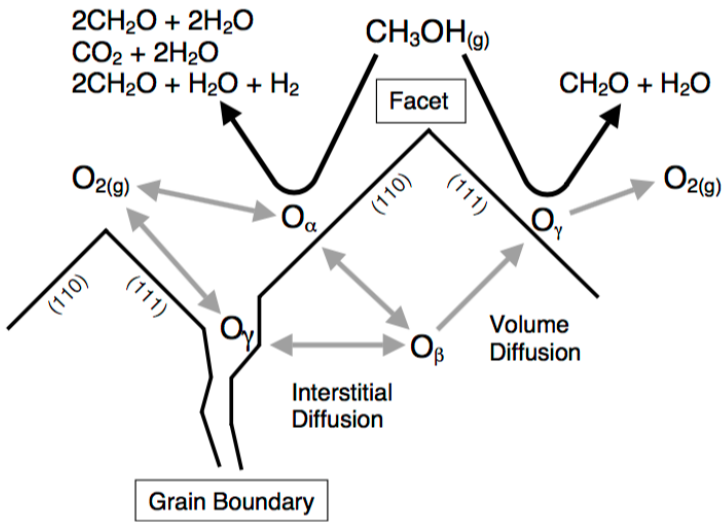

Figure 2.1 – Reaction scheme showing the formation of different oxygen species O_α, O_β and O_γ from gas phase O_2 at 923K, and the initial product distribution on O_α and O_γ [2].

A third oxygen specie was identified as O_β which is atomic oxygen dissolved in the silver sub surface layers. The O_β can segregate to the catalyst surface through grain boundary and interstitial diffusion mechanism and form O_γ. A close packed (111) facet can prevent the segregation of the O_β until the activation barrier for volume diffusion at 900 K is exceeded [2].

At lower temperatures there is a high surface coverage of O_α, while at temperatures exceeding 580 K the surface coverage is lower due to thermal instability [2]. Formaldehyde selectivity is highly dependent on the ratio O_γ/O_α, increasing the temperature will therefore increase the formaldehyde selectivity.

2.2 Mass transfer limitations

In heterogeneous catalysis the reactants have several steps before reaching catalytic surface and then the product have just as many to get back to the bulk fluid. The slowest step of the mechanism dictates therefore the overall reaction rate. If the reaction steps are fast compared to the diffusion steps the diffusion steps will limit the overall reaction rate [4].

External diffusion is the first step for a reactant, this is the mass transfer from the bulk fluid, through the boundary layer, to the external surface of the catalyst pellet. The thickness of the boundary layer is dependent of the velocities of fluid flow through the catalyst bed. At high velocities the boundary layer is smaller than for low velocities. A smaller boundary layer results in a shorter distance for the reactants to diffuse through, thus giving a higher mass transfer across the boundary layer. Figure 2.2 shows an illustration of the boundary layer around a catalyst pellet.

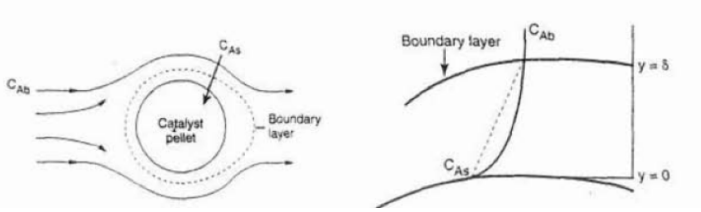

Figure 2.2 – Boundary layer around the surface of a catalyst pellet [4].

If the reaction is limited by the external mass transfer the overall rate is given by equation 2.3 . And the mass transfer coefficient is given by equation 2.4 [4].

$$Rate = k_c(C_{ab} - C_{as}) \tag{2.3}$$

$$k_c = \frac{D_{ab}}{\delta} \tag{2.4}$$

Where k_c is the mass transfer coefficient, C_{Ab} is concentration of A in bulk, C_{As} is concentration of A at the external surface δ is the boundary layer thickness.

From equation 2.4 it can be seen that the mass transfer coefficient is dependent on the thickness of the boundary layer and the diffusion coefficient. The diffusion coefficient for bulk diffusion is then again dependent of the temperature and pressure [4], there might also be concentration and temperature gradients through the boundary layer. This is important to keep in mind when comparing results.

The two most common methods of determining if there are external diffusion limitations are by comparing the conversion with changes in flow when the flow to catalyst is constant, and comparing the reaction rate to increase in gas velocity. The two methods have different advantages over each other. To determine the reaction rate is not always trivial but can be simplified using the assumption that the system is at differential conditions. To compare conversions as the flow increases keeping flow to catalyst constant is easier to measure however, this requires a new catalyst bed for each flow.

Differential reactor

A fixed bed reactor can act as a differential reactor. However, this is under the assumption that differential conditions are present. For a reactor to be differential it is crucial that the conversion is small and the changes of reactant concentration and temperature through the bed are small. Thus, the reaction rate corresponds to the average reactant concentration through the bed, this simplifies the rate expression. The differential reactor rate expression is given by equation 2.5 [4].

$$Rate = \frac{F_{Tot,in}y_{MeOH,in} - F_{Tot,out}y_{MeOH,out}}{m_{cat}} \tag{2.5}$$

Activation energy

Arrhenius proposed that a reaction have an activation energy for it to happen. This is based on the collision model which is built around that molecules must collide for a chemical reaction to occur. Taking the natural logarithm of the Arrhenius equation, equation 2.6, yields equation 2.7. By further derive it gives equation 2.8. Equation 2.8 can be used to either calculate the activation energy or give the fraction of the rate constant at different temperatures. The fraction can be used to see temperature effects on the reaction rate [5].

$$k = Ae^{-\frac{E_a}{RT}} \tag{2.6}$$

$$ln(k) = -\frac{E_a}{R}(\frac{1}{T}) + ln(A) \tag{2.7}$$

$$ln(\frac{k_2}{k_1}) = \frac{E_a}{R}(\frac{1}{T_1} - \frac{1}{T_2}) \tag{2.8}$$

Where, k is the rate constant, A is the pre-exponential factor, E_a is the activation energy, R is the universal gas constant, and T is the absolute temperature.

Production of particular silver catalyst

The particulate silver catalyst is produced in an electrolysis cell. The size and density of the silver crystals are controlled by adjusting the current intensity. Deposited silver crystals on the cathode is scraped of washed and dried before the crystals are sorted in different fractions using a sieve. Figure 2.3 shows a electrolysis cell used for silver catalyst production. Electrolytic silver surfaces are polycrystalline and contain a high proportion of (111) facets.

Figure 2.3 – Electrolysis cell for silver catalyst production, provided by K.A. Rasmussen.

Chapter 3

Characterization

A catalyst performance is often determined by the structure and composition on the surface of the catalyst. Characterization of a catalyst is important to gain knowledge and get a better understanding of the catalyst. There are a variety of characterization techniques available. The following sections describe relevant techniques for characterization of a silver catalyst.

3.1 X-ray Diffraction (XRD)

XRD is used to identify the crystalline phases within a catalyst, and can also give indications of the particle size [6]. XRD works by irradiating the sample with monochromatic X-rays at different angles. The X-rays get scattered by atoms in the sample, which are in a periodic lattice. The diffraction angles are different for each plane within the crystal giving each compound a unique diffraction pattern. The Braggs relations, equation 3.1, describes the lattice spacing of the crystal planes.

$$n\lambda = 2dsin\theta \tag{3.1}$$

Where n is an integer and the order of reflection, λ is the wavelength of the X-rays, d is the distance between the two lattice planes, θ is the angle between the incoming X-rays and normal to the reflection planes.

Braggs equation need to be fulfilled for the scattered X-rays to create constructive interference and create a diffractogram. If the beam is out of phase destructive interference would appear and no distinct diffraction

peak would be created [7]. For powder samples all possible orientation is represented giving a diffraction cone from the illuminated sample, illustrated in figure 3.1.

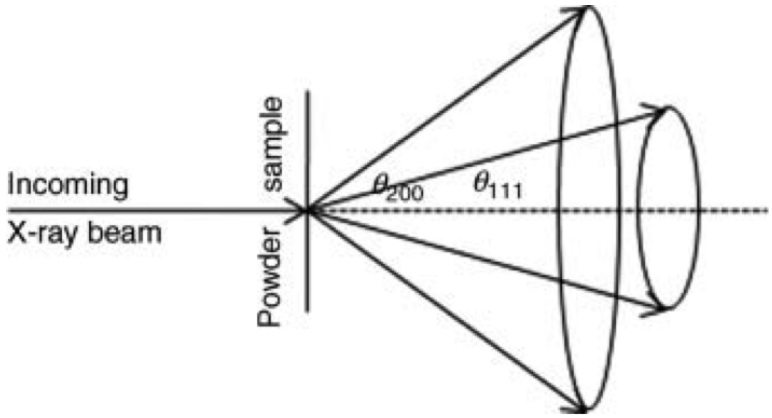

Figure 3.1 – Illustration of the created diffraction cone from a powder sample when irradiated by X-ray beam [7].

The diffraction pattern from a powder sample is dependent of the direction the particles are oriented. If the particles are oriented predominantly along the same direction it may create a diffraction pattern that is not representative. It is therefore essential that the sample is created as random as possible to prevent an anisotropic effect.

Miller indices, (hkl), can be used to explain peaks of different d-space. The miller indices represent the reciprocals of the intercepts to the lattice planes in respect to the unit cell [7]. Scherrer's equation, equation 3.2, can be used to calculate a crude approximation of the crystal size [6, 7]

$$L = \frac{K\lambda}{\beta cos\theta} \tag{3.2}$$

Where L is the dimension of the particle, K is a constant, λ is the X-ray wavelength, β is the peak integral width, θ is the angle between the beam and the normal reflecting plane.

Fitting is a manipulation of a structual model with respect to the observed data. R_{wp} is a weighted difference factor that is used for judge the quality of the fitting. R_{wp} is given by equation 3.3 and should be under 5 %.

$$R_{wp} = \sqrt{\frac{\sum_i |Y_i(obs) - Y_i(calc)^2|^2}{\sum_i W_i Y_i^2(obs)}} \tag{3.3}$$

3.2 Scanning electron microscopy (SEM)

Electron microscopy is a technique to characterize shape and size of a sample. Electron microscopy utilizes the characteristic short wavelength of electrons that is dependent of the acceleration voltage of the electron beam. Higher acceleration voltages shorten the wavelength and increase the penetration of the electrons. When the electrons hit a sample there is a variety of detectable signals [8]. The signals give information about the samples topography, crystallography and chemical composition. Figure 3.2 illustrates the interaction from the primary electron beam and the sample and shows the different detectable signals.

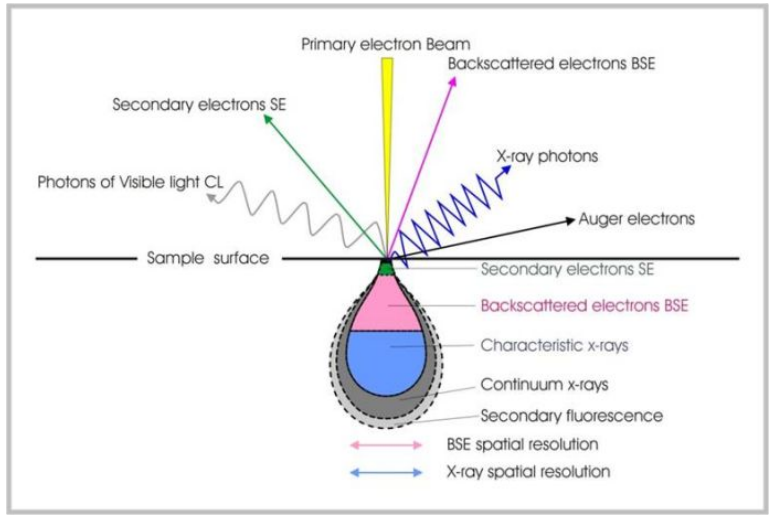

Figure 3.2 – Illustration of interactions between the primary electron beam and the sample in a SEM, the detectable signals with illustration of the depth origin for the various signals [9].

Scanning electron microscopy (SEM) moves a narrow electron beam over the surface and detecting secondary electrons (SE) and back scattered electrons (BSE). Contrast is created depending on the direction of the parts. If the surface faces the detection it would appear brighter than the one not facing the detector [10]. SE origins from the upper part of the surface, as

the electron beam is scanning the sample surface the emitted secondary electrons will vary as a function of the surfaces topography [8], thus giving good depth of field. The BSE comes from deeper within the sample. As heavier elements better scatter electrons than lighter ones [6] the BSE can be used to show contrast between different elements. The electron beam can also excite orbital electrons of the sample, this can be taken advantage of and be used to analyze the composition of the sample. The released energy is characteristic for each element, thus making it possible to determine the chemical composition of the focused part. The detection of the characteristic X-rays is often done by analyzing the energy of the photons, energy dispersive X-ray analysis (EDX). This is described in the X-ray Fluorescence (XRF) chapter below.

3.3 X-ray Fluorescence (XRF)

When a sample get irradiated with high energy X-rays it can either scatter or absorb the X-rays. Contrary to XRD, X-ray fluorescence (XRF) utilize that the X-ray get absorbed and that the atom will release a characteristic energy, in form as a photon with wavelength in the X-ray area. This is a result of interactions with electron beam or high energy X-rays and orbital electrons residing in the K, L, M shell of the sample. If the irradiation has enough energy it can excite electrons from lower energy shale to a higher energy one, this causes the atom to be ionized. As the atom have higher energy than the non excited state, an electron from a higher energy level will jump down, to maintain the energy balance the atom will release energy either in form of auger electrons or as photons [8]. Figure 3.3 illustrate the characteristic X-rays, $K\alpha$, $K\beta$, $L\alpha$ and $L\beta$, an element emits when returning to the non-excited state.

EDX and wave dispersive X-ray fluorescence (WDXRF) are two different XRF systems with different advantages over each other. While EDXRF is a smaller and simpler design often coupled with other systems, i.e. SEM, the WDXRF is a more complex stand-alone system. WDXRF uses crystals to disperse the X-rays from the sample. This utilizes Bragg diffraction, equation 3.1, and provides higher spectral resolution in the low energy region or at longer wavelengths [12]. It also has a wider dynamic range and lower background than EDX. Figure 3.4 is a schematic drawing of a single target WDXRF.

Which element that can be detected is dependent on the crystal used to diffract the incoming X-rays.

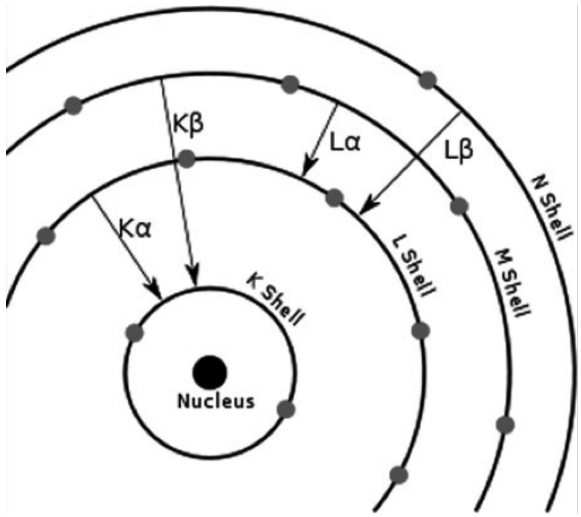

Figure 3.3 – Schematic view of a 2 dimensional orbital transitions due to X-ray fluorescence [11].

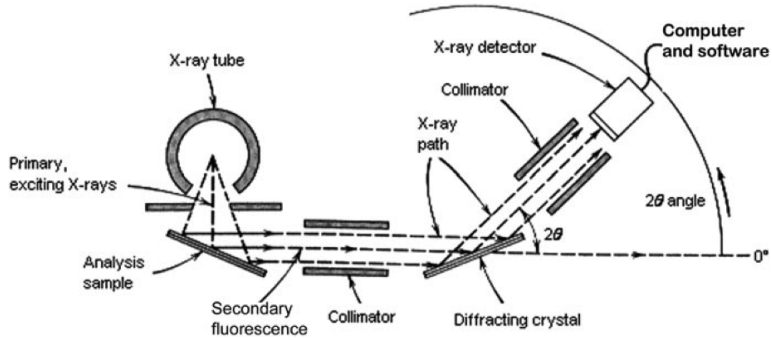

Figure 3.4 – Schematic drawing of a single target WDXRF system [11].

3.4 Chemisorption

Adsorption is divided into physical adsorption, physisorption, and chemical adsorption, chemisorption. Physisorption is weak van der Waal forces between the adsorbed gas and surface, which is taken advantage of when determining surface areas and pore size distribution. Chemisorption is strong valence forces between the adsorbed gas and surface, which only takes place on specific sites on the surface. As for heterogeneous catalysis that requires at least one of the reactant adsorbed to the surface the active site is important and related to the activity of the catalyst.

The dispersion is defined as number of surface atoms of the metal catalyst over the total number of catalyst atoms. Using a gas that only chemisorb on the catalyst surface the dispersion can be determined by measure of the amount gas used [10].

Most used probe gas is hydrogen H_2, carbon monoxide CO and oxygen O_2. Use of the different probes is dependent on the active sites property. As the dispersion is calculated from the amount of probe gas used it is important to apply the correct stoichiometric factor, that is how many active sites each molecule of probe gas occupies.

3.5 Surface area

The surface area of a material can be measured by letting an inert gas like nitrogen, argon or krypton physisorb on the surface. The number of molecules needed to form a monolayer is then measured and the surface area can be calculated knowing the space one molecule occupies. Brunauer, Emmet and Teller (BET) suggested an isotherm for adsorption of physisorbed species, also known as the BET isotherm [6]. The BET isotherm is given in equation 3.4.

$$\frac{p}{V_a(p_0 - p)} = \frac{1}{\chi V_0} + \frac{(\chi - 1)}{\chi V_0}\frac{p}{p_0} \tag{3.4}$$

Where p is equilibrium pressure, V_a is the volume gas adsorbed, V_0 is volume gas adsorbed in the first monolayer, p_0 is saturation pressure, χ is the ratio of desorption rate constants, $\frac{k_1}{k_2}$, for the second and first layer. Equation 3.4 gives a linear approach. By plotting $\frac{p}{V_a(p_0-p)}$ as a function of $\frac{p}{p_0}$ the total volume gas adsorbed in the first monolayer can be calculated from the slope $\frac{(\chi-1)}{\chi V_0}$.

The BET isotherm is based on the following assumptions and has therefore some limitations if these are not met [6]:

- Dynamic equilibrium between adsorbate and adsorptive.
- In the first layer, molecules adsorb on equivalent adsorption sites.
- Molecules in the first layer constitute the adsorption sites for molecules in the second layer, and so on for higher layers.
- Adsorbate-adsorbate interactions are ignores.
- The adsorption-desorption conditions are the same fore all layers but the first.
- The adsorption energy for molecules in the 2^{nd} and higher layers equals the condensation energy.
- The multilayer grows to infinite thickness at the saturation pressure.

3.6 Temperature programmed Techniques

Temperature programmed techniques are based on thermal methods where a chemical reaction is monitored with temperature change. The involved chemical reaction can be a reduction, oxidation, desorption or sulfidation dependent on the desirable information. The instrumentation used for detection of the chemical reaction can be thermal gravimetric analysis (TGA), which measure the change in mass with the temperature change in different conditions. TGA is often coupled with a mass spectrometer (MS) for detecting the reaction products [10].

Temperature programmed reduction (TPR) is a technique in which a chemical reaction is measured while increasing temperature. Hydrogen can be used to induce the reductive conditions for reduction of a metal oxide, given in equation 3.5.

$$MO_n + nH_2 \rightarrow M + nH_2O \tag{3.5}$$

The reduction is dictated by thermodynamics and will proceed when the change in Gibbs free energy (ΔG) is negative. Equation 3.5 describe ΔG dependency of temperature and pressure. For noble metals ΔG^0 is negative and therefore thermodynamically possible to achieve complete reduction [10].

$$\Delta G = \Delta G^0 + nRTln\frac{p_{H_2O}}{p_{H_2}} \tag{3.6}$$

Where ΔG is change in Gibbs free energy, ΔG^0 is change in Gibbs free energy at standard conditions, n is the stoichiometric coefficient of the reaction, R is the gas constant, T is temperature, p is the partial pressure.

TPR provides useful information, on qualitative basis, of the temperature needed for complete reduction of the catalyst. Temperature programmed oxidation (TPO) can be used to determine the degree of reduction for a specie. TPO can be presented as spectrum of oxygen consumption of a catalyst as a function of temperature [10]. At a specific temperature the oxidation reaction will take place. The amount of oxygen consumed is related to the degree of reduction for the specie [13].

Chapter 4

Material

The investigated catalyst is a particle silver catalyst produced by K. A. Rasmusen. It is divided into two fractions, where one has a particle size between 0.15-0.30 mm and the other has a particle size between 0.25-0.50 mm.

The fresh and plant exposed catalyst supplied is from Dynea. The provided plant exposed catalyst was divided into top layer, middle layer and bottom layer. By visually inspecting the catalyst, figure 4.1, it was apparent that the top layer of the catalyst had the largest change from the original form. For further characterization the 0.15-0.30 mm fraction and the top layer of the plant exposed catalyst were used.

Figure 4.1 – Image of the plant exposed catalyst. Visual changes is apparent in the top layer of the silver catalyst.

The silver oxide, Ag_2O, used for XRD and TGA analyses was analytical grade silver oxide produced by MERCK.

Chapter 5

Experimental procedure

This chapter describes the used procedures and parameters for the performed characterization techniques on the silver catalyst and the used experimental set-up.

5.1 Health, safety and environment (HSE)

Before doing any experimental work there was preformed a risk assessment for the experiments to be done. The main risk is associated with explosive, combustible and toxic gases, but also using instruments with radiation and high voltage. To reduce the risk, the instruments working under high voltages were not touched. Before using hazardous gas, a leak test was performed on instruments using gas. Detectors sensitive to hydrogen were also installed in laboratories with equipment where hydrogen was used.

The MTF process are associated with several risks, and working with combustible (H_2 and CO) and/or toxic gases (CO and CH_2O) in particular. To reduce risks, leaks tests are performed prior to all experiments. Leak testing are performed with nitrogen (inert gas) at first, then with small amounts of hydrogen. When applying hydrogen to the system handhold detectors cross sensitive to hydrogen is used to detect leaks. Central gas alarms installed in the laboratories and the experimental setup are sensitive to CO and hydrogen. When handling formaldehyde special filter masks were applied for protection, covering all airways. Lab coat and gloves were used at all time handling the setup. Full risk assessment is attached in appendix A.

5.2 SEM

A total of three SEM instruments has been used to characterize the samples. The first SEM analysis was performed in a Hitachi Analytical Variable Pressure SU6000 Field Emission Scanning electron microscope (FE-SEM), using different acceleration voltage and detecting secondary electrons. The second were a Hitachi TM3000 Tabletop microscope using 15 kV acceleration voltage using BSE and EDX detector. The third was a Hitachi S-5500 in-lens cold field emission Scanning transmission electron microscope (S(T)EM) using SE detector. For all analysis the sample have been mounted on a stage using carbon tape.

5.3 XRD

The XRD studies were preformed in a Bruker D8 Advance DaVinci X-ray Diffractiometer using Cu anode with $K\alpha$ radiation at a wavelength, $\lambda = 1.54$Å. The samples were analyzed at 2θ angles from 20°to 80° with slit V6. V6 is dynamic slit opening so the area of irradiation on the sample is 6 mm regardless of 2θ angle. This will create a higher intensity for the high angle peaks than a fixed slit opening due to how much of the sample that is irradiated.

The X-ray source for the DaVinci instrument is contaminated and therefore emit different wavelengths from the Cu-$K\alpha$. The table 5.1 shows emission line and corresponding wavelength for the irradiation for the Bruker D8 Advance DaVinci X-ray Diffractometer.

Table 5.1 – Emission line and corresponding wavelength for the irradiation from the Bruker D8 Advance DaVinci X-ray Diffractometer.

Emission line	Wavelength [Å]
$Cu - K\alpha 1$	1.5406
$Cu - K\alpha 2$	1.5444
$Cu - K\beta 1$	1.3923
$W - L\alpha 1$	1.4764
$W - L\alpha 2$	1.4875

Catalyst samples were prepared by grinding with a mortar to get as small particle powder as possible before it was assembled in a sample holder.

5.4 XRF

The XRF studies were performed in a Supermini 200 analyser using a Palladium X-ray source produced by Rigaku. The instrument uses LiF (200), PET and RX25 analyzing crystals for analyzing and can detect elements from Fluorine to Uranium. Typically 100 to 200 mg sample were grinded with 2.5 to 3 g boric acid. The pellets were created by taking the mixture of sample and boric acid and pressed into a 40 mm pellet. The pellet was mounted in the sample container covered with a 6 µm polypropylene film.

5.5 Temperature programmed analyses

The temperature programmed analysis was performed in a NETZSCH STA449C TGA/DSC/MS. For each temperature program a correction file with an empty crucible were created to correct for changes in weight introduced without sample. Then typically 0.01 - 0.02 g sample were put in an empty crucible which was placed on an analytical balance. Table 5.2 and 5.3 show used temperature program for the analyses of silver catalyst and silver oxide.

Table 5.2 – Temperature program with used gas in the thermogravimetric analysis instrument for the fresh catalyst.

Task	Start Temp. [°C]	End Temp. [°C]	Argon flow [mL min^{-1}]	Synthetic air flow [mL min^{-1}]	Rate [°C min^{-1}]	Time [min]
Dynamic	30	500	25	50	5.0	-
Isothermal	500	500	25	50	-	30
Dynamic	500	100	25	50	5.0	-
Isothermal	100	100	25	50	-	60

Table 5.3 – Temperature program with used gas in the thermogravimetric analysis instrument for reduction of silver oxide.

Task	Start Temp. [°C]	End Temp. [°C]	Argon flow [mL min^{-1}]	Synthetic air flow [mL min^{-1}]	Rate [°C min^{-1}]	Time [min]
Isothermal	30	30	25	75	-	15
Dynamic	30	700	25	75	5.0	-
Isothermal	700	700	25	75	-	15
Dynamic	700	100	25	75	5.0	-
Isothermal	100	100	25	75	-	60

5.6 Nitrogen adsorption - BET surface area

Catalyst samples were analyzed in a TriStar II 3020 Surface Area and Porosity Analyser produced by Micromeritics. Typically 50 to 100 mg sample were used in the experiments. The samples were degassed at 200°Cin a VacPrep 061 degasser overnight before measurements. Nitrogen gas was used as analyzing gas at liquid nitrogen temperature 77 K.

5.7 O_2 Chemisorption

The volumetric oxygen chemisorption were preformed in an ASAP 2020 surface area and porosity analyser produced by Micromeritics. The experiment was performed in glass reactor using quartz wool over and under the sample. Typically between 0.1 and 0.2 g sample were weighed and put in the glass reactor. The reactor containing the sample was weighted before and after to correct for changes in sample weight during the analysis. A manual leak test was performed before proceeding with the analysis. The used conditions are given in table 5.4.

Table 5.4 – Conditions used for volumetric O_2 chemisorption analysis.

Task	Gas	Temperature [°C]	Rate [min]	Time [°C min^{-1}]
Flow	He	170	10.0	60
Evacuation	-	170	10.0	30
Flow	H_2	170	10.0	120
Evauation	-	170	10.0	60
Analysis	O_2	170	10.0	-

5.8 Catalyst testing with Silver particle catalyst

Experimental Set-up

The experimental setup used for catalyst testing in methanol to formaldehyde (MTF) was previous designed for converting methanol to dimethyl ether (DME). The DME synthesis requires high pressure, and the setup is built to handle a high range of pressure. Several key components as the vaporizer, flow controllers and pressure controller are adapted for this purpose. The pipelines are insulated to keep the temperature stable. The setup consists mainly of quarter-inch stainless steel pipes with Swagelok fittings. Gas is fed to the setup via four high pressure pipelines: two pipelines for N_2 in different volumetric range (4-200 NmL/ min and 30-1500 NmL/ min), one pipeline for synthetic air (10-500 NmL/ min) and a last pipeline for CO/H_2 (20-1000 NmL/ min) which was not applied in this analysis. The setup has two liquid containers, one for methanol mixed with water and one container for formalin solution. The liquid containers are pressurized with helium. The pipelines are equipped with reduction valves, manual valves, filters and manometers. Figure 5.1 shows a process flow diagram (PFD) of the experimental setup. The PFD was created by co-supervisor Jia Yang, no modifications were done on the setup during.

The liquid and gas feed is mixed and sent through an evaporator (Bronkhorst CEM - Controlled Evaporation and Mixing) before entering the reactor. It is possible for the gas feed to bypass the evaporator, when liquids are not applied. The mixed feed stream can bypass the reactor that allows for feed gas analyses.

The pipelines are heated by electric heating bands and insulated, while twelve thermocouples monitor the temperature in the pipelines. It is especially important to keep the pipelines at a certain temperature to avoid condensation when working with methanol and water. One of the thermo-

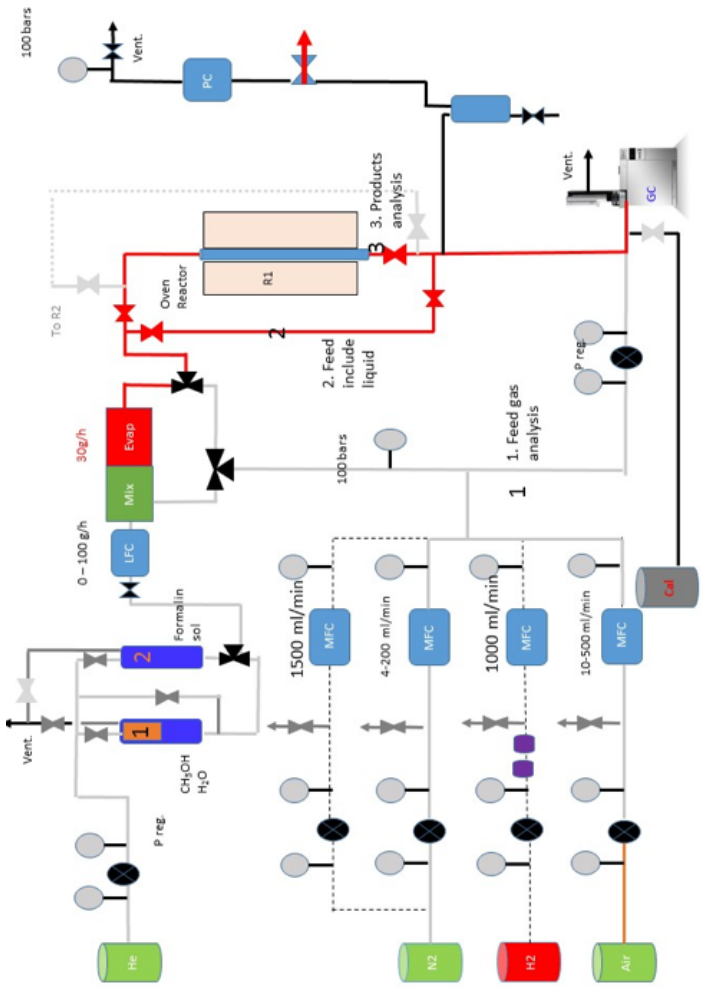

Figure 5.1 – Process flow diagram of the experimental setup for testing silver catalyst in the methanol to formaldehyde process. The flow diagram was designed by co-supervisor Jia Yang.

couple is placed inside the reactor, to monitor the temperature profile in the reactor and catalyst bed. A computer by the setup allows for acquisition of temperature data (EasyView). To control the gas and liquid flow, four Bronkhorst digital mass flow controllers (MFC) and one digital liquid flow controller (LFC) is installed and operated by software (FlowView V1.15) on the computer. All the controllers where calibrated for the gases and liquids connected to the setup, and the calibration curves are shown in appendix B . A Bronkhorst digital back pressure controller is also installed in the setup, but is optimal for a high pressure range. Furthermore, a manometer displays the feed pressure visually.

The experimental setup is connected via piping to an Agilent 7890A gas chromatograph (GC) enabling online analyses of product gas or feed gas. The GC is equipped (see figure 5.2) with two thermal conductivity detectors (TCD-C and TCD-B) and two different columns (molsieve and CP-sil). The molsieve column is applied to separate light/inert gases as H_2, O_2, N_2, CH_4 and CO, which are detected by TCD-C [14]. The CP-sil 5 CB separates components based on boiling point and is customized for separating formaldehyde. The CP-sil is combined with the TCD-B, which detect components as CH_4, CO_2, CH_2O, H_2O and CH_3OH [15]. The GC analyses consisted of two short sequences (6.5 min) and one long sequence (15.5 min), which was repeated throughout the experiment. The long sequence was implemented to remove accumulations in the column.

The GC was calibrated in advance by Jia Yang, but a more profound calibration with a gas mixer (Alytech) was performed during the analyses. The calibration was based on multiple point external standard method, where the analyte response is assumed to be linear over a range of concentrations, calibrations is shown in appendix C. This method is applied when the concentration range is large [16]. A calibration of formaldehyde was performed with a manually injectection by syringe to the GC and through the setup. Unfortunately, this was not optimal and a more reliable calibration is needed. Compounds as formic acid and DME were also injected to identify unknown peaks in the analyses results.

Reactor

A laboratory scale fixed-bed reactor was applied for the catalyst testing in the MTF process. The reactor is made out of quartz and details regarding measurements can be seen in figure 5.3(a). Two flexible metal transitions were attached to the in- and output of the reactor and fitted with Swagelok fittings. A thermowell is centered inside the reactor for a movable thermo-

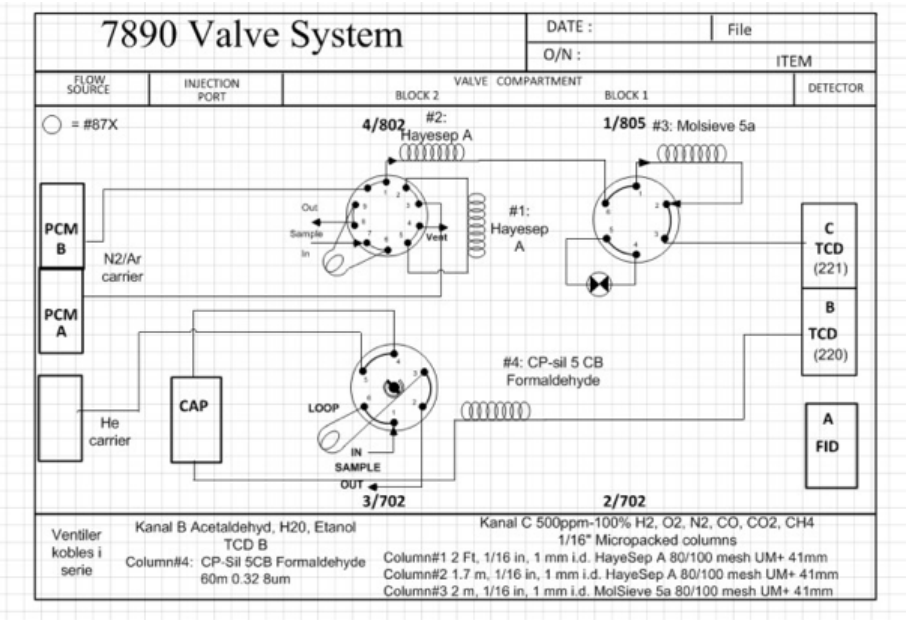

Figure 5.2 – An illustration of the TCD and columns used in Agilent 7890A. In this setup column 3 and 4 was applied. This illustration was provided by Matriks and Jia Yang.

couple. A sinter (porosity 1) was mounted in the reactor to support the catalyst bed. The catalyst bed consists of conventional silver catalyst particles (100 mg, 250-500 µg) diluted with α-alumina (1 g), covered by a top and bottom layer of α-alumina (figure 5.3(b)) to keep the catalyst bed in place.

The reactor is placed inside a high temperature furnace using an Eurotherm temperature controller. Temperature profiles for the catalyst bed was measured by moving the thermocouple along the reactor axis. The catalyst bed temperature was adjusted by modifying the furnace temperature. A pipeline with air was connected inside the furnace to reduce the temperature gradient in the reactor for some analyses.

The product stream exiting the reactor consists of a mixture of unreacted methanol and water vapor, the internal standard nitrogen, formaldehyde, carbon monoxide/dioxide, methane, hydrogen and possible byproducts. The liquids in the product stream are collected in a condenser vessel. The dry product gas is passed through a molecular sieve to remove large particles before the gas is vented.

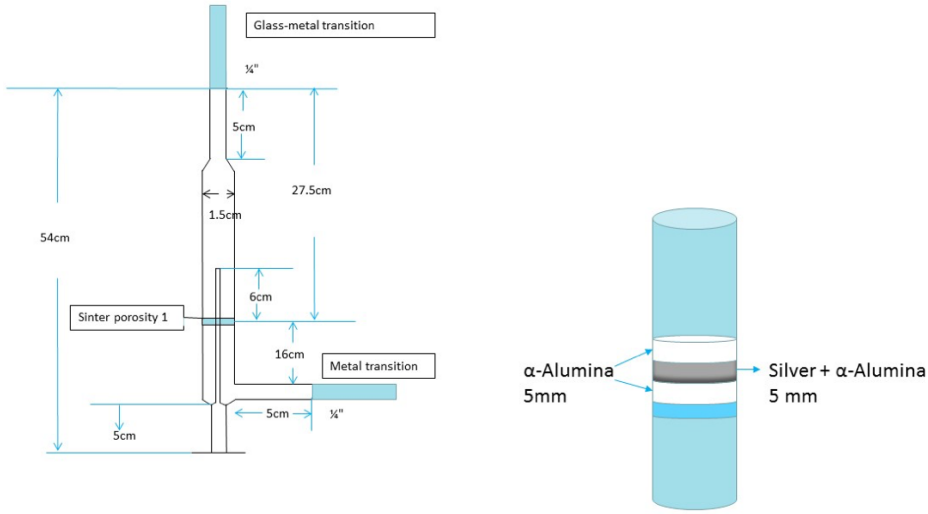

(a) (b)

Figure 5.3 – Illustration of reactor and catalyst bed. Figure 5.3(a) is reactor design of the fixed-bed quartz reactor used in the experimental setup. The design is developed by co-supervisor Jia Yang. Figure 5.3(b) is illustration of the catalyst bed, where to layers of α-alumina is covering the diluted silver catalyst on top of the sinter.

Reaction experiments

Feed composition was based on a chosen molar ratio for H_2O/methanol (1.34) and methanol/O_2 (2.314), these are close to industrial ratios. The feed composition was diluted, with nitrogen, as a compromise between the ability to have high flows and have control at the rig. A solution of methanol (927 g) and water (700 g) was mixed based on this ratio. The reference composition is shown in table 5.5. The feed analyses are found in appendix D.

The complete analyses of the particle catalyst was divided into four main experiments. Several variables and parameters was tested during these analyses, and are presented in table 5.6.

Table 5.5 – Composition of the reference feed based on given molar ratio for H_2O/methanol (1.34) and methanol/O_2 (2.314).

Component	Composition [mol mol^{-1}]
Methanol	0.08
H_2O	0.11
O_2	0.03
N_2	0.78

Table 5.6 – Variables and parameters tested during the four main experiments performed on the particle catalyst.

Analyses	Feed Composition	Temperature [°C]	Total Flow [NmL/ min]	Air Circulation
1. Temperature	Reference	300-650	250 + 375	Off
2. Air circulation	Reference	300-650	250 + 375	On/Off
	50 % less O_2	550	250	Off
	30 % more O_2	550	250	Off
	No O_2	550	250	Off
3. SiC added	Reference	300-650	250 + 375	Off
	4 % MeOH	550	500	Off
4. Empty reactor	Reference	300-650	250 + 375	Off

Data processing

Results from the GC was analyzed in Microsoft Excel. The conversion of methanol was calculated as shown below in equation 5.1. Nitrogen is applied as an internal standard, since nitrogen is inert (neither consumed nor formed).

$$X_{MeOH} = \frac{F_{MeOH,in} - F_{MeOH,out}}{F_{MeOH,in}} \tag{5.1}$$

Where, F_{MeOH} denotes the flow of methanol, and the flow is related to the molar fraction of methanol, y_{MeOH} as shown below in equation 5.2.

$$F_{MeOH,in} = F_{Tot,in} \cdot y_{MeOH,in} \tag{5.2a}$$

$$F_{MeOH,out} = F_{Tot,out} \cdot y_{MeOH,out} \tag{5.2b}$$

Equation 5.3 is given by substituting equation 5.1 and 5.2.

$$X_{MeOH} = \frac{F_{Tot,in} \cdot y_{MeOH,in} - F_{Tot,out} \cdot y_{MeOH,out}}{F_{Tot,in} \cdot y_{MeOH,in}} \tag{5.3}$$

The conversion can be calculated by using the feed analyses for the methanol fraction in the feed $y_{MeOH,in}$ or by basing it on carbon produced is the same amount of carbon as in the feed given by equation 5.4.

$$(F_{Tot} \cdot y_{MeOH})_{in} = (F_{Tot} \cdot \sum y_{c,Tot})_{out} \tag{5.4}$$

The GC had two thermal conductivity detectors, which analyzes the feed and product stream, and gives the concentration of each component. The concentration of a component is related to the peak area and the retention factor for that component as seen below in equation 5.5.

$$y_i = A_i \cdot k_i \tag{5.5}$$

The detectors are concentration sensitive, and any volume changes must be taken into account in the gas stream throughout the process. To minimize errors related to applying the retention factors to determine component concentration, an internal standard (nitrogen) is used to relate total outflow to the total feed as shown in equation 5.6

$$F_{\mathrm{N}_2,in} = F_{\mathrm{N}_2,out} \tag{5.6a}$$

$$F_{Tot,in} \cdot y_{\mathrm{N}_2,in} = F_{Tot,in} \cdot y_{\mathrm{N}_2,in} \tag{5.6b}$$

$$F_{Tot,out} = F_{Tot,in} \frac{y_{\mathrm{N}_2,in}}{y_{\mathrm{N}_2,out}} \tag{5.6c}$$

The carbon based selectivity can be calculated either as a function of the total amount of methanol converted or as a function of the total amount of carbon produced (CO, CO_2, CH_4 and CH_2O) as seen in equation 5.7.

$$S_{c,i} = \frac{F_{Tot,out} \cdot y_{C,i,out}}{F_{Tot,in} \cdot y_{MeOH,in} - F_{Tot,out} \cdot y_{MeOH,out}} \tag{5.7a}$$

$$S_{c,i} = \frac{y_{C,i_{out}}}{\sum y_{C,product_{out}}} \tag{5.7b}$$

Calculating the hydrogen based selectivity implicates limitations because water is a non-desired component in the GC. By assuming that the H_2O in the feed is inert, selectivities for compounds containing hydrogen and H_2O may be calculated as shown in equation 5.8 below.

$$S_{\mathrm{H_2}} = \frac{2F_{Tot,out} \cdot y_{\mathrm{H_2},out}}{4(F_{Tot,in} \cdot y_{MeOH,in} - F_{Tot,out} \cdot y_{MeOH,out})} \tag{5.8a}$$

$$S_{\mathrm{H_2O}} = \frac{2F_{Tot,out} \cdot y_{\mathrm{H_2O},out}}{4(F_{Tot,in} \cdot y_{MeOH,in} - F_{Tot,out} \cdot y_{MeOH,out})} \tag{5.8b}$$

The hydrogen selectivity may also be calculated as a function of the total amount of hydrogen produced (H_2, H_2O, CH_4 and CH_2O) given in equation 5.9.

$$S_{H_n} = \frac{nF_{Tot,out} \cdot y_{H_n,out}}{\sum ny_{H_n,product_{out}}} \tag{5.9}$$

Verification of the mass balances were calculated to identify carbon, hydrogen and oxygen losses. For experiments like this, it is usually always errors in the balances. This could be explained by leakages, simplifications done when treating the GC data etc. If the losses are less than 5 %, it assumed that the error is in the same order of magnitude as other experimental errors (<5 %). The error in the mass balances for carbon, hydrogen and oxygen is presented in equation 5.10.

$$E_C = \frac{F_{Tot,out} \sum y_{C,out} - F_{Tot,in} \cdot y_{MeOH,in}}{F_{Tot,in} \cdot y_{MeOH,in}} \tag{5.10a}$$

$$E_H = \frac{F_{Tot,out} \sum ny_{H_n,out} - F_{Tot,in}(4y_{MeOH,in} + 2y_{\mathrm{H_2O},in})}{F_{Tot,in}(4y_{MeOH,in} + 2y_{\mathrm{H_2O},in})} \tag{5.10b}$$

$$E_O = \frac{F_{Tot,out} \sum ny_{O_n,out} - F_{Tot,in}(y_{MeOH,in} + y_{\mathrm{H_2O},in} + 2y_{\mathrm{O_2},in})}{F_{Tot,in}(y_{MeOH,in} + y_{\mathrm{H_2O},in} + 2y_{\mathrm{O_2},in})} \tag{5.10c}$$

5.9 External mass transfer limitations

To test for external mass transfer limitation there were performed three experiments using different gas flow with an oven temperature starting point at 550 °C. The gas flows chosen were 250 NmL/ min, 500 NmL/ min and 863 NmL/ min. To lower the conversion, the catalyst bed was diluted 1:100 with α-alumina. The catalyst bed was created using 0.0135 g conventional silver catalyst with a particle size 250-500 µm with 1.3677 g α-alumina at the same fraction of particle size. Further 1 g α-alumina was placed under and over the catalyst bed. Then the void volume was reduced using silicon carbide.

For each flow a temperature profile was created and oven setpoint temperature was adjusted to try achieve the same temperature in the catalyst bed. The bed temperature at the experiment with 250 NmL/ min was sat as a reference and the two succeeding experiments the setpoint temperature were changed to respectively 521 °C for 500 NmL/ min and 525 °C for 863 NmL/ min to adjust for the temperature changes.

The heating of feed and product lines were shut off during these experiments. The result is that the feed line had a temperature of 50 °C and product line around 70 °C. This was not intended and might influence the results.

Ideal gas law is applied to convert from volume to mole, using bed temperature and measured pressure.

Chapter 6

Results and Discussion

In this study a fresh and a plat exposed silver catalyst was characterized by SEM, XRD, XRF, TGA, nitrogen adsorption and oxygen chemisorption to determine effects of the plant conditions on the catalyst. The fresh commercial silver catalyst was also tested in a rig to establish a methodology for further reaction experiments. Results from the characterization and rig performance are presented in the following sections.

6.1 SEM

To see the changes in topology for the plant exposed catalyst the fresh and the exposed catalyst were examined using SEM. Figure 6.1 and figure 6.2 show representative images at different magnitude for the fresh catalyst on the left side and the plant exposed on the right hand side.

The images of the fresh catalyst show a terrace structure with crystalline facets. A lot of grain boundaries was apparent. After exposure to plant conditions there were massive changes in the topology. If the silver is exposed to temperature above the tamman temperature for the silver sintering may occur. Tamman temperature for silver is 642 K, half the melting temperature of 1235 K. Exceeding the tamman temperature leads to inter diffusion and surface diffusion [2], and creation of surface area with lowest energy configuration. For silver, the lowest energy configuration is having the facet (111) exposed [17]. The surface- and inter-diffusion is important due to the chemisorbed surface oxygen which is believed to stabilize the (111) facet during restructuring [17].

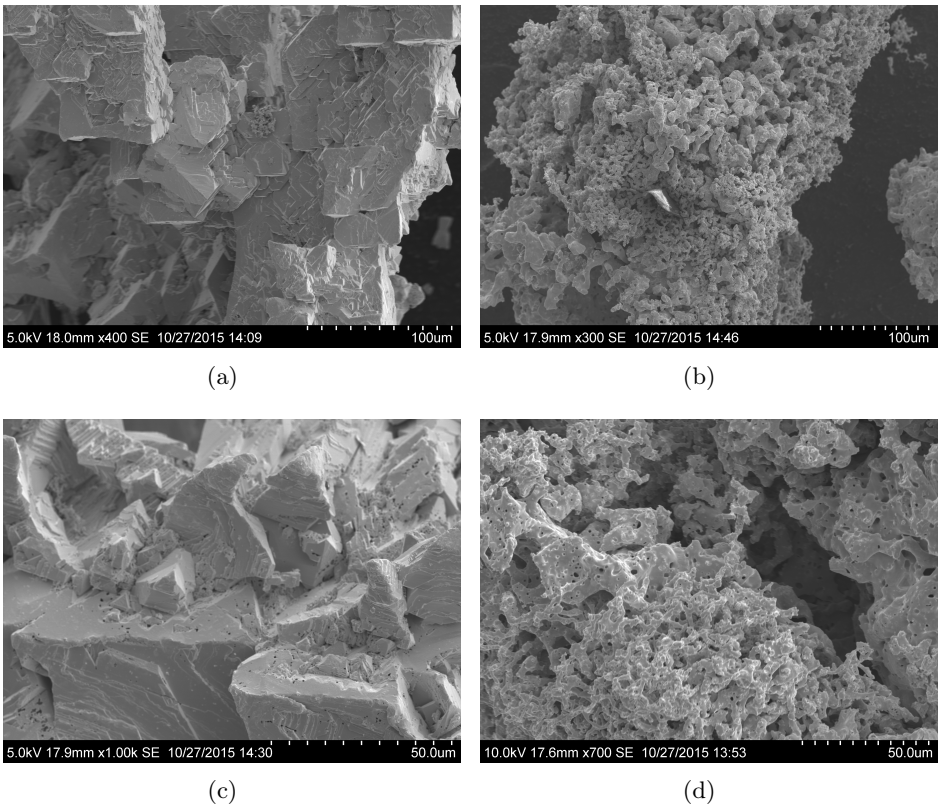

Figure 6.1 – SEM images of the received fresh catalyst (a and c) and the plant exposed catalyst (b and d) at different magnitudes, using secondary electron detector.

Evident pinholes are also observed in the plant exposed catalyst compared to the fresh catalyst. These pinholes are suggested to be created from formation of water in the bulk, which imply bulk diffusion of oxygen and hydrogen is present under industrial plant conditions [17].

The bottom layer of the exposed catalyst shows structures similar to carbon structures, as can be seen in figure 6.3. Due to the feed stock and the structure of the observed features it is assumed to be carbon structures. An elemental analysis of the composition (EDX) was conducted to try identify the elemental composition of the structures but also to try identify elements that is know for promoting carbon formation. For the plant exposed catalyst there is a reason to believe that elements like iron or nickel are present. Both iron and nickel is know for the ability to promote growth of carbon whiskers.

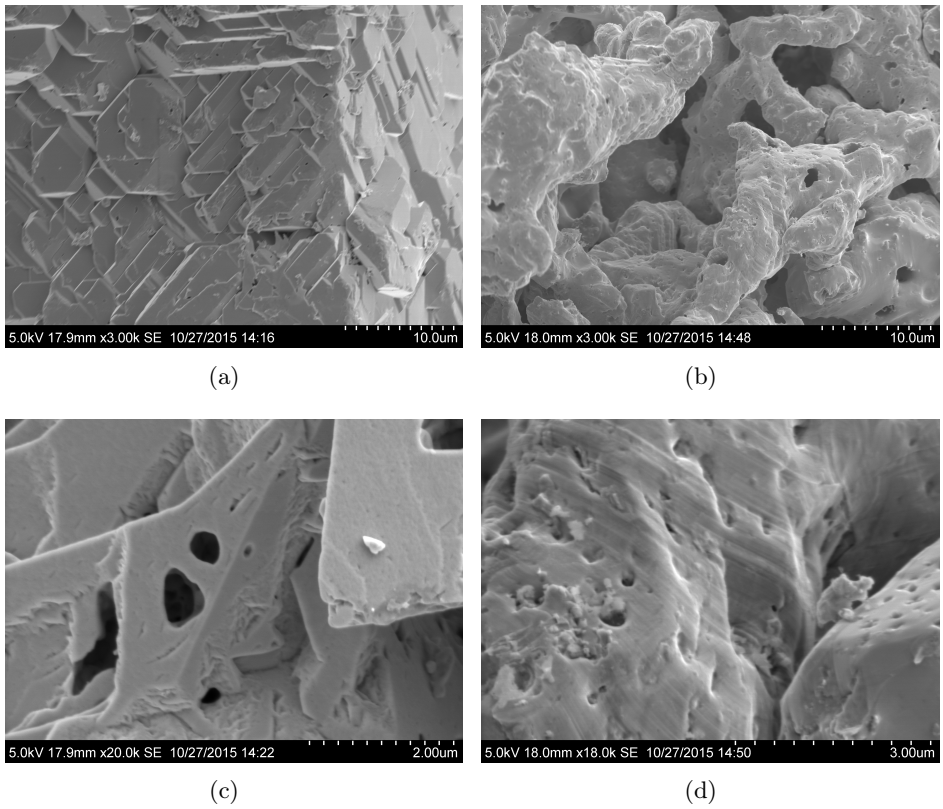

Figure 6.2 – SEM images of the received fresh catalyst (a and c) and the plant exposed catalyst (b and d) at different magnitudes, using secondary electron detector.

Due to the nature of EDX analyses one needs a flat surface to get good results. Examine the carbon whiskers with EDX did not give acceptable signal, so the presence of nickel and iron could not be determined.

There was also seen a different structures than the typical whiskers, show in figure 6.4. Figure 6.4(b) shows EDX maping of the observerd structure. The analysis shows that the structures are carbon. The interesting part is that it looks like carbon is layered from a facet in a structured way. This might be related with how the dark spots, which are visible when inspecting the used catalyst, are formed.

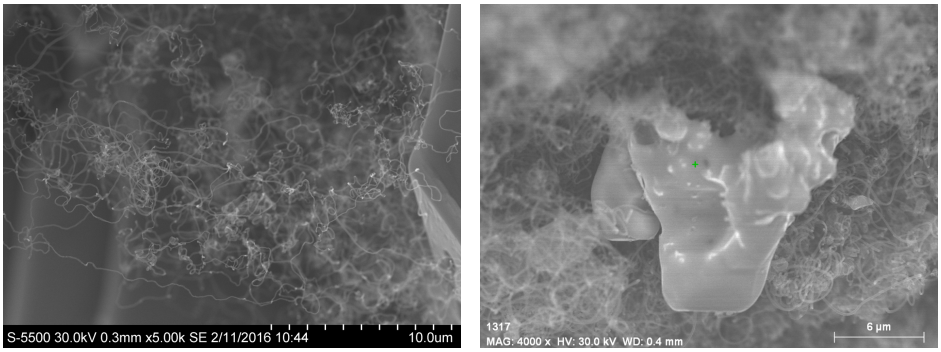

(a) (b)

Figure 6.3 – SEM images of bottom layer of the plant exposed catalyst showing suspected carbon structure.

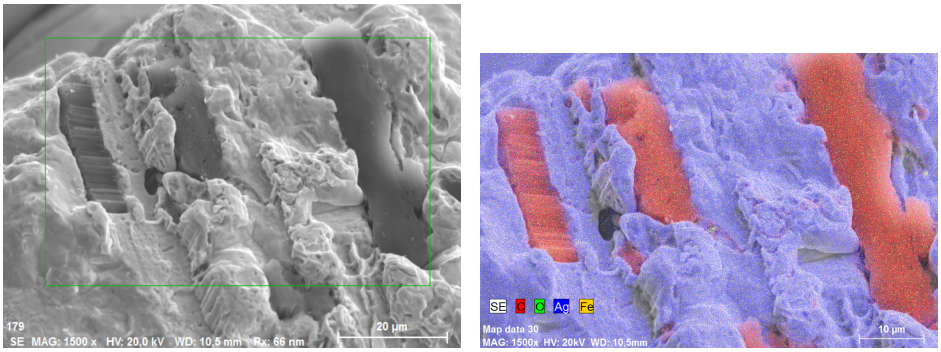

(a) (b)

Figure 6.4 – SEM images of bottom layer of the plant exposed catalyst showing suspected carbon structure. Image 6.4(a) is taken using secondary electron detector. Image 6.4(b) is EDX mapping to show the different elements.

6.2 XRD

The Bruker D8 Advance DaVinci X-ray Diffractiometer was used to analyze the samples. The diffraction patterns for the fresh and top layer of the plant exposed catalyst is given in figure 6.5. The crystalline phases were matched to a reference pattern using DIFFRAC EVA software. Due to the contamination of the X-ray source the reference pattern were also tuned to show peaks for the different wavelengths from the contamination.

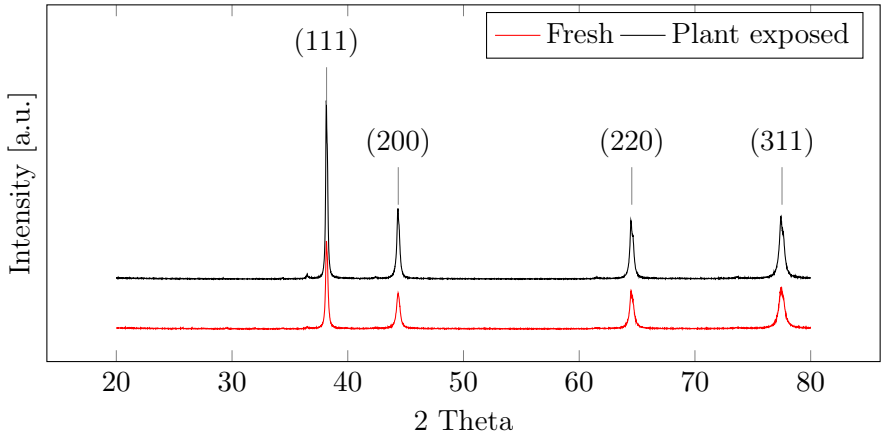

Figure 6.5 – X-ray Diffraction pattern for the silver catalyst. The black line show the fresh catalyst while the red line show the top layer of the plant exposed catalyst.

TOPAS software was used to calculate the crystallite size based on peak size. A Lorentzian convolution was applied. Statistically the R_{wp} should be under 5 % to be within a 95 % confidence interval. The Scherrer's equation was calculated to compare the crystallite size, using $K = 0.89$ and full width at half maximum (FWHM). Results are given in table 6.1.

Table 6.1 – Calculated crystallite size and Rwp for the fresh catalyst and the top layer of the plant exposed catalyst, using TOPAS v.5.0 and Scherrer's equation.

	Crystallite size [nm]	Rwp [%]	Scherrer's equation [nm]
Top layer	65.6	14.36	58.4
Fresh	46.1	13.25	41.0

The intensity has increased for the plant exposed catalyst, thus indicating that the crystallinity of the plant exposed catalyst have increased. This is further reinforced by the calculated crystallite size in table 6.1. The increase in crystallinity is also anticipated due to growth of crystallites when exposed to high temperatures. Due to the high R_{wp} and uncertainty for calculation of the crystallite size the calculated values in table 6.1 values are not exact, however it can still provide a useful comparison for the changes. For the calculation of the crystallite size using Scherrer's equation the K value is an uncertainty, most used values is between 0.89 and 1, however the value can be in the range 0.62 to 2.08. The uncertainty of the K value illustrate that Scherrer's equation is a crude method for calculating the crystallite size, but is useful to compare the relative changes in samples when using the same parameters. For comparison with the provided silver catalysts a silver oxide sample was also analyzed. The diffraction pattern is given in figure 6.6.

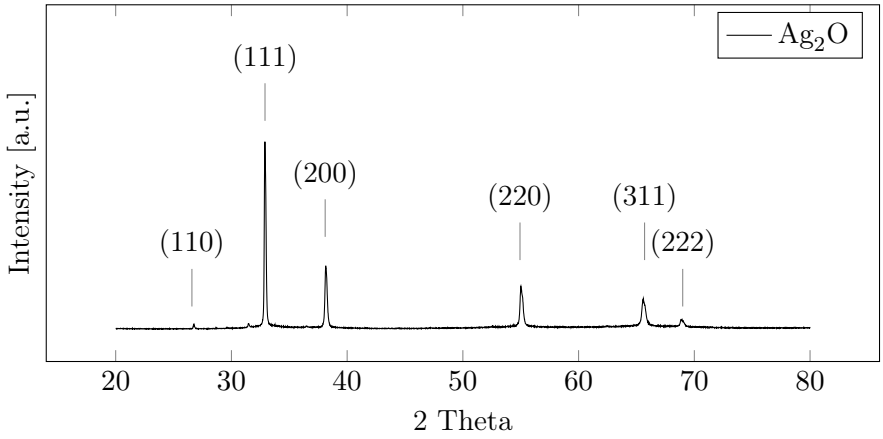

Figure 6.6 – X-ray Diffraction pattern for the silver oxide, Ag_2O.

When comparing figure 6.5 and figure 6.6 there is no evidence of silver oxide peaks in the sample diffractogram. However, as silver creates a stable silver oxide on the surface that prevents further oxidation in ambient conditions the oxide layer would be on the surface. As XRD is a bulk method the silver oxide would be a small part and the bulk silver would be abundant.

For the (111) and (200) facet the normalized intensity are equal while there is a difference in the diffraction pattern of facet (220) and (311), shown in figure 6.7. This might be an effect of the sample preparation as the particles might not be randomly distributed.

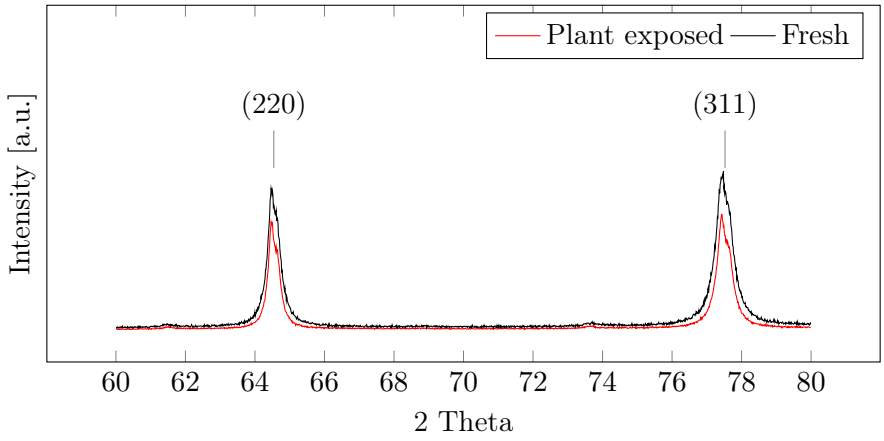

Figure 6.7 – Normalized X-ray diffraction pattern for the silver catalyst. Focused at diffraction pattern of (220) and (311). The black line show the fresh catalyst while the red line show the top layer of the plant exposed catalyst.

6.3 XRF

The XRF studies were performed in a Supermini 200 analyser using a Palladium X-ray source produced by Rigaku. The instrument uses LiF (200), PET and RX25 analyzing crystals for analyzing and can detect elements from Fluorine to Uranium. To quantitatively calculate the $K\alpha$ radiation is used, peaks caused by other irradiation is therefore not used. As the sample is mixed with boric acid as a binder this can introduce contaminants to the sample. The sample specter is therefore qualitatively compared with boric acid as a reference. Peaks that are present in the boric acid spectra are removed before quantitatively calculation using SQX software. The silver content calculated for the silver catalyst is given in 6.2. The XRF charts and SQX calculations are given in appendix E.

Table 6.2 – Silver content in fresh and plant exposed catalyst measured with XRF.

	Silver [%]
Top layer	100
Fresh	100

From SEM analyses there is suspected carbon formation on the used

catalyst, which is not seen in the XRF results. However there is a limit for which elements that can be detected dependent on which detector used. Carbon cannot be detected with the used detector, resulting in that the results is most likely not accurate. The plant exposed catalyst might contain traces of other elements, for example iron from the piping and process equipment. Iron is detected qualitatively, however the detected signal was a second order $K\beta$ and not $K\alpha$ which were used by the SQX software to calculate the present elements. The quantitative calculation gave 100% silver for both the fresh and the plant exposed catalyst. However, this is the result after removal of peaks and might not be correct. The crystal used in the XRF cannot detect elements lighter than Fluorine. It is not likely that there are large amounts of contaminants in the sample total, however the contamination may be predominate at the catalyst surface.

6.4 Temperature programed analyses

The temperature programmed analyses were done in a TGA instrument. The thermogram from the fresh catalyst is given in figure 6.8. This does not show any observable mass change, except the effect of applying gas on the sample at the analysis start. Several experiments were conducted where a TPR with hydrogen was performed before a TPO with synthetic air. The result from the TPR and TPO were inconclusive and different methods were implemented to figure it out. When comparing correction files it was apparent that instrument problem were cause of the results.

Oxygen has a low molecular weight compare to silver. Assuming the whole sample is oxidized and in the form Ag_2O, the weight percent of oxygen would only account for 7 %. This raises a question if the weight change is detectable due to the oxide layer is only on the surface of low surface area specie. To further investigate this an analysis with silver oxide (Ag_2O) was performed in synthetic air atmosphere, after the instrument was recovered. The thermogram form the analysis is given in figure 6.9.

From the figure 6.9 it is seen that the silver is reduced at around 400 °C and does not show any mass change during further heating nor cooling in synthetic air. The change in mass at the start is due to weight changes when the gas is turned on. The sample mass is reduced 7 %, this shows that the silver oxide is fully reduced. As no mass change was apparent, after the reduction of silver oxide, further analyses was not conducted.

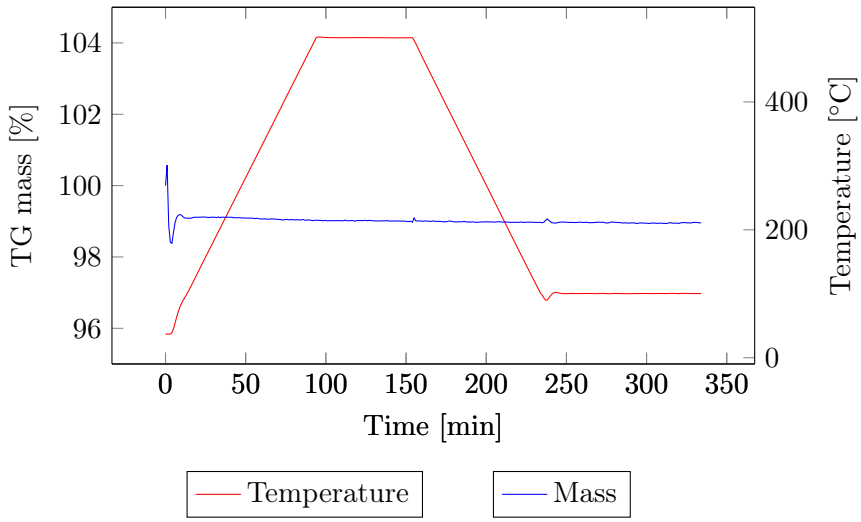

Figure 6.8 – Thermogram of fresh catalyst. Change in mass and temperature is plotted as a function as time. Sample is heated to 700 °C and cooled down to 30 °C in a synthetic air and argon atmosphere.

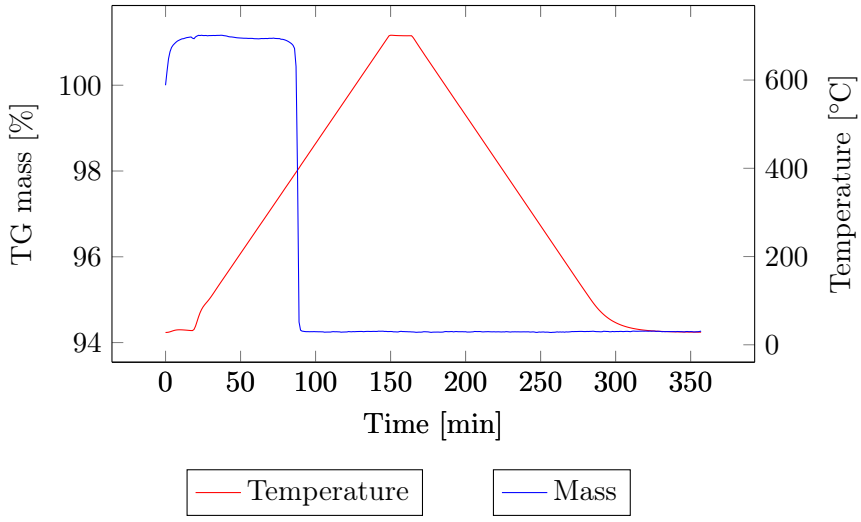

Figure 6.9 – Thermogram of silver oxide. Change in mass and temperature is plotted as a function as time. Sample is heated to 700 °C and cooled down to 30 °C in a synthetic air and argon atmosphere.

6.5 Nitrogen adsorption - Bet surface area

The nitrogen adsorption did not yield any results for the surface area. A general rule of thumb to get reliable result is to have at least 20 m^2 of surface area when measuring the BET surface area with Nitrogen adsorption. As electrolytic silver is not a porous metal, and having a surface area of 70 $cm^2\,g^{-1}$ for particle size 0.85-2.0 mm [3], makes Nitrogen adsorption not suitable to measure the surface area due to high vapor pressure at 77 K. Using a gas with lower vapor pressure, like krypton, would give a larger pressure change for the same relative pressures than for nitrogen. This makes krypton adsorption superior to nitrogen for measuring compounds with smaller surface area.

6.6 Chemisorption

No reliable result was received from the oxygen chemisorption. Negative adsorption does not make sense. Silver has low surface area that might contribute to making the chemisorption difficult. Low surface area compounds is also more prone to instrumental errors and detection limitations. Low surface area on the sample can to some extent be countered by increasing the amount of sample used. There have also been registered problems with the oxygen line in to the instrument, which might also have contributed to the non-reliable results obtained.

6.7 Operation of methanol to formaldehyde (MTF) rig

Operation of Experimental Setup

The experimental setup used for MTF production was previously used for DME synthesis. This indicated that the setup was not necessarily optimal for MTF synthesis. Henceforth, making it operational is one of the main motivations behind the thesis.

Before the analysis could take place, a customization of detectors and columns in the GC were required. This would cause a delay in the project, and a microGC was installed to the setup. The original idea was to run side reactions and to investigate oxidation of CO and burning of H_2, since a microGC would not be able to analyze formaldehyde. MFC was calibrated for the required gases and calculations needed to calibrate the microGC by using the gas mixer (Alytech) was prepared. The availability of the

gas mixer was limited and after a period of latency, the original GC was operational. This lead to the decision of using the microGC as a backup plan, and continuing the analysis with the GC and MTF synthesis. Following, the LFC was calibrated for methanol and a single point calibration of a formalin solution (roughly 37 % CH_2O, 13 % CH_3OH and 50 % H_2O) was performed.

The GC was already calibrated for methanol (0.5 % MeOH in CH_4), but a calibration for CH_2O was required. Calibration was performed with a formalin solution sent through the setup and a direct injection with a syringe in the GC. The calibration performed with the setup applied a mix of nitrogen (75 %) and formalin (25 %, ca. 9.25 % CH_2O). The results from the calibration were highly unstable, and a more profound calibration is essential. This could be due to instability of the formalin solution, due to the unknown concentrations of each component in the solution. Dynea will perform a more accurate calibration with a stable formalin solution in the future. It is important to keep in mind the absence of an accurate calibration for formaldehyde when analyzing the data from the experiments.

After the formaldehyde calibration, a feed analysis was performed at 200 °C. The goal was to ensure a stabilized feed composition, but there were evident traces of CH_2O left in the system. To remove the contaminations, the pressure was increased from 1.3 bar to 3.3 bar. This resulted in a decrease of CH_2O contaminations, but there were still traces. The pressure was decreased toward 2 bars, and left for an hour to clean out the system. A considerable decrease was discovered afterwards, but there were still traces left. The methanol/water mix and formalin solution containers are connected by shared pipelines. To ensure that the contaminations were not located in these pipelines, the methanol/water mix was flushed through. This did not result in a stable feed analysis. The problems regarding an instable feed analysis continued and the feed was stopped. The setup contains large amounts of pipelines, and a cold spot in the pipelines could be a reason for the instability. All the pipelines are insulated, but the insulation started showing signs of a replacement need. Several pipelines were given new insulation, especially pipelines going into the GC. The pipelines into the reactor are quite long and contains a large volume, which is not ideal conditions for the GC and makes it vulnerable. This will influence the GC results and should be taken into consideration.

The original molar percentage of methanol in the feed was set to 16 %, but after having considerable challenges regarding a stable feed analysis, this was changed. The methanol/water mix was reduced to a halved molar percentage of methanol (8 %). This gave a significant positive impact on the feed analysis, and was chosen as the reference feed composition for methanol.

From a GC point of view, water is less than ideal component. Problems associated with water include large vapor expansion volume, inadequate wettability and solubility in several stationary phases, detector difficulties, and perceived chemical harm to the stationary phase [18]. Water is an essential component in the analysis, and its influence will complicate the GC analysis. This was taken into consideration during the experiments and a stable GC value for water was not expected. Because of the difficulties associated with water and GC, the calculations for hydrogen selectivity and mass balances including water is not optimal.

During the analysis, a common factor for all the feed analysis is that the oxygen amount is higher than expected. It is supposed to be around 3 mol%, but was closer to 4 mol%. A test was performed to see if a new setpoint for synthetic air MFC would improve the oxygen fraction. The results can be found in appendix B, and shows evident signs of improvement. The new MFC setpoint was calculated from the low range of calibration performed for air (see appendix B). The new setpoint was not applied, since it would complicate the comparison of data. But an improvement of setpoint would improve the feeds composition, making it more similar to the target value. Additionally, there was some difficulties getting the LFC for the methanol/water mix stable. Throughout the analysis the He pressure was increased/decreased in the liquid tank to keep the liquid flow stable. When running the flow controllers at a low setpoint, the accuracy decreases. This influenced the feed analysis and thereby the calculations. This was also the situation for the MFC for air, which started to destabilize later in the analysis.

After some runtime in the setup, a large pressure increase in the pipelines was discovered. The reason for this pressure increase appeared to come from a blockage in the vaporizer (CEM). Thereby, the vaporizer was detached and disassembled to examine the interior. A blockage was discovered in outlet of the CEM. The blockage appeared to consist of some unidentified dark organic matter, and with the help of a thin metal rod, heat and pressurized air was removed. To ensure that a blockage in the vaporizer was avoided for further work, a certain temperature (about 100 °C is kept in the CEM with a continuous flow of inert during downtime.

Another significant variable for the experimental setup is the absence of pressure control for the feed. There is a Bronkhorst pressure controller installed, but it is not operational at pressures below two bar. When installed, it was supposed to control pressures in a range from 50-60 bar. The MTF synthesis is at low pressure (about atmospheric), and the pressure controller installed would not stabilize at such a low range. The pressure controller

has been used to monitor the pressure on the computer, but could not be used as a controlling element. During the analysis, when changing the total flow, a change in pressure has been observed. The pressure changes are not major, but the influence cannot be disregarded.

While running the experiments, several minor peaks were discovered during the long run sequence for the GC. Attempts were made to identify these peaks by calibrating DME and formic acid. DME was applied from a calibration mix (0.5 mol% DME) and diluted formic acid (0.1-2 mol%) was injected by syringe into the GC. None of these components seemed to match these unidentified peaks. It is possible that the peaks could originate from formaldehyde polymers, but further testing is required to make a conclusion.

Feed Analysis

Before starting the analysis for the different experiments, a feed analysis was performed, given in appendix D. This to ensure stable feed and the average composition of these analyses were used in the calculations. Due to instability regarding flow controllers (MFC and LFC) and their calibrations, deviations from the desired composition were observed in the feed analyses.

When calculating the average composition for each feed analysis, data showing large deviations were excluded (marked red in appendix D). During the analysis, time limitations were a fact, and the feed analysis was run for a short period. The goal was to get it as constant as possible, but it would undoubtedly favor from a longer run time. Hence, calculations independent of the feed analysis were favored.

Conversion and selectivity can be calculated using different methods. Either by using formed products or by total conversion of methanol. Both methods will have advantages and disadvantages. Calculations based on total conversion of methanol take all product formed and not only the analyzed ones into account. Nevertheless, this method is based on a fixed feed analysis and variations of feed will affect the result. By using the analyzed products, variations of feed are taken into account. However, this will exclude all products not analyzed by the GC.

The presented conversion and selectivities is on a product basis, since there was no apparent carbon formation in the reactor nor any large unidentified peaks in the GC analysis.

Errors due to a proper calibration of formaldehyde were inevitable. An attempt to reduce this error was conducted by recalibrating the GC value based on stable areas of the mass balance. At a low conversion the mass

balance showed minor errors, but at high conversion the deviation grows. Due to this, the formaldehyde data were adjusted to 90 % of the original GC value, by applying the stable regimes of the carbon mass balance in test 2.

6.8 Experimental methodology for MTF rig

First objective is to achieve conversion and formaldehyde selectivities close to whats obtainable industrially, then determine what may be manipulated to increase the selectivity towards formaldehyde. Four formaldehyde synthesis experiments has been performed to establish the experimental methodology for reaction experiments and the influence of different conditions on the system. Three tests were performed with a commercial silver catalyst and one test with empty reactor. For the test using catalyst, the catalyst was diluted 1:10 with α-alumina and the methanol fraction was kept low to keep control of the reaction temperature and safe operation. Temperature profiles were taken during experiments to get information about the temperature gradient in the reactor. For each run the oxygen was fully consumed when reactions took place.

Test 1 - Preliminary test, changes in temperature and flow

Test 1 was performed to determine at which temperature the reaction takes place and the desired products are formed. The test was done with constant gas composition. Table 6.3 gives changes in oven setpoint temperature and total flow.

Methanol conversion, carbon and hydrogen products selectivity were calculated as shown in appendix F . The selectivity is based on total methanol conversion, thus including all products formed. The results were plotted as a function of TOS and given in figure 6.10.

Figure 6.10 shows there is no activity before a reactor temperature of 500 °C, increasing the temperature gives an increase in conversion. Increasing the flow gives a lower conversion. To better illustrate the applied changes impact, is the carbon selectivity plotted at different time on stream intervals in figure 6.11.

From figure 6.11 there is seen that oven setpoint temperature of 500 °C is needed to start the reactions. By further increasing oven temperature to 550 °C the formaldehyde selectivity increases, while carbon dioxide selectivity is reduced. Increasing oven temperature to 600 °C drastically changes product composition, carbon monoxide is favored while formaldehyde and

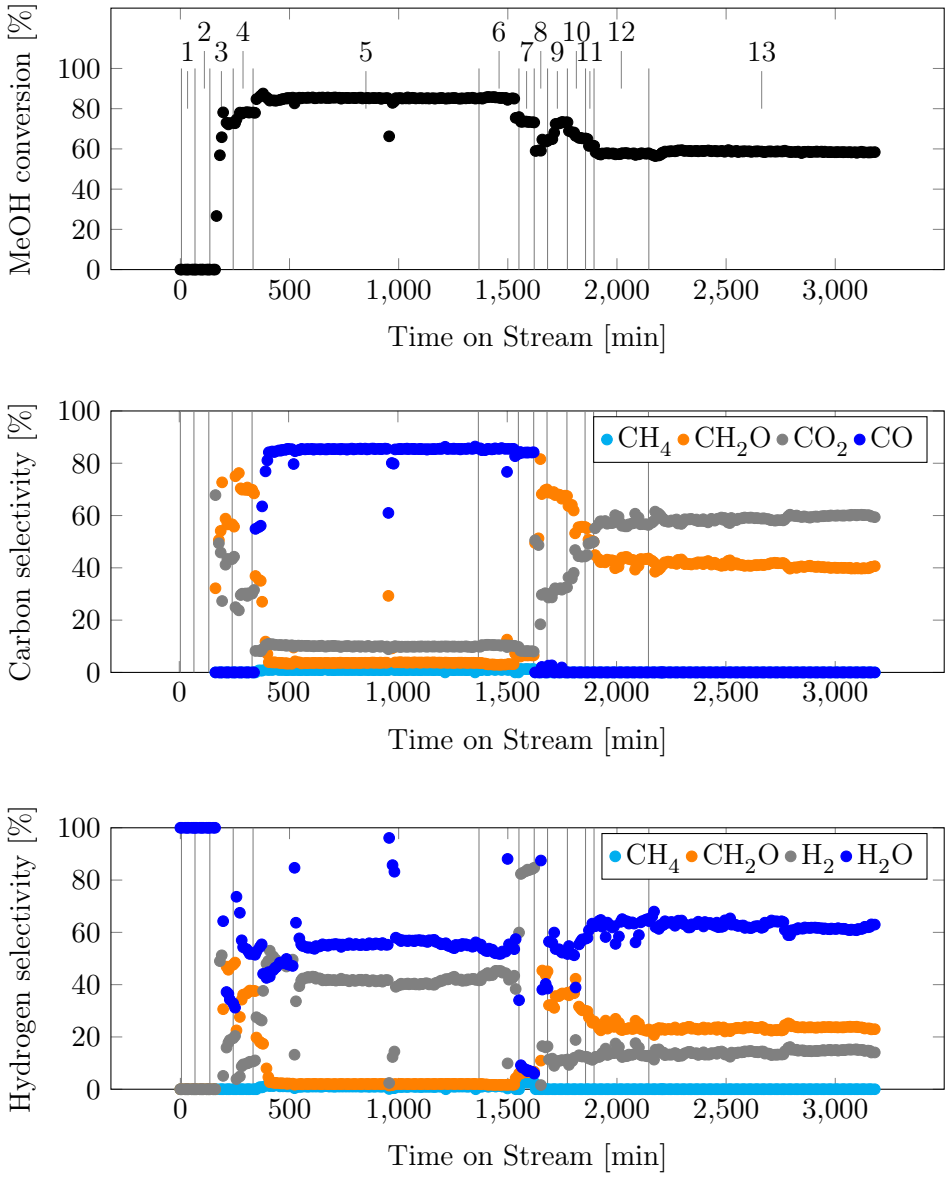

Figure 6.10 – Conversion, carbon selectivities and hydrogen selectivities as a function of time on stream (TOS), with temperature and gas composition changes indicated with gray lines. Section 1, 2, 3, 4, 5 and 6 have oven setpoint temperature respectively 300, 400, 500, 550, 600, and 650 °C. Section 7 is increase in total flow to 375 NmL/ min. Section 8 is decreasing the temperature to 500 °C. Section 9 is reducing the total flow to 250 NmL/ min. Section 10, 11, 12 og 13 have temperature respectively 450, 420, 405 and 390 °C. All use reference feed composition, table 5.5.

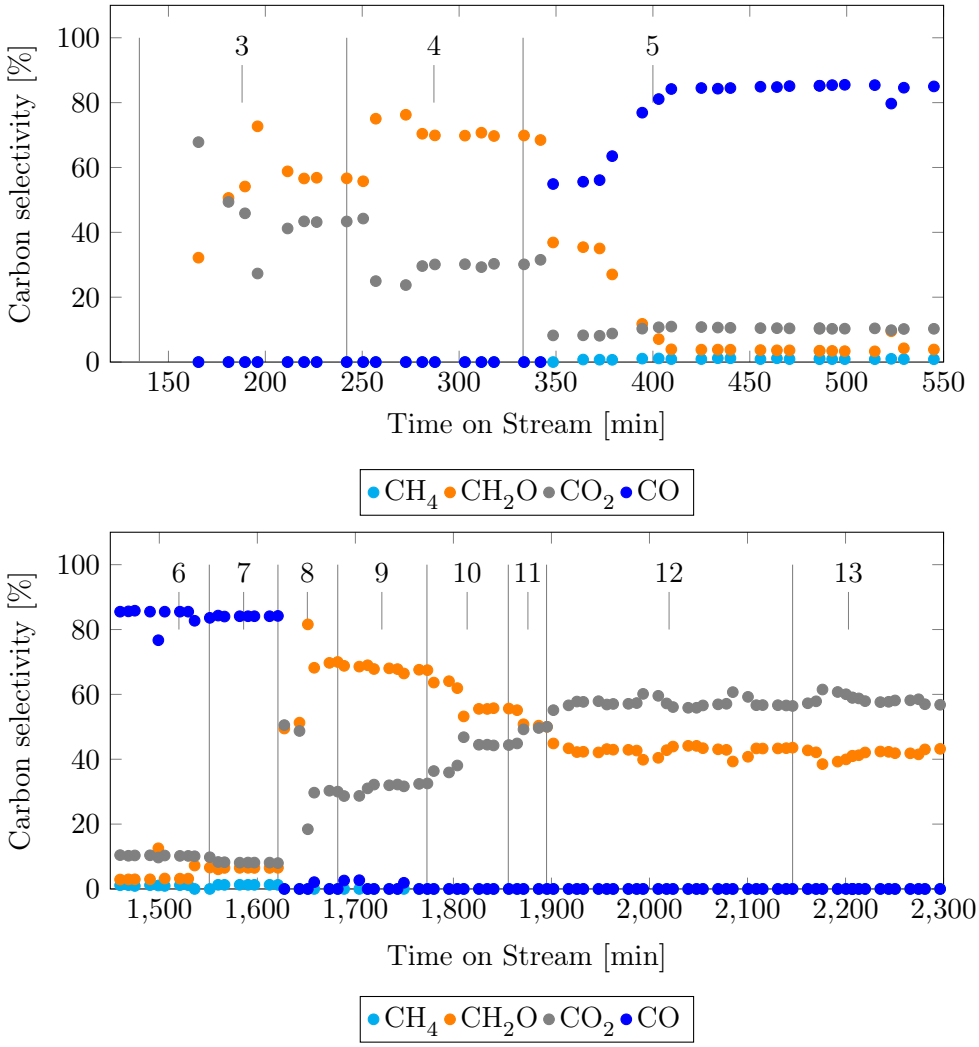

Figure 6.11 – Carbon selectivities as a function of time on stream (TOS), with temperature and gas composition changes indicated with gray lines. Section 3, 4, 5 and 6 is oven setpoint temperature respectively 500, 550, 600, and 650 °C. Section 7 is increase in total flow to 375 NmL/ min. Section 8 is decreasing the temperature to 500 °C. Section 9 is reducing the total flow to 250 NmL/ min. Section 10, 11, 12 og 13 have temperature respectively 450, 420, 405 and 390 °C. All uses reference feed composition, table 5.5.

Table 6.3 – Section with temperature, gas composition and total flow changes for test 1. The gas composition is shown in table 5.5.

Section	TOS [min]	Gas composition	Oven temperature [°C]	Total flow [NmL/ min]
1	0-67	Reference	300	250
2	67-135	Reference	400	250
3	135-242	Reference	500	250
4	242-333	Reference	550	250
5	333-1368	Reference	600	250
6	1368-1551	Reference	650	250
7	1551-1621	Reference	650	375
8	1621-1682	Reference	500	375
9	1682-1773	Reference	500	250
10	1773-1856	Reference	450	250
11	1856-1895	Reference	420	250
12	1895-2146	Reference	405	250
13	2146-3181	Reference	390	250

carbon dioxide is dropping down. A change in gas flow to 375 NmL/ min increases formaldehyde selectivity while some what reducing carbon dioxide selectivity. By reducing the temperature to 500 °C carbon monoxide selectivity drops to zero while formaldehyde and carbon dioxide increases. By reducing the gas down to 250 NmL/ min at 500 °C the formaldehyde and carbon dioxide selectivity increases while carbon monoxide shows little to non change. Further reduction of temperature to 450 °C and 420 °C gives an increase in carbon dioxide selectivity while a reduction of formaldehyde selectivity. Small temperature changes form 420 °C to 390 °C gives little to none change in selectivities for the products.

The first test showed that an oven setpoint of 500 °C was needed to get ignition of the catalyst bed. After the bed ignites the methanol conversion rises rapidly from 0 to 70 %. After the reactions takes place all oxygen is consumed for further reactions. At lower temperatures than 500 °C there is a high carbon dioxide selectivity, which indicates a large amount of the methanol, goes to complete combustion, this combustion might provide the heat for the reaction. Increasing the temperature to 550 °C the conversion gets an increase to 78 % and the formaldehyde selectivity increases from 56 % to 70 %, while the carbon dioxide is reduced from 44 % to 30 %. Higher temperature increase formaldehyde selectivity, this is expected due to the

increasing ratio O_γ/O_α.

When increasing the oven setpoint temperature to 600 °C the conversion stabilizing at 85 % gas phase reaction takes over as no apparent increase in catalyst bed area. Decomposing of methanol rise the carbon monoxide selectivity from 0 % to 85 % and remaining formaldehyde selectivity is 3.5 %. By increasing the total gas flow to 375 NmL/ min gives a small increase in formaldehyde selectivity while reducing carbon dioxide selectivity, the methanol conversion is unchanged. If methanol is directly decomposing to carbon monoxide and hydrogen gas or if it goes through intermediate steps where formaldehyde is formed is difficult to determine. However, the temperature plays a significant role. Increasing the flow will reduce the residence time, as the silver catalyst is also suspected to participate [19], not only in oxidative dehydrogenation of methanol but also further decomposition of formaldehyde, lower residence time should provide advantages for keeping high formaldehyde selectivity. By reducing the oven temperature to 500 °C, the formaldehyde selectivity increases back around 65 %, carbon dioxide is increased to 30 % and conversion is reduced to 70 %.

By reducing the total flow to 250 NmL/ min, thus reducing the amount of reactants, there is a slight reduction in formaldehyde selectivity and a slight increase in carbon dioxide selectivity, while the conversion is increased to 73 %.

By further reducing temperature the selectivity for formaldehyde is reduced before it stabilizes at 42-43 %. The carbon dioxide selectivity increases before t stabilizes at 57 %. The same trend is seen in the conversion where it is reduced with decreasing temperatures before to stabilizes at 60 % regardless of the applied temperature reduction. A lower conversion that the reaction started at, this indicates that after the ignition the reaction is self sustained at lower temperature. This might indicate that at lower temperature, the exothermic reactions provide energy for the endothermic reactions. The high pressence of CO_2 further indicates that the combustion reactions is providing the heat. This is also seen in the increasing hydrogen selectivity as the oxygen is consumed before hydrogen is formed.

When increasing the temperature, the performed temperature profiles, figure 6.12 show that there are temperature increasing in the area of the catalyst bed at oven setpoint temperature 450 °C. This increase in bed temperature is noticeable until the oven setpoint is 600 °C. At 600 °C and 650 °C the temperature profile does not show an increase nor a flattening at the catalyst bed area. This indicates that at oven setpoint temperatures at 600 °C and above the gas phase and decompositions reactions is favoured, where carbon monoxide and hydrogen is major products. This is

also further confirmed by the product composition. By lowering the setpoint temperatures after the ignition of the bed there is seen an increase in bed temperatures at lower oven setpoint temperatures than when heating up the reactor. This indicates that there is catalytic activity in the catalyst bed, which further confirmed in the change of the product composition.

Due to the reactor design, it was only possible to measure the lower one third part of the reactor, yet still the temperature profiles showed a large temperature gradient. To improve this an air line was implemented to get some air circulation in the reactor oven.

The temperature profiles obtained during the different temperature changes for ordinary feed composition (8 % MeOH) with a total flow of 250 NmL/ min are presented in figure 6.12 . The figure illustrate a large temperature gradient for the oven, with high temperatures in the top. This imply that the oven set up is not optimal. Temperature profiles for 500 and 550 °C shows peaks in the catalyst bed, indicating that the catalyst reaction is ignited and the exothermic reactions takes place at the catalyst bed. Temperature profiles for 600 and 650 °C does not show any clear peaks in this area and indicates that the homogeneous gas phase reaction and decomposition is dominating.

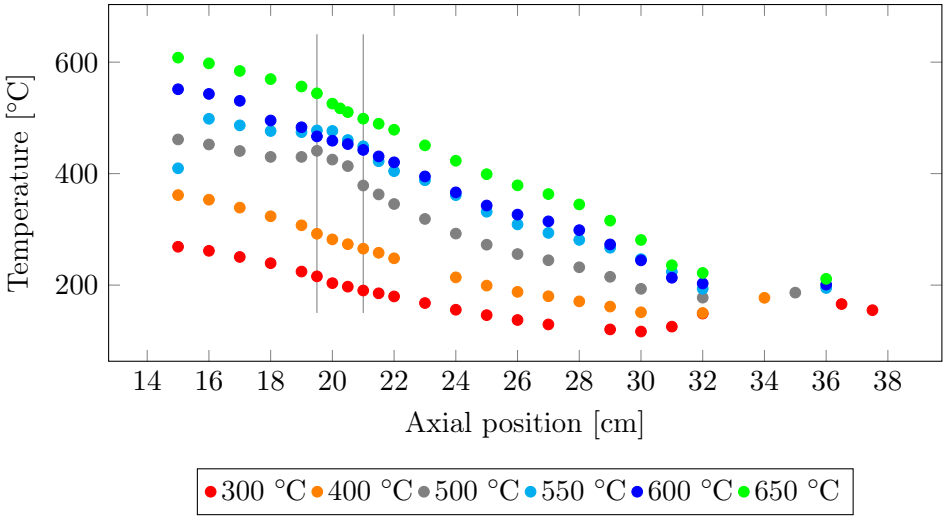

Figure 6.12 – Temperature profiles obtained for different temperatures (300, 400, 500, 550, 600 and 650 °C) changes with a total flow of 250 NmL/ min with reference feed composition, table 5.5. Gray lines indicate start and stop of catalyst bed.

Mass balances for carbon, oxygen and hydrogen were performed too show

deviations in the results and thus verify the conversion and selectivity data. The mass balance for carbon, hydrogen and oxygen is shown as a function of TOS and given in figure 6.13.

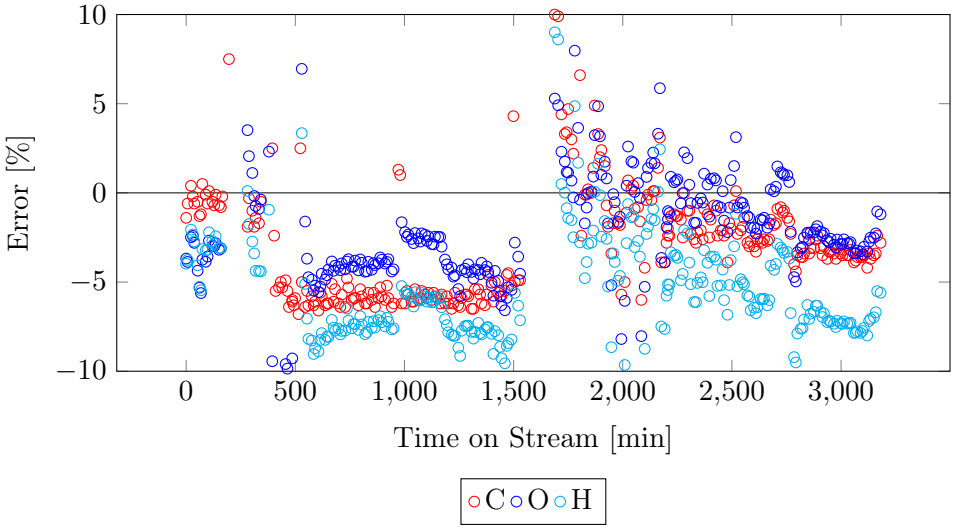

Figure 6.13 – Error in mass balance for for carbon, oxygen and hydrogen as a function of time on stream.

Test 2 - Effects of variations of gas compositions and improving temperature gradient in oven, using circulated air.

Test 2 was performed to determine effects of different oxygen concentrations and to improve the large observed temperature gradient in the reactor oven, shown in appendix G. Table 6.4 gives changes in conditions during the experiment. A pipeline with air was implemented in reactor oven. For the test it was seen that oxygen is fully consumed as soon as some reactions take place.

Methanol conversion, carbon and hydrogen products selectivities were calculated as shown in appendix F. The selectivity is based on total methanol conversion, thus including all products formed. The results were plotted as a function of TOS and given in figure 6.14.

Figure 6.14 shows that an increase in temperature from 300 °C to 500 °C and 550 °C gives an increase in conversion. By reducing the oxygen fraction

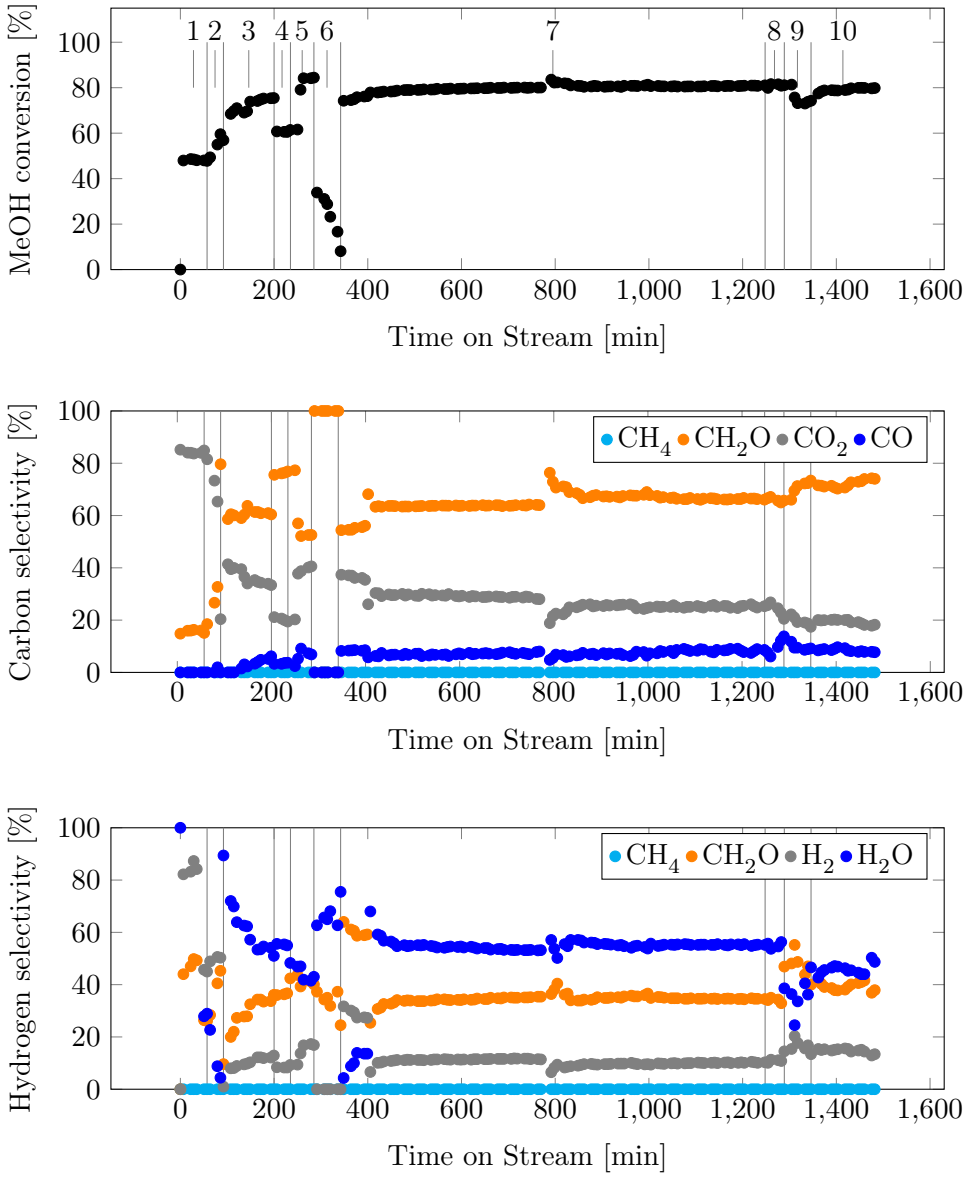

Figure 6.14 – Conversion with carbon and hydrogen selectivities as a function of time on stream. The gray lines indicate when changes are applied to the system. Section 1, 2 and 3 increase in temperature respectively to 300, 500 and 550 °C, Section 3 is reducing oxygen with 50 %, section 4 oxygen concentration is increased with 30 %, Section 5 is reducing oxygen to 0 %, section 6 is ordinary feed composition on 550 °C, section 7 is turning air circulation in reactor oven, section 8 and 9 is increasing gas flow to respectively 375 NmL/ min and 500 NmL/ min.

Table 6.4 – Time sections with changes is gas compositions, oven temperature, total flow and circulated air in oven for Test 2. Reference feed is given in table 5.5.

Section	TOS [min]	Gas composition	Temperature [°C]	Total flow [NmL/ min]	Air circulation
1	0-57	Reference	300	250	Off
2	57-92	Reference	500	250	Off
3	92-200	Reference	550	250	Off
4	200-235	50% O_2	550	250	Off
5	235-285	+30% O_2	550	250	Off
6	285-342	No O_2	550	250	Off
7	342-1248	Reference	550	250	Off
8	1248-1289	Reference	550	250	On
9	1289-1346	Reference	550	375	On
10	1346-1482	Reference	550	500	On

the methanol conversion is reduced, by removing all oxygen the conversion of methanol also is reduced to 34 % and continues to decrease. Increasing oxygen gives an increase in conversion. Turning the air circulation does not give an obvious change in the conversion. Increasing the gas flow gives a decrease in conversion before it stabilizing at the same conversion.

A decrease in oxygen concentration gives an increase in formaldehyde selectivity and a drop in carbon dioxide selectivity. An increase in oxygen concentration reduces formaldehyde selectivity, and increase of carbon monoxide and carbon dioxide selectivity, zero oxygen gives high formaldehyde selectivity but no conversion. Turning on air circulation in the oven gives no apparent change in formaldehyde selectivity, while a small decrease in carbon dioxide selectivity and a small increase in carbon monoxide selectivity. An increase in flow gives a higher formaldehyde selectivity.

After test 1 and prior to this test the catalyst was exposed to a low nitrogen flow for 11 days at ambient temperature, before the reactor oven was heated to 300 °C over night. When feed was applied it was seen catalytic activity already at 300 °C. This is interesting to the fact that fresh catalyst did not show any activity before passing 500 °C. The activity at lower temperatures indicate that some changes have happened to the silver catalyst or the α-alumina. However, the α-alumina should be stable up to 1400 K [20].

The conversion was at 50 % while selectivity towards carbon dioxide was at 83 % and formaldehyde at 16 %. The suspected active phase for

silver catalyst is the different adsorbed oxygen species where O_α is active in complete oxidation of methanol to carbon dioxide and water and also formation of formaldehyde. At lower temperatures the O_α is predominate on the silver surface.

Figure 6.15 illustrates the temperature profile for reduced oxygen (halved amount), increased amount of oxygen (30 %) and no oxygen compared to ordinary composition of oxygen. Temperature in reactor is highly dependent of the oxygen concentration.

Reducing the oxygen fraction to 50 % reduces the methanol conversion to 60 % and give an increase in formaldehyde selectivity to 76 % and a reduction in carbon dioxide. The reactions that uses the oxygen are all exothermic, by reducing the oxygen amount it is expected to lead to a lower temperature in the reactor, which is seen in the temperature profile, figure 6.15. As these reactions have to share the oxygen it is expected to lower carbon dioxide formation.

By removing all oxygen, the methanol conversion drops from 84 % to 34 % and continue to decrease. The test should have been performed at a longer interval as it would be interesting to seen if the conversion would completely stop or that some methanol would decompose to formaldehyde and hydrogen gas. As the conversion did not stop during the 0 % oxygen period there might be some adsorbed oxygen at the silver surface and some bulk dissolved oxygen. This shows the importance of some oxygen in the reaction. Little or none methanol dehydrogenation takes place when no oxygen is supplied. The subsequent analyses shows a higher selectivity towards CO_2 at the start, which is decreased in the following analyses. Qian et. al. [21] found that the dynamic equilibrium development of oxygen species were interrupted by treatment with nitrogen gas. Resulting in O_α is the predominant specie up to 30 min after reintroducing oxygen. This effect is seen at the start of each test as CO_2 selectivity is gradually decreased at the start for each new experiment.

When the reaction was supplied with more oxygen the temperature in the catalyst bed was increased, as expected. The formaldehyde selectivity was decreased and carbon monoxide and carbon dioxide was increased.

By adding the air circulation, the temperature increased in the bed area, the temperature gradient was improved. Turning on air circulation gives no apparent change in formaldehyde selectivity, while a small decrease in carbon dioxide selectivity and a small increase in carbon monoxide selectivity. As seen earlier is the carbon monoxide selectivity influenced by the temperature and an increase in the temperature will favor formation of carbon monoxide. The conversion is not influenced by the increase in bed temperature.

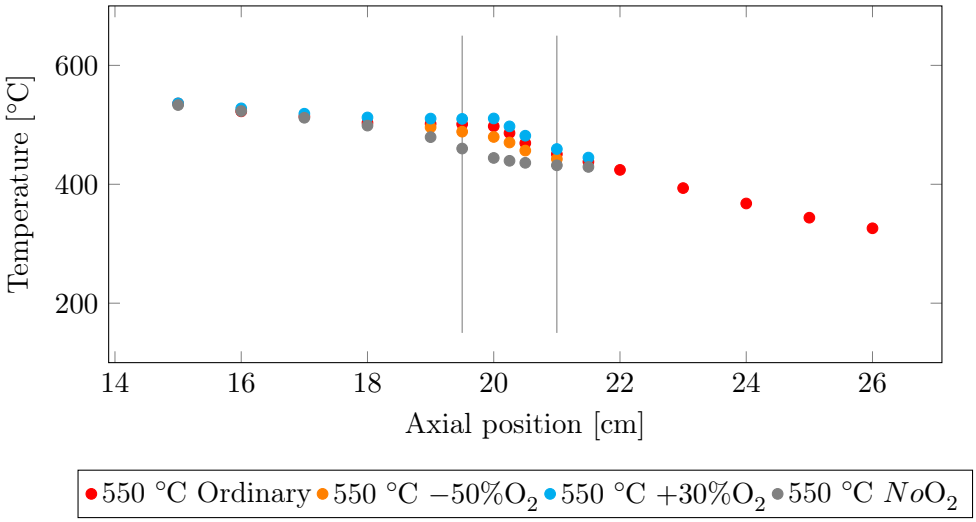

Figure 6.15 – Temperature profile for the oxygen analysis. Different amounts of oxygen were analyzed, reduced (halved), increased (30 %) and no oxygen (w/o) compared to the original oxygen composition.

Increasing the total gas flow to 375 NmL/ min gives a decrease in conversion to 73 % while increasing to 500 NmL/ min the conversion is increased to 79 %. When increasing the total gas flow to 500 NmL/ min the bed temperature also increases, which is expected due the increased amount of reactants. There is seen an increase formaldehyde selectivity and lower carbon monoxide and carbon dioxide selectivity. Increasing the total gas flow will also give lower residence time resulting in less time for the formaldehyde at the catalyst, this might indicate that the silver catalyst also plays a role in decomposing formaldehyde. That silver is active for complete oxidation of formaldehyde is also suggested by literature [22].

During the overnight run, where no changes was applied to the system, there is a jump in formaldehyde selectivity and a drop in the remaining carbon products. The formaldehyde selectivity is also stabilizing at a higher level than before the spike. This effect is unknown but it might be due to accumulation of water and formaldehyde at the spike was an increase in these compounds. This might be due to a cold spot in the system leading to condensation of products in the lines before analyses. However, it does not seem to affect the overall trend.

Mass balances for carbon, oxygen and hydrogen were performed too show deviations in the results and thus assess the accuracy of the conversion and

selectivity data. The mass balance for carbon, hydrogen and oxygen is shown as a function of TOS and given in figure 6.16.

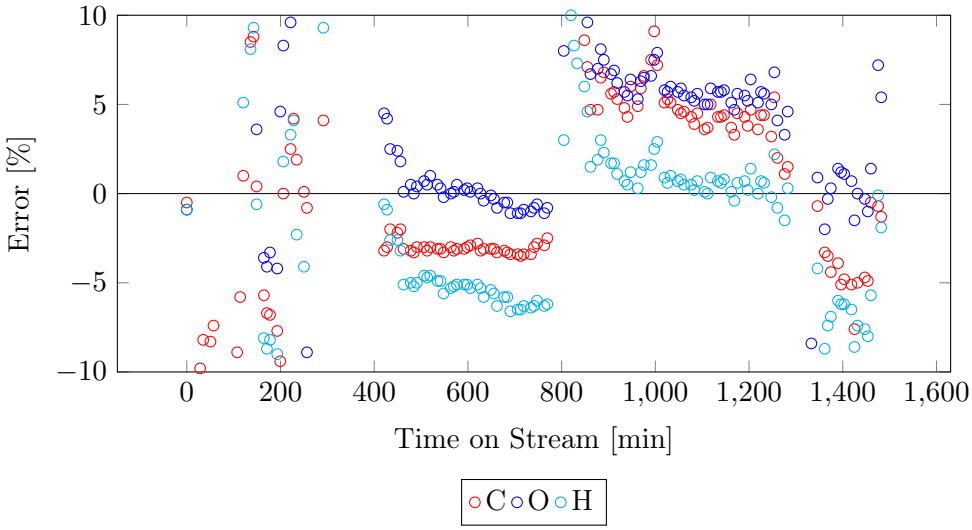

Figure 6.16 – Error in mass balance for for carbon, oxygen and hydrogen as a function of time on stream.

Figure 6.16 show an error in carbon mass balance from 400 to 800 min to be stabilizing at -2 %, before it jumps to +5 % at 850 min without any changes to the system. The error in oxygen mass balance is stabilizing at 0 % before it does a jump to +6 % at 850 min without any changes to the system. The error in hydrogen mass balance is quite similar to the mass balance of oxygen but at a different scale.

Test 3- Use of silicon carbide to fill void space.

Due to the reactor design and reactor oven there is a large heated volume in the reactor, a large heated volume increases the extent of gas phase reactions. Test 3 was performed to try exclude the suspected gas phase reactions. A 1 mm particle size silicon carbide, a supposed inert material, was added prior to the catalyst bed to reduce the void space. Table 6.5 gives changes in the experiment.

Methanol conversion, carbon and hydrogen products selectivities were calculated as shown in appendix F. The selectivity is based on total methanol conversion, thus including all products formed. The results were plotted as a function of TOS and given in figure 6.17.

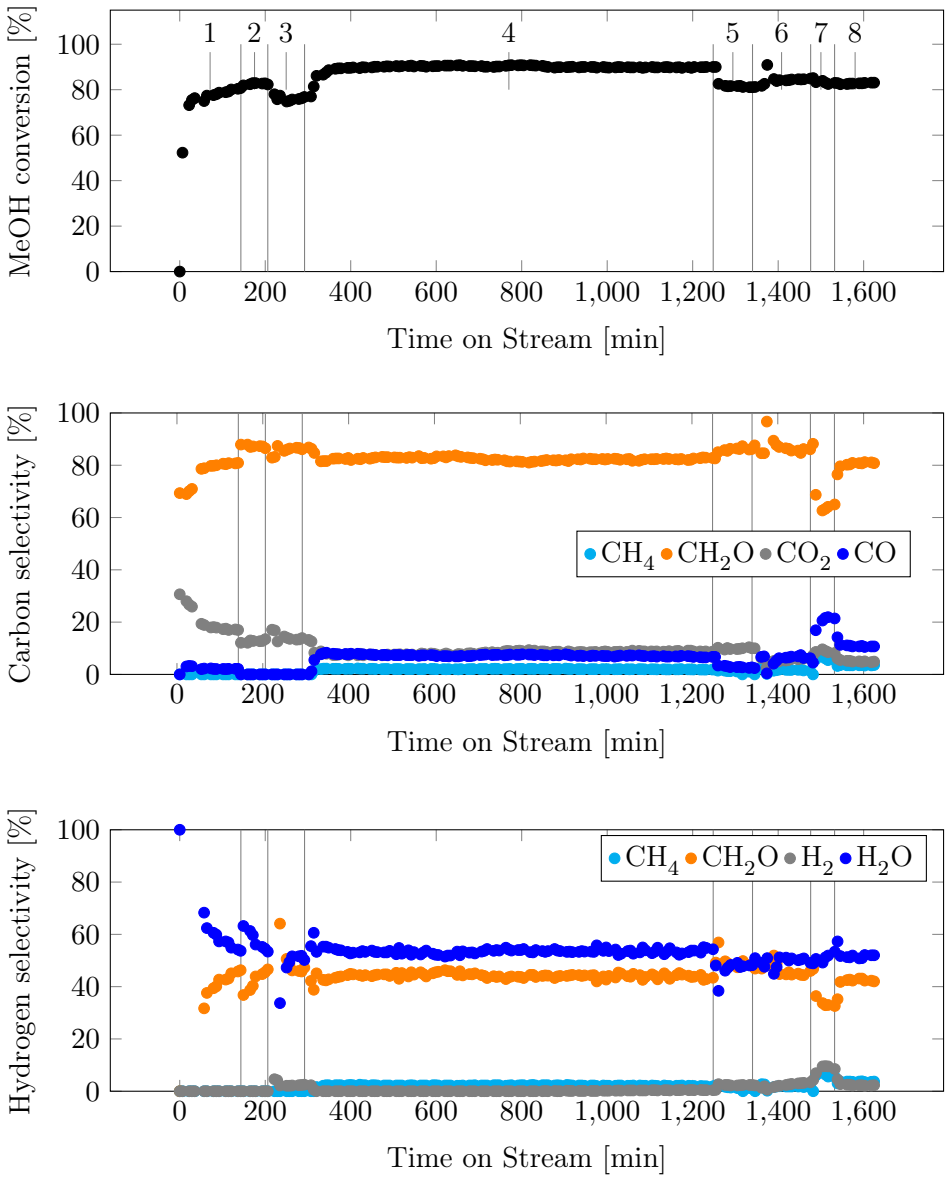

Figure 6.17 – Conversion with carbon and hydrogen selectivities as a function of time on stream. The gray lines indicate when changes are applied to the system. Section 1 is reference composition with total flow of 250 NmL/ min. Section 2 increase in nitrogen flow so total flow is 500 NmL/ min thus reducing concentration of other components by 50 %. Section 3 is reference gas composition at 500 NmL/ min. Section 4 is reducing flow to 250 NmL/ min and increase of temperature to 600 °C. Section 5 is increase total flow to 500 NmL/ min. Section 6 is turning on air circulation, section 7 is increase of temperature to 650 °C, section 8 is the air flow turned off.

Table 6.5 – Time sections with changes is gas compositions, oven temperature, total flow and circulated air in oven for Test 3. Reference feed is given in table 5.5

Section	TOS [min]	Gas composition	Temperature [°C]	Total flow [NmL/ min]	Air circulation
1	0-143	Reference	550	250	Off
2	143-206	Diluted with N_2	550	500	Off
3	206-292	Reference	550	500	Off
4	292-1248	Reference	600	250	Off
5	1248-1340	Reference	600	500	Off
6	1340-1476	Reference	600	500	On
7	1476-1517	Reference	650	500	On
8	1517-1625	Reference	650	500	Off

Section 4 in test 1, section 7 in test 2 and section 1 in test 3 have the same conditions except for added SiC in test 3. The conversion lies around 80 % for each test, but there is seen an increase in selectivity towards formaldehyde with SiC, the selectivity is 80 %. Without SiC a formaldehyde selectivity is around 70 %. The CO_2 selectivity is 19 % with SiC and around 30 % without. H_2 selectivity is 0 % for test 3 while for test 1 and 2 it is at 10 %. This points towards less use of present oxygen to complete combustion for test 3 so hydrogen react with oxygen to form water. Comparing section 5 in test 1 and section 4 in test 3, there is seen a increase in conversion from 85 % to 90 % with SiC. For test 1 the gas phase reactions takes over with 85 % selectivity towards CO while test 3 have 85 % selectivity towards formaldehyde.

By increasing the reactant concentration the conversion gets a slight decrease. Air circulation in the reactor oven gives a slight increase in conversion and. Figure 6.17 shows that increasing flow gives higher formaldehyde selectivity and reduces carbon monoxide and carbon dioxide. An increase in reactant concentration gives little to non change. Turning on air circulation lower carbon dioxide while increasing carbon monoxide, formaldehyde is unchanged, by turning up oven temperature to 650 °C gives a sudden drop in formaldehyde selectivity before it stabilizing at 80 %.

Due to the reactor design and reactor oven there is a large heated volume in the reactor prior to the catalyst bed, this increase the chance of gas phase reactions. To try counter this, α-silicon carbide was added in the heated volume prior to the catalyst bed. Silicon carbide is a stable material

and is supposed to be an inert material at these conditions. The silicon carbide removes the heated volume and increases the linear flow, this will suppress gas phase reactions. In addition silicon carbide give more surface, more surface will contribute to terminate the free radical gas phase driven reactions [23].

By adding silicon carbide, higher temperature made it possible to reach higher conversions, selectivity towards formaldehyde and higher catalyst bed temperatures without gas phase reactions. By reducing the heated volume, the residence time in heated are is significant reduced. This will reduce the decompositions and gas phase reactions. However, what is also interesting is the increase in conversion, which can indicate a more controlled reaction at the catalyst bed and reduced gas phase reactions. Reduction of void space took the reaction one step closer to the industrially performance. Formaldehyde selectivity and conversion is close but carbon monoxide selectivity is still to high.

Mass balances for carbon, oxygen and hydrogen were performed too show deviations in the results and thus verify the conversion and selectivity data. The mass balance for carbon, hydrogen and oxygen is shown as a function of TOS and given in figure 6.18.

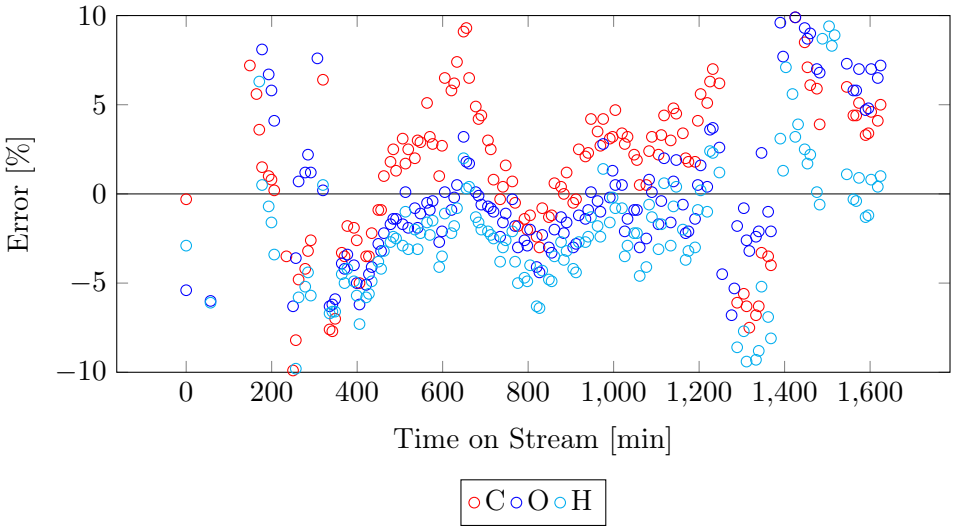

Figure 6.18 – Error in mass balance for for carbon, oxygen and hydrogen as a function of time on stream.

Test 4 – Reference test, using empty reactor without silicon carbide.

A reference test was performed with an empty reactor and with previous used temperatures, flows and gas compositions to get comparable results with tests using the particular silver catalyst. Table 6.6 gives temperature, flow and gas compositions at certain times.

Table 6.6 – Time sections with changes is gas compositions, oven temperature and total flow for test 4. Reference feed is given in table 5.5.

Section	TOS [min]	Gas composition	Temperature [°C]	Total flow [NmL/ min]
1	0-35	Reference	300	250
2	35-134	Reference	550	250
3	134-246	Reference	600	250
4	246-308	Feed off overnight	600	0
5	308-358	Reference	600	500
6	358-476	Reference	650	500
7	476-539	Reference	650	250

Methanol conversion, carbon and hydrogen products selectivities was calculated as shown in appendix F . The selectivity is based on total methanol conversion, thus including all products formed. The results were plotted as a function of TOS and given in figure 6.19.

Figure 6.19 shows no gas phase activity in the empty reactor before a reactor temperature of 600 °C. This indicates that the gas phase reaction is negligible at oven setpoint temperature of 550 °C. Increasing the total flow to 500 NmL/ min gives a slight decrease in conversion. Increasing the temperature to 650 °C gives a small increase in conversion and decreasing the total flow to 250 NmL/ min also give a higher conversion. The major product for the gas phase is carbon monoxide with a selectivity at 84 %. The selectivities did not show a significant change when changing the residence time and temperature, but there is seen a lower conversion at lower residence times. Experiments in an empty reactor will have different residence time and temperature profiles compared to experiments with catalyst and especially when using SiC filling.

It would be interesting to do the same experiments with both silicon carbide and alumina, to verify that these actual have no catalytic property in this synthesis.

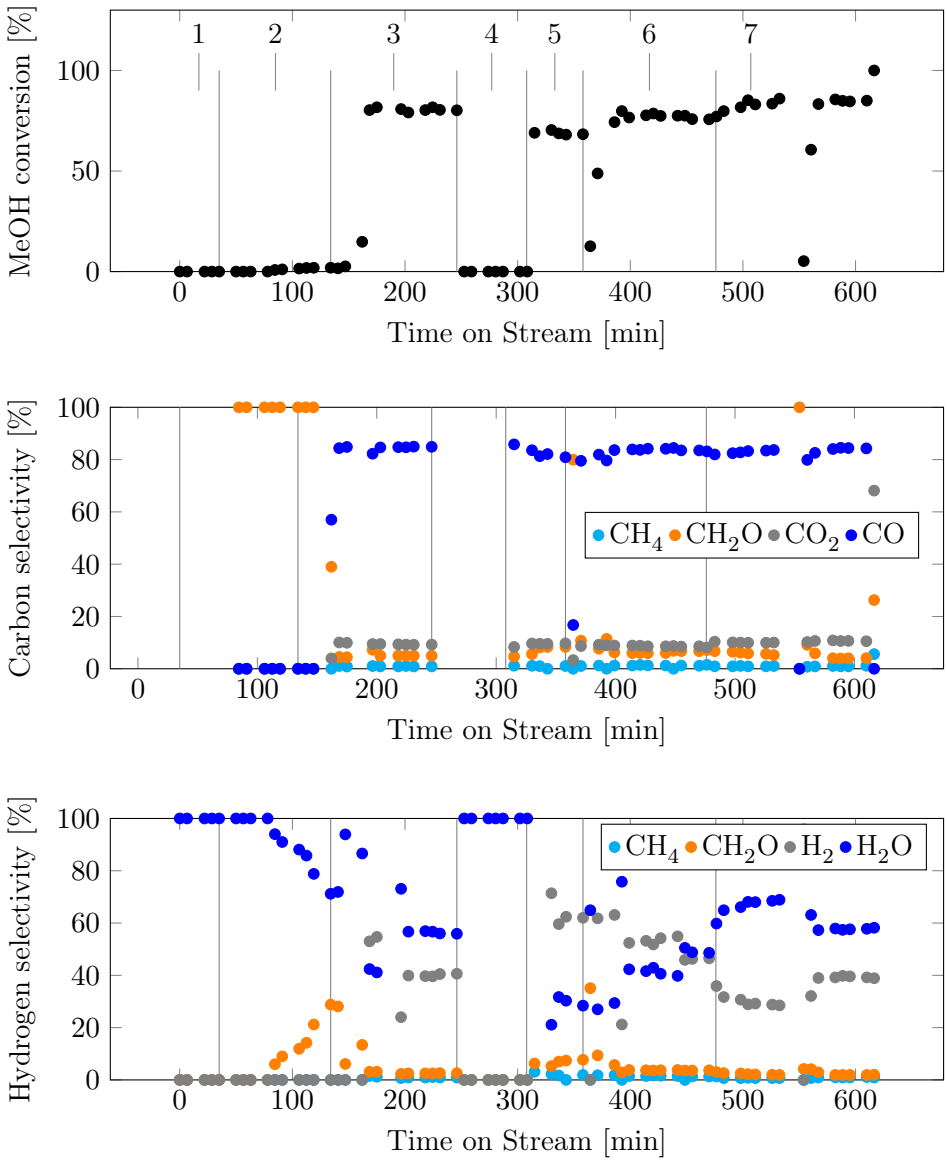

Figure 6.19 – Conversion with carbon and hydrogen selectivities as a function of time on stream. The gray lines indicate when changes are applied to the system. Section 1 is 300 °C with reference feed composition and 250 NmL/ min. Section 2 is increase of temperature to 550 °C, section 3 is increase temperature to 600 °C, section 4 feed is shut off, section 5 is 600 °C with a total flow of 500 NmL/ min, section 6 is increase of temperature to 650 °C, section 7 is 650 °C and total flow of 250 NmL/ min. Reference feed is shown in table 5.5.

Mass balances for carbon, oxygen and hydrogen were performed too show deviations in the results and thus verify the conversion and selectivity data. The mass balance for carbon, hydrogen and oxygen is shown as a function of TOS and given in figure 6.20.

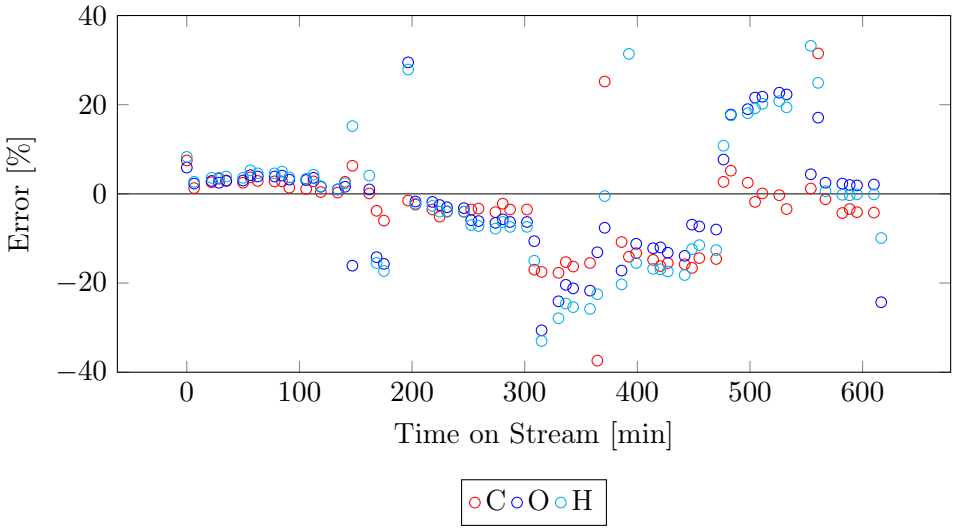

Figure 6.20 – Error in mass balance for for carbon, oxygen and hydrogen as a function of time on stream.

Mass balances

The error is deviations from what is fed and what is measured, this is highly dependent on the feed analysis. Since the mass balances illustrate large deviations, calculations based on formed products and not data from feed analysis were preferred. The mass balances are based on calculations including feed analysis data and offers another interpretation of the data. When basing the conversion and selectivity on formed products, the assumption being that the same amount of C/H produced is the same as in the feed, the mass balances are forced to equal zero. By presenting the mass balances based on different calculations, it provides a more nuanced illustration. An interpretation of the mass balances could show that the product based calculations were a bold choice. However, the feed analysis can not be deemed reliable so a conclusion based on the mass balances should be avoided.

A negative error in the mass balances is a general trend for the analysis. The oxygen mass balance is less stable than the carbon mass balance but

at lower values. The hydrogen mass balance is quite similar to the mass balance of oxygen but at a factor 2, a first suspicion is that the analysis of water might be the reason. Because of the complications with water and GC, this is a probable cause.

Additionally, it is important to remember that the GC value for formaldehyde is adjusted to 90 % of the original value, due to lack of proper calibration. This will influence the mass balances and may not be the optimal and most likely not the correct value for formaldehyde.

External mass transfer limitations

Three experiments were performed with a total gas flow respectively 250 NmL/ min, 500 NmL/ min and 863 NmL/ min. The conversion and calculated observed reaction rate is presented in figures 6.21 - 6.23 as a function of time on stream. This to show the effect over time on the calculated reaction rate.

Changing the total flow from 250 to 500 NmL/ min total flow the temperature increased in the reactor. This was expected as the supplied reactants were doubled and the conversion was not halved. The oxidation reactions are exothermic so the increase in temperature is due to more reactants is converted. For the experiment at 863 NmL/ min the temperature was changed but a continues decrease happened over night resulting in a 12 °C lower bed temperature. The effect is seen both in the conversion and the reaction rate.

The observed reaction rate, bed temperature and conversion used from figures 6.21 - 6.23 are shown in table 6.7.

Table 6.7 – Total flow, reaction rate, conversion and bed temperature for the external mass transfer limitation experiment.

Total flow NmL/ min	Reaction rate [mmol g^{-1} s^{-1}]	Conversion [%]	Bed temperature [°C]
250	46.3	67.5	444.2
500	67.5	56.2	442.8
863	45.7	18.5	430.2

The reaction rate peaks at 500 NmL/ min then the reaction rate decreases at higher flow. The boundary layer will decrease as the velocity across the catalyst particle is increased, this will result in an increase in mass transfer. If the reaction is limited by external mass transfer the reaction rate should increase, if the reaction is limited by kinetics the reaction

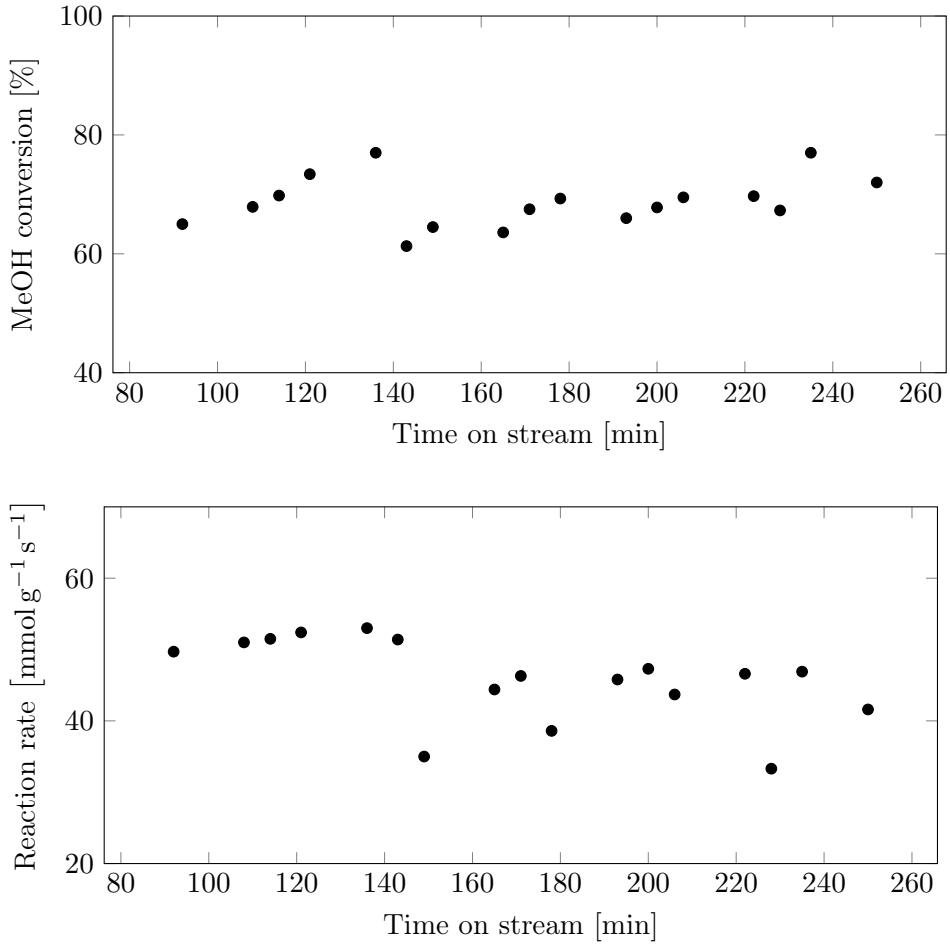

Figure 6.21 – Methanol conversion and observed reaction rate as a function of time on stream with a total flow 250 NmL/ min.

rate should not change due to increase in mass transfer. A reduction in reaction rate is not expected when the flow increases. The reaction is relatively far from equilibrium conditions and no deactivation is observed at earlier tests, it is believed that the reduction of reaction rate at the highest flow is due to the decrease in bed temperature. The decrease in temperature is most likely a combination of decrease in amount reactants converted and also convection effects from the colder feed. To determine the temperature effect is an activation energy is needed. From literature [24] where activation energy for oxidation of methanol over a Ag (110) facet is proposed to be in

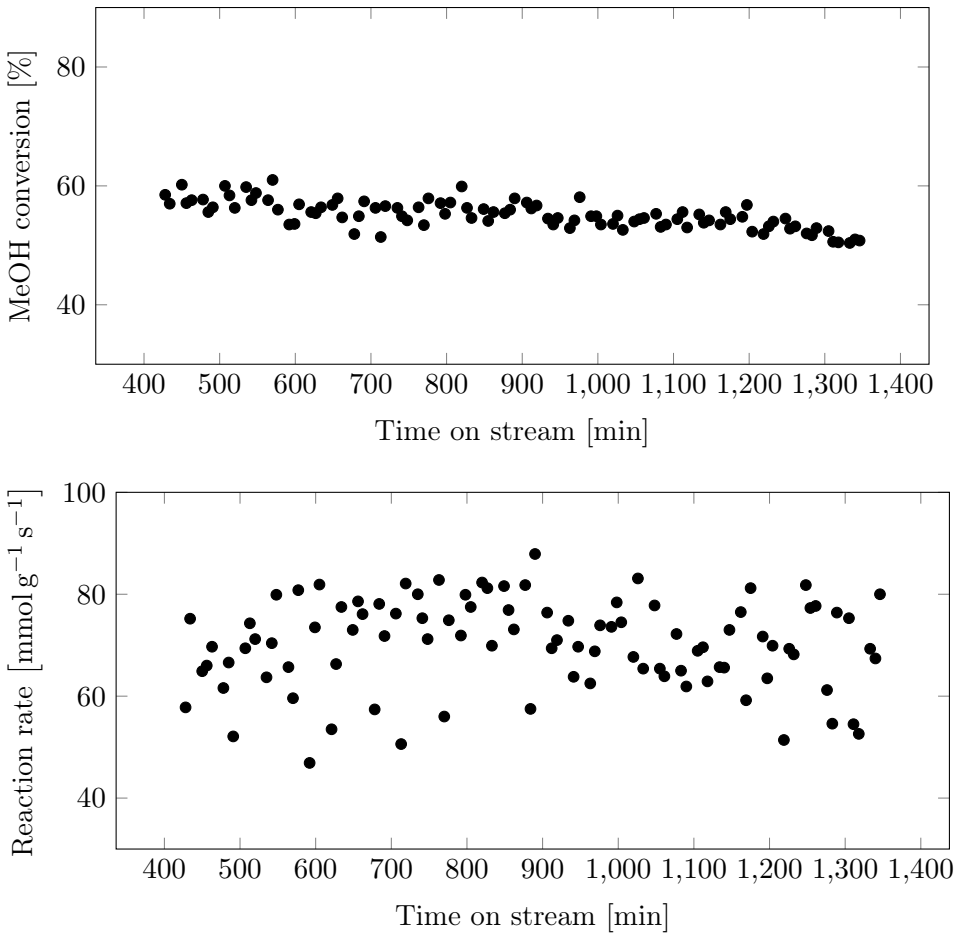

Figure 6.22 – Methanol conversion and observed reaction rate as a function of time on stream with a total flow 500 NmL/ min.

range of 61-82 kJ mol^{-1}. Using an activation energy of 80 kJ mol^{-1} with the bed temperature in equation 2.8, derived form Arrhenius equation, gives a rate constant ratio $\frac{k_{863}}{k_{500}} = 0.78$. This give an adjusted observed reaction rate of 59 mmol g^{-1} s^{-1} for the experiment with 863 NmL/ min.

For the experiments at 250 and 500 NmL/ min the reaction rate is increased by almost a factor 2, this can indicate that there are mass transfer limitations in that area. However, the increase in rate can also be due to concentration effect. There is a significant difference in conversion, thus resulting in a higher reactant concentration for every point in the reactor for

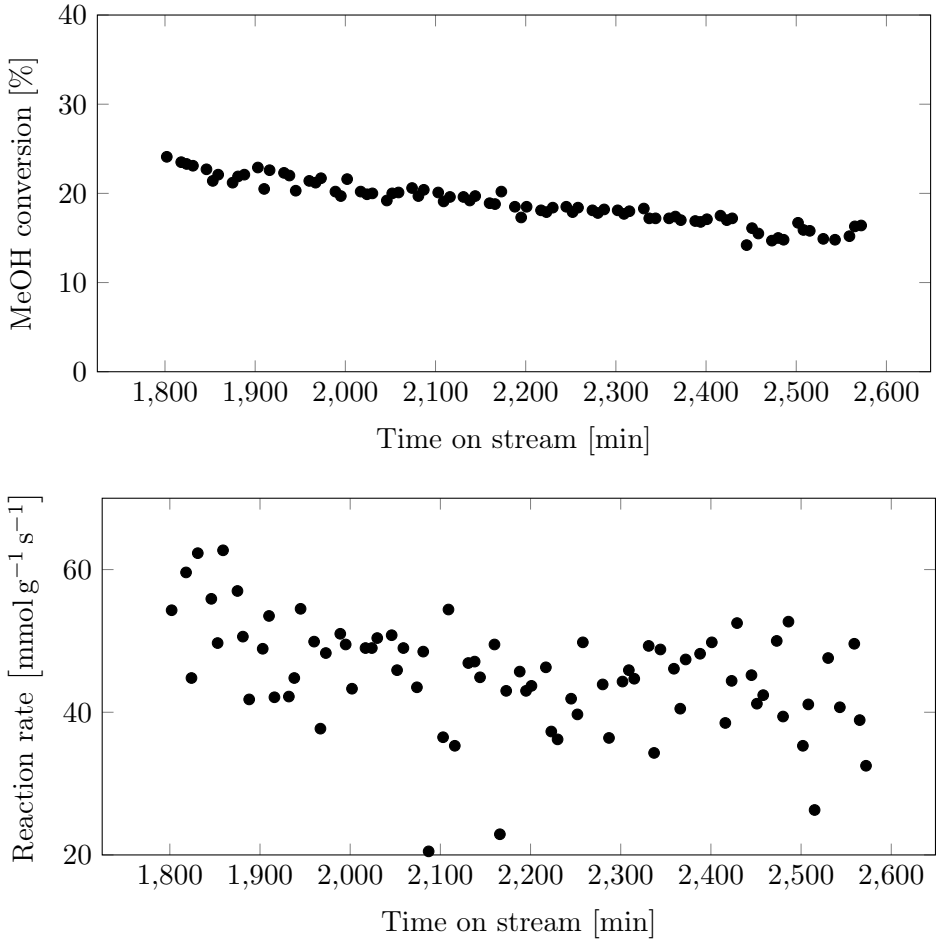

Figure 6.23 – Methanol conversion and observed reaction rate as a function of time on stream with a total flow 863 NmL/ min.

the run at 500 NmL/ min than for 250 NmL/ min.

The reaction rate is calculated using the assumption that differential conditions is present. However, for the experiments with total flow 250 and 500 NmL/ min the conversion is high. Even the experiment at the highest flow, the conditions is at borderline to be differential conditions. This indicate that the calculated reaction rate might be inaccurate.

The feed analyses shows a change in reactant concentration when applying change to the flow. This gives an uncertainty in the partial pressures of reactants which directly affects the reaction rate.

Determination of possible mass transfer limitation need a better temperature control, this requires probably as further dilution of the catalyst and low conversion that it is not necessarily relevant. The conditions at the catalyst surface is not necessary the same for a reaction with low conversion as with high conversion. Investigate at low conversions might not be representative to the reaction at higher conversions.

Chapter 7

Conclusion

Fresh and plant exposed electrolytic silver particles have been characterized in order to establish a suitable characterization toolbox and identify possible changes in the structures and composition during use.

Images from SEM reveal a massive change in the topology from the terrace structure in the fresh catalyst. Exceeding Tammann temperature will lead to formation of surface with lowest energy configuration dependent on conditions. There are observed pinholes created in the structure of the plant exposed catalyst which is believed are due to water formation in bulk. Structures similar to carbon deposits were also observed.

The XRD diffraction shows a higher intensity but no changes in lattice structure for the plant exposed catalyst compared to the fresh catalyst. An increase in crystallite size is observed. No sign of silver oxide peaks in the silver catalyst were apparent.

The quantitative XRF analyses gave 100 % silver for both the fresh and the plant exposed catalyst.

Temperature programmed analysis in the thermo gravimetric analysis with heating in synthetic air did not show any apparent weight change. Silver is a low surface area specie, if the oxide layer is only at the surface the TGA instrument might not be able to detect the weight change. Heating and cooling silver oxide confirmed that there was no mass change after reduction of silver oxide to silver.

The nitrogen adsorption did not yield any results for the surface area. Using krypton as adsorption gas is better for low surface area compounds.

The oxygen chemisorption did not give any reliable results. As silver has low surface area, increasing the amount sample used for the analysis might

enhance the result.

Creating a rig suitable for MTF synthesis is not a trivial, an ideal setup is not necessary a practically one so compromises were made. Several aspect as calibration of MFC, LFC and CG, stabilized vaporization, avoiding condensation in pipelines, accurate temperature and control, and suppressing gas phase reactions have been taken into consideration.

The significance of temperature and flow is seen in both selectivity and conversion. The methanol conversion was highly dependent on oxygen concentration.

The reactor oven had a large temperature gradient and a large heated area, the reactor had a large heated void volume. This promotes gas phase reactions. By reducing the void space in the reactor with SiC the conversion and selectivities is approaching industrially performance. The conversion reached was 90 % with 84 % formaldehyde selectivity 7.5 % selectivity to CO and CO and 1 % selectivity towards CH_4. This was achieved using a feed composition of 8 % methanol 11 % water 3 % oxygen and 78 % nitrogen with 250 NmL/ min and 600 °C oven set point temperature.

Both reactor design and oven design should be reconsidered combined with reducing the pipelines in the rig.

From the experiment testing for external mass transfer it is hard to determine if there are any external mass transfer limitations. The temperature effect on reaction rate is exponential resulting in deviation from isotherm conditions have effect on kinetic data. The decrease in reaction rate from 500 to 863 NmL/ min might be due to the temperature decrease. The increase in reaction from 250 NmL/ min to 500 NmL/ min might indicate that there are mass transfer limitations in that area, or can be a concentration effect due to lower conversion at 500 NmL/ min.

Chapter 8

Suggestions for Further Work

In this section, some suggestions and ideas for further work are presented.

The different adsorbed oxygen species is of particular interest for the selectivity towards formaldehyde. For the characterization part it might be interesting to go into more advanced characterization methods to better get an understanding of the roll of the different adsorbed oxygen species. Different methods to quench the silver so the adsorbed oxygen species can be investigated. Studies like raman, temperature programed desorption (TPD) and X-ray photoelectron spectroscopy (XPS) can be used to characterize the oxygen species.

The experimental setup has room for several improvements, but one of the key components, the reactor, gives several opportunities. The current design results in a large temperature gradient and significant amount of homogeneous gas phase reaction and formaldehyde decomposition. By experimenting with different kinds of heating and reactor design, optimization of diameter and volume (increasing linear gas velocity), reaching industrial conditions may be achievable.

Another significant issue with the experimental setup are the large amount of volume in pipelines from the reactor to the GC. By decreasing the amount of pipelines, a more accurate analysis with less room for defects can be achieved. To analyze the unidentified peaks, a combination of GC and MS could be of interest.

Changing the flow and pressure controllers into low pressure favorable controllers, would ensure a more stable feed composition. With new con-

trollers a more stable calibration for the relevant gases and liquids could be achieved. A more profound calibration of formaldehyde is required. The formalin solution need to be stable, to ensure accuracy. With an accurate calibration for formaldehyde, a review of the calculations should be performed.

Only one reference test was performed, an empty reactor without silicon carbide. Silicon carbide, a supposedly inert material, need to analyzed and a reference test performed with an empty reactor containing silicon carbide. The inert properties of α-alumina should also be tested. Additionally, feed analyses run over a longer period could have positive influence on the calculations. Running the different analyses over longer periods should be performed for all the different compositions and variables tested.

Bibliography

[1] Sharon S Chadwick. Ullmann's encyclopedia of industrial chemistry. *Reference Services Review*, 16(4):31–34, 1988.

[2] Geoffrey I. N. Waterhouse, Graham A. Bowmaker, and James B. Metson. Mechanism and active sites for the partial oxidation of methanol to formaldehyde over an electrolytic silver catalyst. *Applied Catalysis A: General*, 265(1):85–101, 2004.

[3] Geoffrey I. N. Waterhouse, Graham A. Bowmaker, and James B. Metson. Oxygen chemisorption on an electrolytic silver catalyst: a combined tpd and raman spectroscopic study. *Applied Surface Science*, 214(1–4):36–51, 2003.

[4] H.S. Fogler. *Elements of Chemical Reaction Engineering*. Elements of Chemical Reaction Engineering. Prentice Hall PTR, 2006.

[5] Steven Zumdahl and Donald J DeCoste. *Chemical principles*. Nelson Education, 2012.

[6] Ib Chorkendorff and Johannes W Niemantsverdriet. *Concepts of modern catalysis and kinetics*. John Wiley & Sons, 2007.

[7] Michel Che and Jacques C. Vedrine. *Characterization of Solid Materials and Heterogeneous Catalysts : From Structure to Surface Reactivity*. Wiley, Hoboken, 2013.

[8] J. Hjelen. *Scanning elektron-mikroskopi*. SINTEF, Avdeling for metallurgi, Metallurgisk Institutt NTH, 1986.

[9] Scanning electron microscopy, 2015.

[10] J. W. Niemantsverdriet. *Spectroscopy in Catalysis*. Wiley, Hoboken, 2007.

[11] M. Steven Shackley. *An Introduction to X-Ray Fluorescence (XRF) Analysis in Archaeology*, book section 2, pages 7–44. Springer New York, 2011.

[12] Burkhard Beckhoff, Birgit Kanngießer, Norbert Langhoff, Reiner Wedell, and Helmut Wolff. *Handbook of practical X-ray fluorescence analysis*. Springer Science & Business Media, 2007.

[13] Paul A Webb. Introduction to chemical adsorption analytical techniques and their applications to catalysis. *Micromeritics Instrument Corp. Technical Publications*, 2003.

[14] Eugene F Barry and Robert L Grob. *Columns for gas chromatography: performance and selection*. John Wiley & Sons, 2007.

[15] Agilent Technologies. Cp-sil 5 cb, 2016.

[16] Alltech Associates. *Quantitation Methods in Gas Chromatography*. In GC Education, 1998.

[17] X. Bao, G. Lehmpfuhl, G. Weinberg, R. Schlögl, and G. Ertl. Variation of the morphology of silver surfaces by thermal and catalytic etching. *Journal of the Chemical Society, Faraday Transactions*, 88(6):865–872, 1992.

[18] Eberhardt R Kuhn. Water injections in gc-how wet can you get? *LC GC NORTH AMERICA*, 20(5):474–478, 2002.

[19] Alejandro Montoya and Brian S Haynes. Dft analysis of the reaction paths of formaldehyde decomposition on silver. *The Journal of Physical Chemistry A*, 113(28):8125–8131, 2009.

[20] Claudio Morterra and Giuliana Magnacca. A case study: surface chemistry and surface structure of catalytic aluminas, as studied by vibrational spectroscopy of adsorbed species. *Catalysis Today*, 27(3):497–532, 1996.

[21] Min Qian, M.A Liauw, and G Emig. Formaldehyde synthesis from methanol over silver catalysts. *Applied Catalysis A: General*, 238(2):211 – 222, 2003.

[22] Xingfu Tang, Junli Chen, Yonggang Li, Yong Li, Yide Xu, and Wenjie Shen. Complete oxidation of formaldehyde over ag/mno x–ceo 2 catalysts. *Chemical Engineering Journal*, 118(1):119–125, 2006.

[23] T.R. Baldwin, R. Burch, G.D. Squire, and S.C. Tsang. Influence of homogeneous gas phase reactions in the partial oxidation of methane to methanol and formaldehyde in the presence of oxide catalysts. *Applied Catalysis*, 74(1):137 – 152, 1991.

[24] Israel E Wachs and Robert J Madix. The oxidation of methanol on a silver (110) catalyst. *Surface Science*, 76(2):531–558, 1978.

Appendix A

Health, Safety and Environment

Detaljert Risikorapport

ID	1731	**Status**	**Dato**
Risikoområde	Risikovurdering: Helse, miljø og sikkerhet (HMS)	Opprettet	11.11.2015
Opprettet av	Cristian Ledesma Rodriguez	Vurdering startet	11.11.2015
Ansvarlig	Vegard Naustdal	Tiltak besluttet	
		Avsluttet	

CAT, Master student 2016, Vegard Andreas Naustdal

Gyldig i perioden:

10/7/2015 - 7/1/2016

Sted:

3 - Gløshaugen / 315 - Kjemi 5

Mål / hensikt

This risk assessment contains all the activities that the master student Vegard Naustdal will perform in the labs of the Catalysis group.

Bakgrunn

[Ingen registreringer]

Beskrivelse og avgrensninger

Forutsetninger, antakelser og forenklinger

[Ingen registreringer]

Vedlegg

[Ingen registreringer]

Referanser

[Ingen registreringer]

Oppsummering, resultat og endelig vurdering

I oppsummeringen presenteres en oversikt over farer og uønskede hendelser, samt resultat for det enkelte konsekvensområdet.

Farekilde: **Use of silver catalyst**

Uønsket hendelse: **Inhalation of small particles**

Konsekvensområde:		
	Helse	Risiko før tiltak: Risiko etter tiltak:
	Ytre miljø	Risiko før tiltak: Risiko etter tiltak:
	Materielle verdier	Risiko før tiltak: Risiko etter tiltak:

Uønsket hendelse: **Spill on skin**

Konsekvensområde:		
	Helse	Risiko før tiltak: Risiko etter tiltak:
	Ytre miljø	Risiko før tiltak: Risiko etter tiltak:
	Materielle verdier	Risiko før tiltak: Risiko etter tiltak:

Farekilde: **Use of high temperature furnace**

Uønsket hendelse: **Electric shock**

Konsekvensområde:		
	Helse	Risiko før tiltak: Risiko etter tiltak:
	Ytre miljø	Risiko før tiltak: Risiko etter tiltak:
	Materielle verdier	Risiko før tiltak: Risiko etter tiltak:

Uønsket hendelse: **Uncontrolled heating**

Konsekvensområde:		
	Helse	Risiko før tiltak: Risiko etter tiltak:
	Ytre miljø	Risiko før tiltak: Risiko etter tiltak:
	Materielle verdier	Risiko før tiltak: Risiko etter tiltak:

Uønsket hendelse: **Fire**

Konsekvensområde:		
	Helse	Risiko før tiltak: Risiko etter tiltak:
	Ytre miljø	Risiko før tiltak: Risiko etter tiltak:
	Materielle verdier	Risiko før tiltak: Risiko etter tiltak:

Uønsket hendelse: **Burn damage**

Konsekvensområde:		
	Helse	Risiko før tiltak: Risiko etter tiltak:
	Ytre miljø	Risiko før tiltak: Risiko etter tiltak:
	Materielle verdier	Risiko før tiltak: Risiko etter tiltak:

Farekilde: **Use of non-toxic compressed gases**

Uønsket hendelse: **Uncontrolled expansion and depleiton of O2**

Konsekvensområde:		
Helse	Risiko før tiltak:	Risiko etter tiltak:
Ytre miljø	Risiko før tiltak:	Risiko etter tiltak:
Materielle verdier	Risiko før tiltak:	Risiko etter tiltak:

Uønsket hendelse: **Gas leakage**

Konsekvensområde:		
Helse	Risiko før tiltak:	Risiko etter tiltak:
Ytre miljø	Risiko før tiltak:	Risiko etter tiltak:
Materielle verdier	Risiko før tiltak:	Risiko etter tiltak:

Farekilde: **Use of flammable gases**

Uønsket hendelse: **Gas leakage**

Konsekvensområde:		
Helse	Risiko før tiltak:	Risiko etter tiltak:
Ytre miljø	Risiko før tiltak:	Risiko etter tiltak:
Materielle verdier	Risiko før tiltak:	Risiko etter tiltak:

Uønsket hendelse: **Fire, explosion**

Konsekvensområde:		
Helse	Risiko før tiltak:	Risiko etter tiltak:
Ytre miljø	Risiko før tiltak:	Risiko etter tiltak:
Materielle verdier	Risiko før tiltak:	Risiko etter tiltak:

Farekilde: **Use of compressed gas**

Uønsket hendelse: **uncontrolled expansion**

Konsekvensområde:		
Helse	Risiko før tiltak:	Risiko etter tiltak:
Ytre miljø	Risiko før tiltak:	Risiko etter tiltak:
Materielle verdier	Risiko før tiltak:	Risiko etter tiltak:

Uønsket hendelse: **Depletion of O2**

Konsekvensområde:		
Helse	Risiko før tiltak:	Risiko etter tiltak:
Ytre miljø	Risiko før tiltak:	Risiko etter tiltak:
Materielle verdier	Risiko før tiltak:	Risiko etter tiltak:

Farekilde: **Use of flammable gas**

Uønsket hendelse: **Small gas leak**

Konsekvensområde:		
	Helse	Risiko før tiltak: Risiko etter tiltak:
	Ytre miljø	Risiko før tiltak: Risiko etter tiltak:
	Materielle verdier	Risiko før tiltak: Risiko etter tiltak:

Uønsket hendelse: **Big gas leak**

Konsekvensområde:		
	Helse	Risiko før tiltak: Risiko etter tiltak:
	Ytre miljø	Risiko før tiltak: Risiko etter tiltak:
	Materielle verdier	Risiko før tiltak: Risiko etter tiltak:

Farekilde: **Use of toxic gas**

Uønsket hendelse: **toxic if swallowed, in contact with skin or if inhaled**

Konsekvensområde:		
	Helse	Risiko før tiltak: Risiko etter tiltak:
	Ytre miljø	Risiko før tiltak: Risiko etter tiltak:
	Materielle verdier	Risiko før tiltak: Risiko etter tiltak:

Farekilde: **Use of electrical furnace**

Uønsket hendelse: **Electric shock**

Konsekvensområde:		
	Helse	Risiko før tiltak: Risiko etter tiltak:
	Ytre miljø	Risiko før tiltak: Risiko etter tiltak:
	Materielle verdier	Risiko før tiltak: Risiko etter tiltak:

Uønsket hendelse: **Uncontrolled heating**

Konsekvensområde:		
	Helse	Risiko før tiltak: Risiko etter tiltak:
	Ytre miljø	Risiko før tiltak: Risiko etter tiltak:
	Materielle verdier	Risiko før tiltak: Risiko etter tiltak:

Uønsket hendelse: **Fire**

Konsekvensområde:		
	Helse	Risiko før tiltak: Risiko etter tiltak:
	Ytre miljø	Risiko før tiltak: Risiko etter tiltak:
	Materielle verdier	Risiko før tiltak: Risiko etter tiltak:

Farekilde: **Use of electrical furnace**

Uønsket hendelse: **Burn damage**

Konsekvensområde:		
Helse	Risiko før tiltak:	Risiko etter tiltak:
Ytre miljø	Risiko før tiltak:	Risiko etter tiltak:
Materielle verdier	Risiko før tiltak:	Risiko etter tiltak:

Endelig vurdering

Oversikt involverte enheter og personell

En risikovurdering kan gjelde for en, eller flere enheter i organisasjonen. Denne oversikten presenterer involverte enheter og personell for gjeldende risikovurdering.

Enhet /-er risikovurderingen omfatter

- Institutt for kjemisk prosessteknologi

Deltakere

Cristian Ledesma Rodriguez
Karin Wiggen Dragsten
Hilde Johnsen Venvik
Jia Yang
Rune Lødeng
Stine Lervold

Lesere

[Ingen registreringer]

Andre involverte/interessenter

[Ingen registreringer]

Følgende akseptkriterier er besluttet for risikoområdet Risikovurdering: Helse, miljø og sikkerhet (HMS):

Helse	Materielle verdier	Omdømme	Ytre miljø
			

Oversikt over eksisterende, relevante tiltak som er hensyntatt i risikovurderingen

I tabellen under presenteres eksisterende tiltak som er hensyntatt ved vurdering av sannsynlighet og konsekvens for aktuelle uønskede hendelser.

Farekilde	Uønsket hendelse	Tiltak hensyntatt ved vurdering
Use of silver catalyst	Inhalation of small particles	HSE documentation
	Inhalation of small particles	Working alone regulations at NTNU
	Inhalation of small particles	Personal protective equipment
	Inhalation of small particles	Ventilation
	Spill on skin	HSE documentation
	Spill on skin	Working alone regulations at NTNU
	Spill on skin	Personal protective equipment
	Spill on skin	Ventilation
Use of high temperature furnace	Electric shock	HSE documentation
	Electric shock	Working alone regulations at NTNU
	Electric shock	Personal protective equipment
	Uncontrolled heating	HSE documentation
	Uncontrolled heating	Working alone regulations at NTNU
	Uncontrolled heating	Personal protective equipment
	Fire	HSE documentation
	Fire	Working alone regulations at NTNU
	Fire	Personal protective equipment
	Fire	Ventilation
	Fire	Gas detectors
	Burn damage	HSE documentation
	Burn damage	Working alone regulations at NTNU
	Burn damage	Personal protective equipment
	Burn damage	Ventilation
Use of non-toxic compressed gases	Uncontrolled expansion and depleiton of O2	HSE documentation
	Uncontrolled expansion and depleiton of O2	Working alone regulations at NTNU
	Uncontrolled expansion and depleiton of O2	Personal protective equipment
	Uncontrolled expansion and depleiton of O2	Ventilation
	Uncontrolled expansion and depleiton of O2	Leak test procedure
	Uncontrolled expansion and depleiton of O2	Installation and change of gas cylinders
	Gas leakage	HSE documentation
	Gas leakage	Working alone regulations at NTNU
	Gas leakage	Personal protective equipment

Use of non-toxic compressed gases	Gas leakage	Ventilation
	Gas leakage	Leak test procedure
	Gas leakage	Installation and change of gas cylinders
Use of flammable gases	Gas leakage	HSE documentation
	Gas leakage	Working alone regulations at NTNU
	Gas leakage	Personal protective equipment
	Gas leakage	Ventilation
	Gas leakage	Gas detectors
	Gas leakage	Leak test procedure
	Gas leakage	Installation and change of gas cylinders
	Fire, explosion	HSE documentation
	Fire, explosion	Working alone regulations at NTNU
	Fire, explosion	Personal protective equipment
	Fire, explosion	Ventilation
	Fire, explosion	Gas detectors
	Fire, explosion	Leak test procedure
	Fire, explosion	Installation and change of gas cylinders
Use of compressed gas	uncontrolled expansion	HSE documentation
	uncontrolled expansion	Working alone regulations at NTNU
	uncontrolled expansion	Ventilation
	uncontrolled expansion	Gas detectors
	uncontrolled expansion	Leak test procedure
	Depletion of O2	HSE documentation
	Depletion of O2	Working alone regulations at NTNU
	Depletion of O2	Ventilation
	Depletion of O2	Gas detectors
	Depletion of O2	Leak test procedure
Use of flammable gas	Small gas leak	HSE documentation
	Small gas leak	Working alone regulations at NTNU
	Small gas leak	Ventilation
	Small gas leak	Gas detectors
	Small gas leak	Leak test procedure
	Big gas leak	Ventilation
	Big gas leak	Gas detectors
	Big gas leak	Leak test procedure
Use of toxic gas	toxic if swallowed, in contact with skin or if inhaled	HSE documentation
	toxic if swallowed, in contact with skin or if inhaled	Working alone regulations at NTNU
	toxic if swallowed, in contact with skin or if inhaled	Personal protective equipment

Use of toxic gas	toxic if swallowed, in contact with skin or if inhaled	Ventilation
	toxic if swallowed, in contact with skin or if inhaled	Gas detectors
	toxic if swallowed, in contact with skin or if inhaled	Leak test procedure
Use of electrical furnace	Electric shock	
	Uncontrolled heating	HSE documentation
	Uncontrolled heating	Working alone regulations at NTNU
	Uncontrolled heating	Ventilation
	Fire	
	Burn damage	

Eksisterende og relevante tiltak med beskrivelse:

HSE documentation

The laboratories have an updated Room Card and the unit 2.4 has a copy of the risk assessment, operating instructions and apparatus card with information regarding safety and information in case of emergency stop.

Different phone numbers are provided to contact in case of emergency.

Working alone regulations at NTNU

NTNU students and employee are not allowed to work alone after 7pm and during the weekends.

Working after 19:00 or in the weekends, you need to be at least 2 in the lab or in the building with regularly check-ups (every 30 minutes). Both of the people needs to have access to the labs

Personal protective equipment

The hall contains googles, other safety measures and a first-aid kit.. There are also gloves, lab coats and more protective equipment available upon request.

Ventilation

The reactor system is installed inside a cabinet with ventilation.

Gas detectors

The cabinet has CO/H2 and CH4/H2 detectors which trigger the alarms in case of leakage. There are portable detectors that must be used during the leak tests before running experiments.

Leak test procedure

Before running experiments, a leak test must be performed following the procedure attached.

Installation and change of gas cylinders

This will be done by authorized personnel only.

Risikoanalyse med vurdering av sannsynlighet og konsekvens

I denne delen av rapporten presenteres detaljer dokumentasjon av de farer, uønskede hendelser og årsaker som er vurdert. Innledningsvis oppsummeres farer med tilhørende uønskede hendelser som er tatt med i vurderingen.

Følgende farer og uønskede hendelser er vurdert i denne risikovurderingen:

- **Use of silver catalyst**
  - Inhalation of small particles
  - Spill on skin
- **Use of high temperature furnace**
  - Electric shock
  - Uncontrolled heating
  - Fire
  - Burn damage
- **Use of non-toxic compressed gases**
  - Uncontrolled expansion and depleiton of O2
  - Gas leakage
- **Use of flammable gases**
  - Gas leakage
  - Fire, explosion
- **Use of compressed gas**
  - uncontrolled expansion
  - Depletion of O2
- **Use of flammable gas**
  - Small gas leak
  - Big gas leak
- **Use of toxic gas**
  - toxic if swallowed, in contact with skin or if inhaled
- **Use of electrical furnace**
  - Electric shock
  - Uncontrolled heating
  - Fire
  - Burn damage

Oversikt over besluttede risikoreduserende tiltak med beskrivelse:

Use of silver catalyst (farekilde)

Use of silver catalyst/Inhalation of small particles (uønsket hendelse)

Samlet sannsynlighet vurdert for hendelsen: Lite sannsynlig (2)

Kommentar til vurdering av sannsynlighet:

[Ingen registreringer]

Vurdering av risiko for følgende konsekvensområde: Helse

Vurdert sannsynlighet (felles for hendelsen): Lite sannsynlig (2)

Vurdert konsekvens: Middels (2)

Kommentar til vurdering av konsekvens:

[Ingen registreringer]

Use of silver catalyst/Spill on skin (uønsket hendelse)

Samlet sannsynlighet vurdert for hendelsen: Svært lite sannsynlig (1)

Kommentar til vurdering av sannsynlighet:

[Ingen registreringer]

Vurdering av risiko for følgende konsekvensområde: Helse

Vurdert sannsynlighet (felles for hendelsen): Svært lite sannsynlig (1)

Vurdert konsekvens: Liten (1)

Kommentar til vurdering av konsekvens:

[Ingen registreringer]

Use of high temperature furnace (farekilde)

Use of high temperature furnace/Electric shock (uønsket hendelse)

Samlet sannsynlighet vurdert for hendelsen: Lite sannsynlig (2)

Kommentar til vurdering av sannsynlighet:

[Ingen registreringer]

Vurdering av risiko for følgende konsekvensområde: Helse

Vurdert sannsynlighet (felles for hendelsen): Lite sannsynlig (2)

Vurdert konsekvens: Middels (2)

Kommentar til vurdering av konsekvens:

[Ingen registreringer]

Use of high temperature furnace/Uncontrolled heating (uønsket hendelse)

Samlet sannsynlighet vurdert for hendelsen: Lite sannsynlig (2)

Kommentar til vurdering av sannsynlighet:

[Ingen registreringer]

Vurdering av risiko for følgende konsekvensområde: Helse

Vurdert sannsynlighet (felles for hendelsen): Lite sannsynlig (2)

Vurdert konsekvens: Liten (1)

Kommentar til vurdering av konsekvens:

[Ingen registreringer]

Use of high temperature furnace/Fire (uønsket hendelse)

Samlet sannsynlighet vurdert for hendelsen: Svært lite sannsynlig (1)

Kommentar til vurdering av sannsynlighet:

[Ingen registreringer]

Vurdering av risiko for følgende konsekvensområde: Helse

Vurdert sannsynlighet (felles for hendelsen): Svært lite sannsynlig (1)

Vurdert konsekvens: Middels (2)

Kommentar til vurdering av konsekvens:

[Ingen registreringer]

Use of high temperature furnace/Burn damage (uønsket hendelse)

Samlet sannsynlighet vurdert for hendelsen: Lite sannsynlig (2)

Kommentar til vurdering av sannsynlighet:

[Ingen registreringer]

Vurdering av risiko for følgende konsekvensområde: Helse

Vurdert sannsynlighet (felles for hendelsen): Lite sannsynlig (2)

Vurdert konsekvens: Middels (2)

Kommentar til vurdering av konsekvens:

[Ingen registreringer]

Use of non-toxic compressed gases (farekilde)

Use of non-toxic compressed gases/Uncontrolled expansion and depleiton of O2 (uønsket hendelse)

Samlet sannsynlighet vurdert for hendelsen: Svært lite sannsynlig (1)

Kommentar til vurdering av sannsynlighet:

[Ingen registreringer]

Vurdering av risiko for følgende konsekvensområde: Helse

Vurdert sannsynlighet (felles for hendelsen): Svært lite sannsynlig (1)

Vurdert konsekvens: Middels (2)

Kommentar til vurdering av konsekvens:

[Ingen registreringer]

Use of non-toxic compressed gases/Gas leakage (uønsket hendelse)

Samlet sannsynlighet vurdert for hendelsen: Sannsynlig (3)

Kommentar til vurdering av sannsynlighet:

[Ingen registreringer]

Vurdering av risiko for følgende konsekvensområde: Helse

Vurdert sannsynlighet (felles for hendelsen): Sannsynlig (3)

Vurdert konsekvens: Liten (1)

Kommentar til vurdering av konsekvens:

[Ingen registreringer]

Use of flammable gases (farekilde)

Use of flammable gases/Gas leakage (uønsket hendelse)

Samlet sannsynlighet vurdert for hendelsen: Lite sannsynlig (2)

Kommentar til vurdering av sannsynlighet:

[Ingen registreringer]

Vurdering av risiko for følgende konsekvensområde: Helse

Vurdert sannsynlighet (felles for hendelsen): Lite sannsynlig (2)

Vurdert konsekvens: Middels (2)

Kommentar til vurdering av konsekvens:

[Ingen registreringer]

Use of flammable gases/Fire, explosion (uønsket hendelse)

Samlet sannsynlighet vurdert for hendelsen: Svært lite sannsynlig (1)

Kommentar til vurdering av sannsynlighet:

[Ingen registreringer]

Vurdering av risiko for følgende konsekvensområde: Helse

Vurdert sannsynlighet (felles for hendelsen): Svært lite sannsynlig (1)

Vurdert konsekvens: Stor (3)

Kommentar til vurdering av konsekvens:

[Ingen registreringer]

Use of compressed gas (farekilde)

Use of compressed gas/uncontrolled expansion (uønsket hendelse)

Samlet sannsynlighet vurdert for hendelsen: Lite sannsynlig (2)

Kommentar til vurdering av sannsynlighet:

Pressure should be relived with care

Vurdering av risiko for følgende konsekvensområde: Helse

Vurdert sannsynlighet (felles for hendelsen): Lite sannsynlig (2)

Vurdert konsekvens: Stor (3)

Kommentar til vurdering av konsekvens:

[Ingen registreringer]

Use of compressed gas/Depletion of O2 (uønsket hendelse)

Samlet sannsynlighet vurdert for hendelsen: Svært lite sannsynlig (1)

Kommentar til vurdering av sannsynlighet:

[Ingen registreringer]

Vurdering av risiko for følgende konsekvensområde: Helse

Vurdert sannsynlighet (felles for hendelsen): Svært lite sannsynlig (1)

Vurdert konsekvens: Stor (3)

Kommentar til vurdering av konsekvens:

[Ingen registreringer]

Use of flammable gas (farekilde)

Use of flammable gas/Small gas leak (uønsket hendelse)

Samlet sannsynlighet vurdert for hendelsen: Sannsynlig (3)

Kommentar til vurdering av sannsynlighet:

[Ingen registreringer]

Vurdering av risiko for følgende konsekvensområde: Helse

Vurdert sannsynlighet (felles for hendelsen): Sannsynlig (3)

Vurdert konsekvens: Liten (1)

Kommentar til vurdering av konsekvens:

[Ingen registreringer]

Use of flammable gas/Big gas leak (uønsket hendelse)

Samlet sannsynlighet vurdert for hendelsen: Svært lite sannsynlig (1)

Kommentar til vurdering av sannsynlighet:

[Ingen registreringer]

Vurdering av risiko for følgende konsekvensområde: Helse

Vurdert sannsynlighet (felles for hendelsen): Svært lite sannsynlig (1)

Vurdert konsekvens: Stor (3)

Kommentar til vurdering av konsekvens:

[Ingen registreringer]

Use of toxic gas (farekilde)

Use of toxic gas/toxic if swallowed, in contact with skin or if inhaled (uønsket hendelse)

Samlet sannsynlighet vurdert for hendelsen: Svært lite sannsynlig (1)

Kommentar til vurdering av sannsynlighet:

[Ingen registreringer]

Vurdering av risiko for følgende konsekvensområde: Helse

Vurdert sannsynlighet (felles for hendelsen): Svært lite sannsynlig (1)

Vurdert konsekvens: Stor (3)

Kommentar til vurdering av konsekvens:

[Ingen registreringer]

Use of electrical furnace (farekilde)

Use of electrical furnace/Electric shock (uønsket hendelse)

Samlet sannsynlighet vurdert for hendelsen: Svært lite sannsynlig (1)

Kommentar til vurdering av sannsynlighet:

keep an eye on the quality of the insulation material.

Vurdering av risiko for følgende konsekvensområde: Helse

Vurdert sannsynlighet (felles for hendelsen): Svært lite sannsynlig (1)

Vurdert konsekvens: Stor (3)

Kommentar til vurdering av konsekvens:

[Ingen registreringer]

Use of electrical furnace/Uncontrolled heating (uønsket hendelse)

Samlet sannsynlighet vurdert for hendelsen: Svært lite sannsynlig (1)

Kommentar til vurdering av sannsynlighet:

[Ingen registreringer]

Vurdering av risiko for følgende konsekvensområde: Helse

Vurdert sannsynlighet (felles for hendelsen): Svært lite sannsynlig (1)

Vurdert konsekvens: Stor (3)

Kommentar til vurdering av konsekvens:

[Ingen registreringer]

Use of electrical furnace/Fire (uønsket hendelse)

Samlet sannsynlighet vurdert for hendelsen: Svært lite sannsynlig (1)

Kommentar til vurdering av sannsynlighet:

[Ingen registreringer]

Vurdering av risiko for følgende konsekvensområde: Helse

Vurdert sannsynlighet (felles for hendelsen): Svært lite sannsynlig (1)

Vurdert konsekvens: Stor (3)

Kommentar til vurdering av konsekvens:

[Ingen registreringer]

Use of electrical furnace/Burn damage (uønsket hendelse)

Samlet sannsynlighet vurdert for hendelsen: Lite sannsynlig (2)

Kommentar til vurdering av sannsynlighet:

[Ingen registreringer]

Vurdering av risiko for følgende konsekvensområde: Helse

Vurdert sannsynlighet (felles for hendelsen): Lite sannsynlig (2)

Vurdert konsekvens: Stor (3)

Kommentar til vurdering av konsekvens:

[Ingen registreringer]

Oversikt over besluttede risikoreduserende tiltak:

Under presenteres en oversikt over risikoreduserende tiltak som skal bidra til å reduseres sannsynlighet og/eller konsekvens for uønskede hendelser.

Oversikt over besluttede risikoreduserende tiltak med beskrivelse:

Appendix B

Calibration of Flow Controllers

The used mass flow controllers were calibrated for synthetic air and nitrogen gas. Two mass flow controllers were used for nitrogen, line 4 with a flow interval 4-200 NmL/ min and line 1 with a flow interval 30-1500 NmL/ min. The calibrations were performed using 0-100 mL bubble flow meter. Figure B.1 shows the calibration.

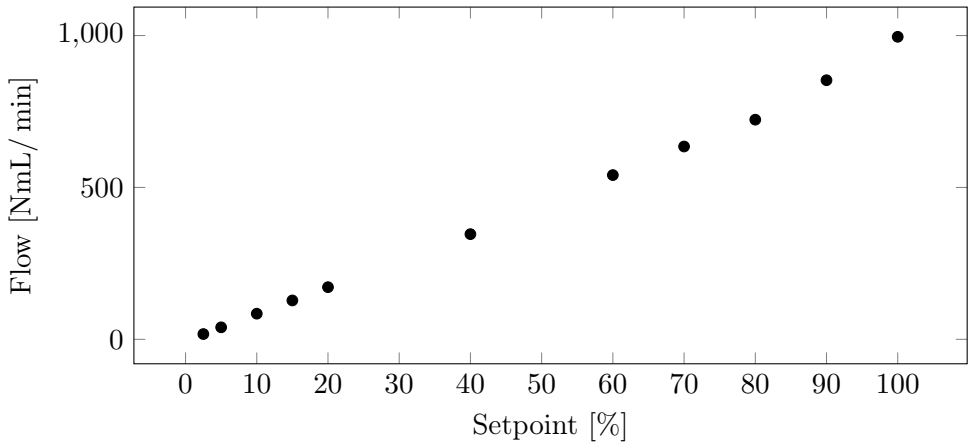

Figure B.1 – Calibration of mass flow controller for synthetic air.

A linear regression line was applied at desired flow range of synthetic air,

given in figure B.2 .

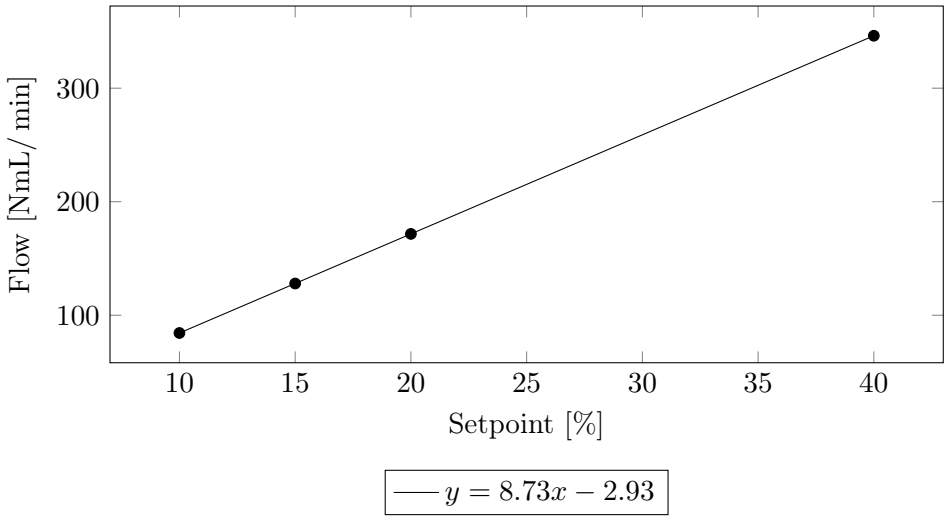

Figure B.2 – Calibration of mass flow controller for synthetic air with linear regression line.

The calibration of mass flow controllers for nitrogen gas line is given in figure B.3 and figure B.4.

The liquid flow controller used was calibrated using needle valve and weighing the collected sample at a time. The methanol/water reservoir was pressurized with 10 bar helium. The calibration is given in figure B.5 .

Due to deviation from linearity at the desired setpoint range, the calibration line was divided in an upper region, figure B.6, and a lower region, figure B.7, within the desired setpoint range.

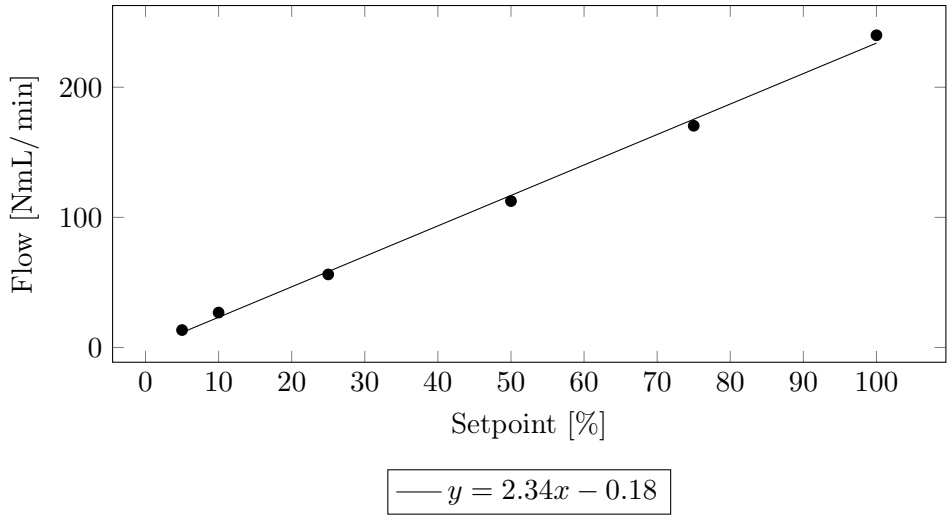

Figure B.3 – Calibration of mass flow controller for nitrogen, line 4, with linear regression line.

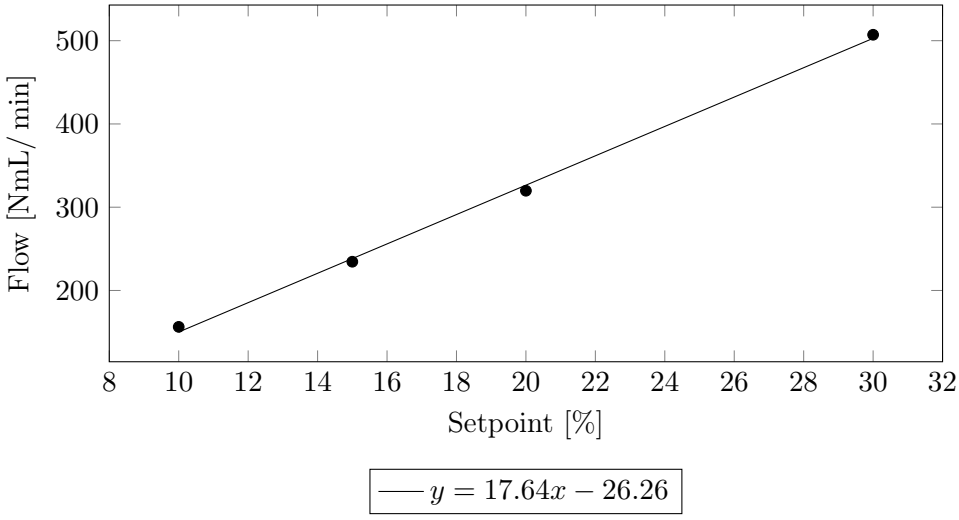

Figure B.4 – Calibration of mass flow controller for nitrogen, line 1, with linear regression line.

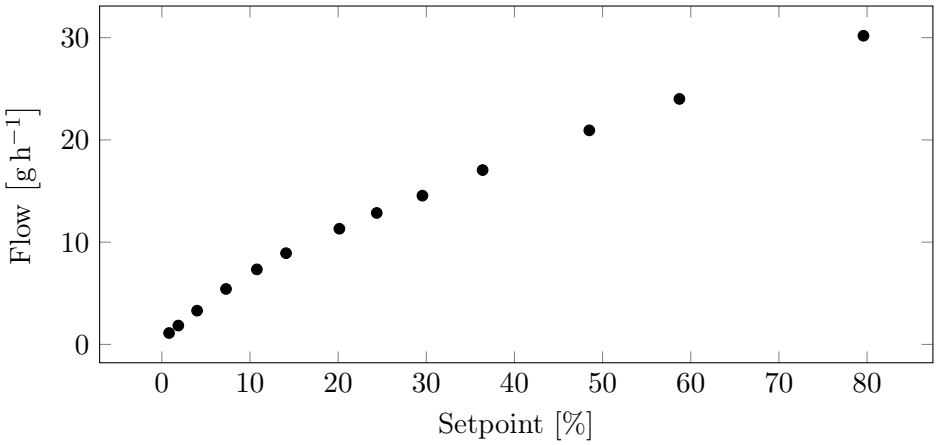

Figure B.5 – Calibration of liquid flow controller for methanol/water mixture.

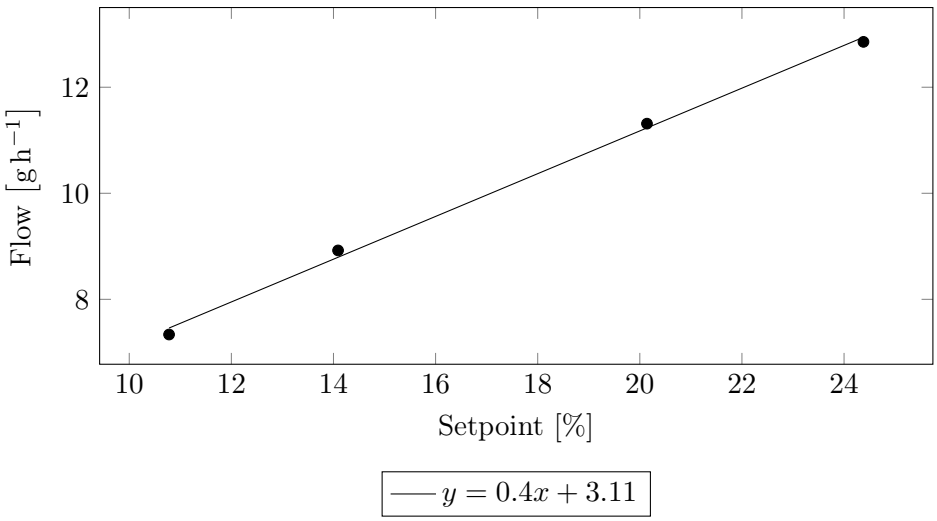

Figure B.6 – Calibration curve for methanol/water mixture at upper region with linear regression line.

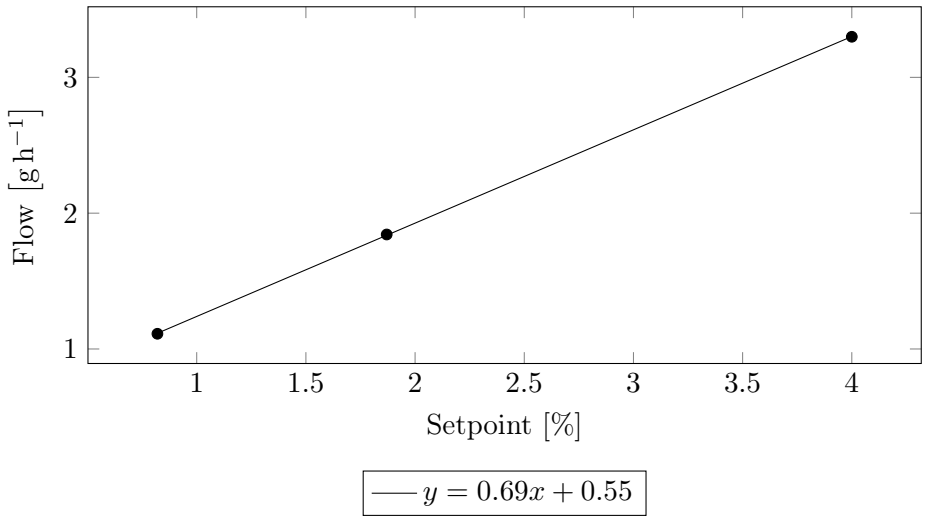

Figure B.7 – Calibration curve for methanol/water mixture at lower region with linear regression line.

Appendix C

Calibration of Gas Chromatograph

The gas chromatograph was calibrated for oxygen gas, hydrogen gas, and carbon monoxide using external standard method. A AlyTech GasMix was used to dilute the given gases in nitrogen gas. Figure C.1, C.2 and C.3 gives respectively calibration curves for oxygen, hydrogen and carbon monoxide gas.

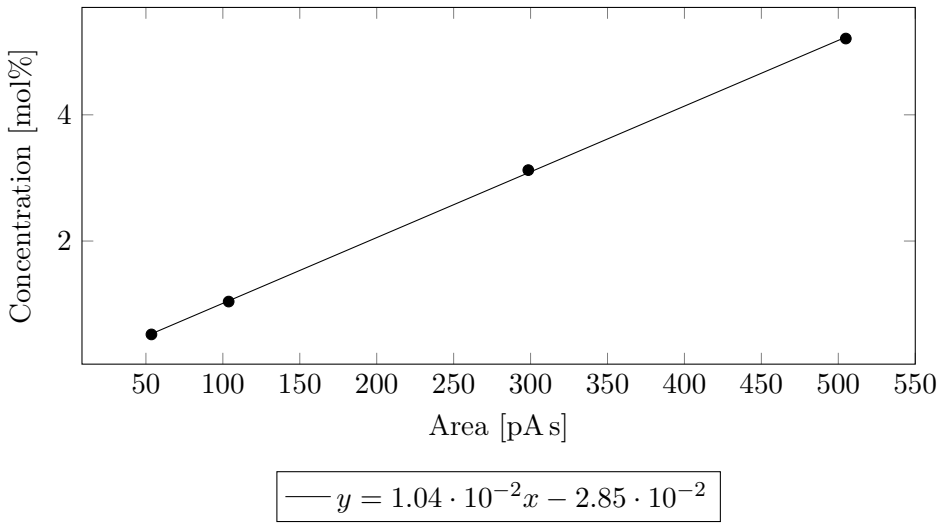

Figure C.1 – Calibration curve for oxygen gas in GC, where concentration is a function of area. Linear regression line is applied.

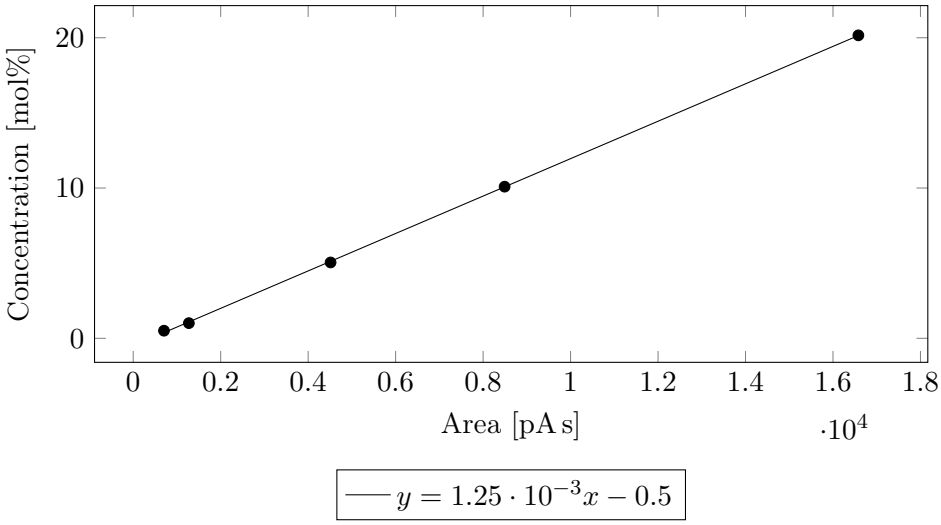

Figure C.2 – Calibration curve for hydrogen gas in GC, where concentration is a function of area. Linear regression line is applied.

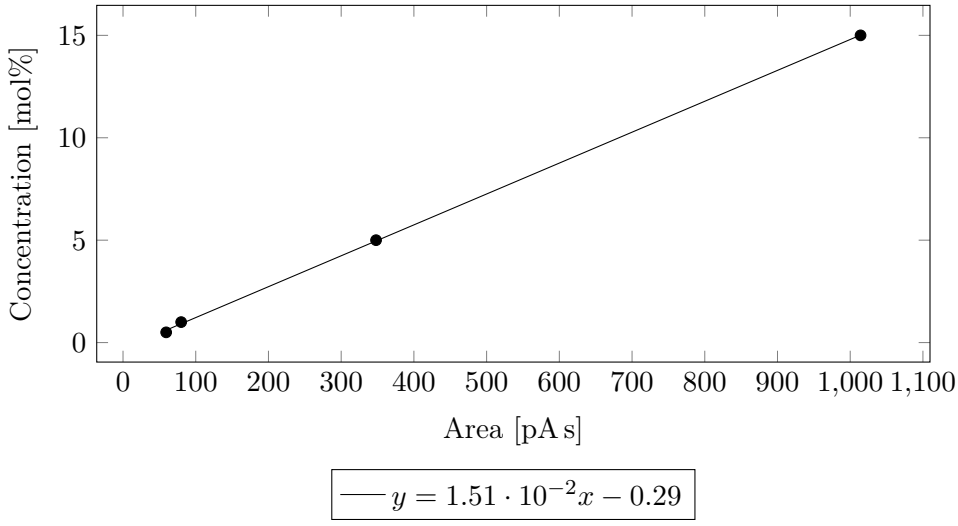

Figure C.3 – Calibration curve for carbon monoxide gas in GC, where concentration is a function of area. Linear regression line is applied.

Appendix D

Feed analyses

For each of different experiments a feed analysis was ran to examine the feed composition. The different feed analysis is presented below in table D.1-D.6 with GC data. Values that stand out are assumed non-reliable, and is not included in the calculations.

Table D.1 – Feed analysis for 250 NmL/ min 8 % MeOH

Date	Seq	MeOH	H_2O	O_2	N_2
17.03.2016	1	8.28	10.64	3.97	80.78
	2	8.28	10.84	3.98	80.89
	3	8.18	10.96	3.98	80.74
	4	8.26	10.59	3.95	80.32
	5	8.27	10.57	3.97	80.63
	6	8.25	10.53	3.99	81.01
	7	8.25	10.10	3.94	80.76
	8	8.20	9.82	3.99	81.48
	Average	8.25	10.58	3.97	80.76
31.03.2016	1	4.04	5.01	4.19	87.24
	2	3.96	4.71	4.23	88.27
	3	3.78	4.99	4.26	88.44
	4	8.01	9.62	3.79	79.07
	5	8.01	9.65	3.84	79.41
	6	7.98	9.70	3.86	79.64
	7	8.02	9.50	3.82	79.41
	8	8.03	9.47	3.84	79.73
	9	8.02	9.46	3.84	80.00
	Average	8.01	9.57	3.83	79.54
05.04.2016	1	7.98	8.87	3.78	79.72
	2	8.08	9.33	3.80	79.48
	3	8.00	9.52	3.79	79.47
	4	8.15	9.79	3.77	78.69
	5	8.23	9.83	3.78	78.63
	6	8.12	9.91	3.79	78.71
	7	8.05	9.97	3.79	78.50
	8	8.07	9.82	3.79	78.79
	9	8.08	9.69	3.80	78.96
	Average	8.08	9.86	3.79	78.71
14.04.2016	8	8.10	9.19	3.77	78.79
	9	10.27	9.56	3.98	82.71
	10	8.26	9.35	3.71	77.83
	11	8.06	9.29	3.76	78.44
	12	8.05	9.34	3.76	78.65
	13	8.12	9.37	3.72	78.05
	14	8.04	9.34	3.76	78.51
	15	8.10	9.48	3.75	78.44
	Average	8.07	9.34	3.76	78.51

Table D.2 – Feed analysis for 500 NmL/ min 8 % MeOH

Date	Seq	MeOH	H_2O	O_2	N_2
07.04.2016	11	9.32	9.19	3.42	79.41
	12	9.41	10.03	3.41	78.68
	13	9.48	12.03	3.30	76.31
	14	9.47	11.50	3.37	77.27
	15	9.46	11.31	3.37	77.61
	16	9.48	11.99	3.32	76.39
	Average	9.47	11.60	3.36	77.49
15.04.2016	1	9.26	10.25	3.49	78.56
	2	9.31	10.21	3.50	78.83
	3	9.25	10.17	3.51	78.93
	4	9.35	10.17	3.47	78.21
	5	9.28	10.16	3.50	78.74
	6	9.30	10.17	3.50	78.79
	Average	9.29	10.17	3.50	78.79

Table D.3 – Feed analysis for 500 NmL/ min 4 % MeOH

Date	Seq	MeOH	H_2O	O_2	N_2
07.04.2016	1	4.66	6.18	1.92	88.49
	2	4.74	6.04	1.91	88.91
	3	4.82	6.25	1.92	88.72
	4	4.98	6.33	1.88	87.69
	5	4.84	6.32	1.91	88.54
	6	4.82	6.34	1.90	88.41
	7	5.02	6.31	1.88	88.04
	8	4.51	6.17	1.91	88.92
	9	4.81	6.66	1.90	88.46
	10	4.86	6.24	1.88	88.32
	Average	4.83	6.33	1.91	88.55

Table D.4 – Feed analysis for 375 NmL/ min 8 % MeOH

Date	Seq	MeOH	H_2O	O_2	N_2
07.04.2016	38	9.72	12.22	3.37	74.51
	39	9.72	12.49	3.35	74.05
	40	9.75	12.46	3.33	73.76
	41	9.74	12.53	3.38	74.25
	42	9.70	12.44	3.38	74.40
	43	9.75	12.53	3.34	73.77
	Average	9.74	12.50	3.36	74.23

Table D.5 – Change of oxygen setpoint

Date	Seq	MeOH	H_2O	O_2	N_2
07.04.2016	44	9.73	12.59	3.39	74.25
	45	9.73	12.54	3.38	74.34
	46	8.35	11.10	3.08	75.65
	47	8.31	10.91	3.13	76.33
	48	8.29	10.90	3.12	76.45
	49	8.41	10.74	3.10	75.95
	50	8.37	10.73	3.13	76.42
	Average	8.74	11.36	3.19	75.63

Table D.6 – Oxygen analyses for different oxygen analyses.

Date	Composition	Seq	MeOH	H_2O	O_2	N_2
07.04.2016	250 NmL/ min	17	8.06	10.04	2.33	78.34
	1/2 O_2	18	8.05	10.00	2.32	78.45
		19	8.07	9.97	2.30	77.98
		20	8.02	9.94	2.32	78.47
		21	8.02	9.96	2.32	78.46
		22	8.04	10.14	2.29	77.88
		23	8.02	10.09	2.32	78.35
		24	8.03	10.14	2.32	78.43
		Average	8.02	10.00	2.32	78.42
	250 NmL/ min.	25	8.12	10.21	4.46	75.24
	+30 % O_2	26	8.08	10.17	4.51	75.75
		27	8.09	10.17	4.52	75.83
		28	8.10	10.45	4.46	75.03
		29	8.08	10.43	4.49	75.33
		30	8.09	10.45	4.50	75.51
		31	8.12	10.46	4.46	75.04
		Average	8.09	10.45	4.51	75.46
	250 NmL/ min	32	8.37	10.55	0.00	79.96
	0 % O_2	33	8.38	10.75	0.00	79.89
		34	8.40	10.80	0.00	79.32
		35	8.38	10.80	0.00	79.78
		36	8.36	10.79	0.00	79.93
		37	8.12	10.72	0.00	80.88
		Average	8.38	10.78	0.00	79.89

Appendix E

Qualitative analysis chart for XRF

The qualitative XRF analyes spectra are given in figure E.1 for the fresh silver catalyst and figure E.2 for the toplayer of the plant exposed catalyst.

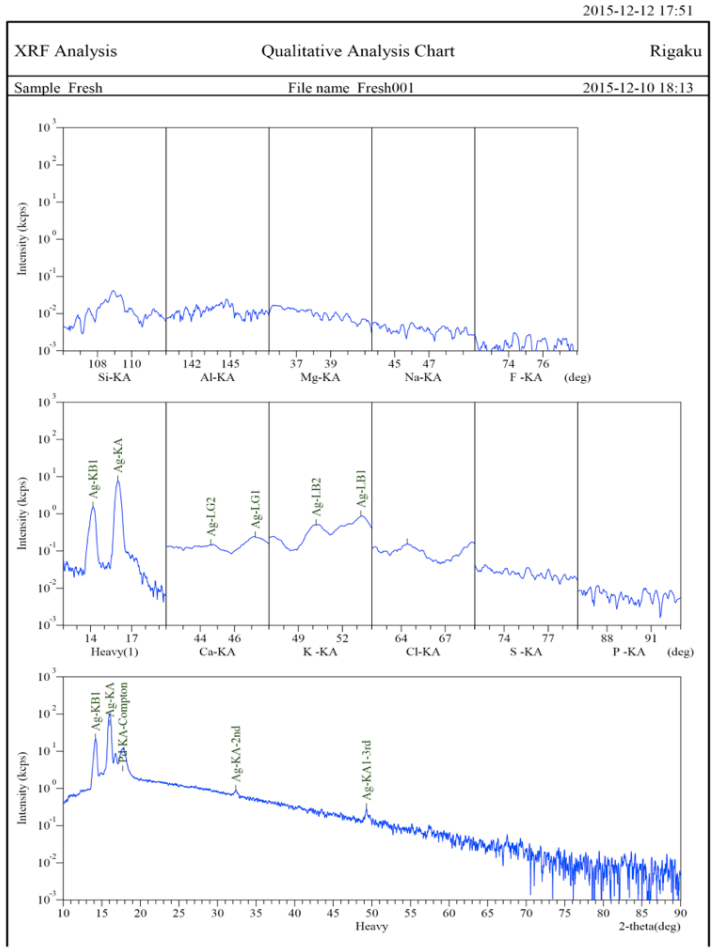

Figure E.1 – XRF spectra for fresh silver catalyst.

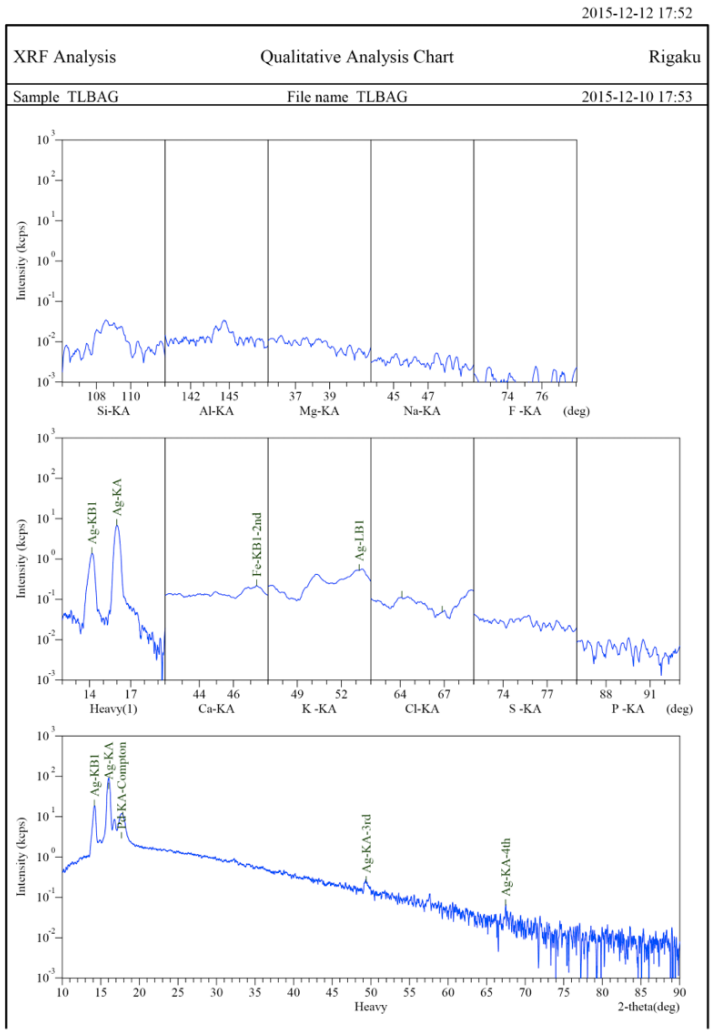

Figure E.2 – XRF spectra for toplayer of the plant exposed silver catalyst.

Appendix F

Calculations

The data from the GC analyses were processed in Excel, applying the formulas presented in the method chapter (see Chapter 5). Presenting all the data would demand tenfold of pages, and it was therefore made a decision to not present the data in Appendix. Instead, a calculation example of conversion, selectivity and mass balance are presented below. By using equation 5.3, two different methods were used to calculate the conversion. First one basing the methanol fraction and total flow in to the feed analysis. As can be seen in equation F.1.

$$X_{MeOH} = \frac{8.25 \cdot 204.91 - 1.89 \cdot 261.65}{8.25 \cdot 240.91} = 0.75 \tag{F.1}$$

The data used in the example is taken from Test 1, with a target value of 8 mol% methanol and 250 NmL/ min total flow. The other method is based on the product distribution, assuming that the same amount of carbon out is the same as in the feed, equation F.2. Calculations are shown in equation F.3 below, with the same data.

$$(F_{Tot} \cdot y_{MeOH})_{in} = (F_{Tot} \cdot \sum y_{c,Tot})_{out} \tag{F.2}$$

$$X_{MeOH} = \frac{(1.89 + 5.06 + 1.71 + 0 + 0) - 1.89}{1.89 + 5.06 + 1.71 + 0 + 0} = 0.78 \tag{F.3}$$

Carbon selectivity may also be calculated through these two methods, and the equations are illustrated in equations F.4 and F.5.

$$S_{c,i} = \frac{F_{Tot,out} \cdot y_{C,i,out}}{F_{Tot,in} \cdot y_{MeOH,in} - F_{Tot,out} \cdot y_{MeOH,out}} \tag{F.4a}$$

$$S_{c,i} = \frac{y_{C,i_{out}}}{\sum y_{C,product_{out}}} \tag{F.4b}$$

$$S_{\mathrm{CH_2O}} = \frac{261.65 \cdot 4.56}{240.91 \cdot 8.25 - 261.65 \cdot 1.89} = 0.799 \tag{F.5a}$$

$$S_{\mathrm{CH_2O}} = \frac{4.56}{4.56 + 1.17 + 0 + 0} = 0.727 \tag{F.5b}$$

The hydrogen based selectivities is calculated by assuming that the H_2O in the feed is inert, selectivities for H_2 and H_2O may be calculated as shown in equations F.6 and F.7 below.

$$S_{\mathrm{H_2}} = \frac{2F_{Tot,out} \cdot y_{\mathrm{H_2},out}}{4(F_{Tot,in} \cdot y_{MeOH,in} - F_{Tot,out} \cdot y_{MeOH,out})} \tag{F.6a}$$

$$S_{\mathrm{H_2O}} = \frac{2F_{Tot,out} \cdot y_{\mathrm{H_2O},out}}{4(F_{Tot,in} \cdot y_{MeOH,in} - F_{Tot,out} \cdot y_{MeOH,out})} \tag{F.6b}$$

Hydrogen selectivity is chosen for the example and is based on the same data as the previous examples.

$$S_{\mathrm{H_2}} = \frac{2 \cdot 261.65 \cdot 0.76}{4(240.91 \cdot 8.25 - 261.65 \cdot 1.89)} = 0.067 \tag{F.7}$$

Verification of the mass balances were calculated to identify carbon, hydrogen and oxygen losses. The mass balances are calculated through equation F.8. By applying the same data as from previous examples, error in carbon mass balance is calculated in equation F.9.

$$E_C = \frac{F_{Tot,out} \sum y_{C,out} - F_{Tot,in} \cdot y_{MeOH,in}}{F_{Tot,in} \cdot y_{MeOH,in}} \tag{F.8a}$$

$$E_H = \frac{F_{Tot,out} \sum n y_{H_n,out} - F_{Tot,in}(4y_{MeOH,in} + 2y_{\mathrm{H_2O},in})}{F_{Tot,in}(4y_{MeOH,in} + 2y_{\mathrm{H_2O},in})} \tag{F.8b}$$

$$E_O = \frac{F_{Tot,out} \sum n y_{O_n,out} - F_{Tot,in}(y_{MeOH,in} + y_{\mathrm{H_2O},in} + 2y_{\mathrm{O_2},in})}{F_{Tot,in}(y_{MeOH,in} + y_{\mathrm{H_2O},in} + 2y_{\mathrm{O_2},in})} \tag{F.8c}$$

$$E_C = \frac{261.65 \cdot (1.89 + 4.56 + 1.71 + 0 + 0) - 240.91 \cdot 8.25}{240.91 \cdot 8.25} = 0.075 \tag{F.9}$$

Appendix G

Temperature profiles

Temperature profiles have been obtained during the analysis. The different profiles are illustrated in this chapter. The catalyst bed is at 19.5-21 cm and the diluted silver catalyst is located at 20-20.5 cm.

G.1 Temperature profile in reactor without feed

Temperature profiles for the reactor and catalyst bed, without feed, was obtained at 200 °C. In figure G.1 are two different profiles, measured at different days, presented. This was performed to illustrate the error obtained during measurement of the temperature.

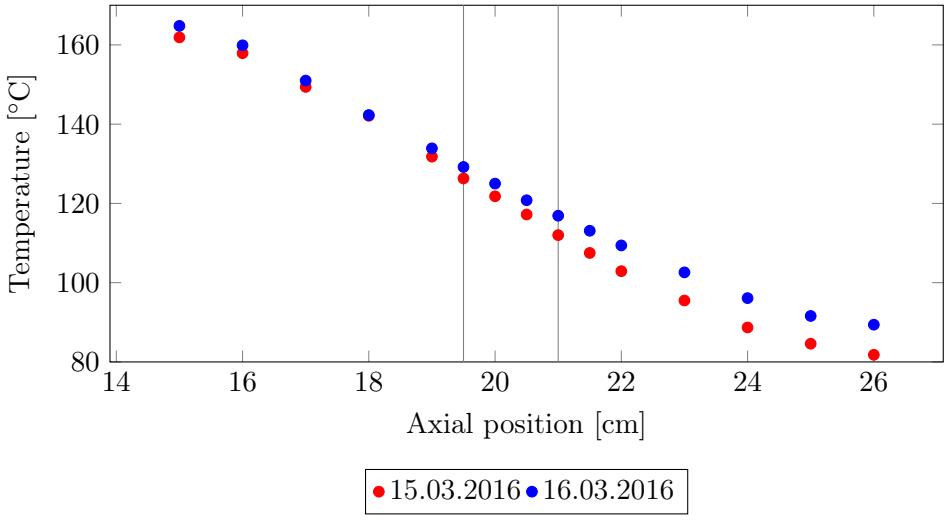

Figure G.1 – Comparison of temperature profiles obtained at 200 °C in the oven, without feed. The two profiles are obtained at different days, and compared to illustrate measurement errors. The gray lines indcate the catalyst bed area.

G.2 Temperature profiles for test 1

Test 1 was an analysis of the temperature effect on the MTF synthesis. Figure G.2 shows a comparison of temperature profiles in the reactor with and without (w/o) feed (ordinary feed composition) at 300 °C. The temperature range for the feed profile is slightly higher than for the non-feed profile, but no ignition of the reaction is observed at this temperature.

The temperature profiles obtained during the different temperature changes for ordinary feed composition (8 % MeOH) with a total flow of 250 NmL/ min are presented in figure G.3 . The figure illustrate a large temperature gradient for the oven, with high temperatures in the top. Temperature profiles for 500 and 550 °C shows peaks in the catalyst bed, indicating that the catalyst reaction is ignited. Temperature profiles for 600 and 650 °C does not show any clear peaks in this area and indicates that the homogeneous gas phase reaction and decomposition is dominating. The present setup is not optimal for high temperatures (industrial conditions), and improving the temperature gradient is further tested.

To further investigate when the catalyst reaction extinguishes, several temperatures 390, 405, 420 and 450 °C were performed. The different tem-

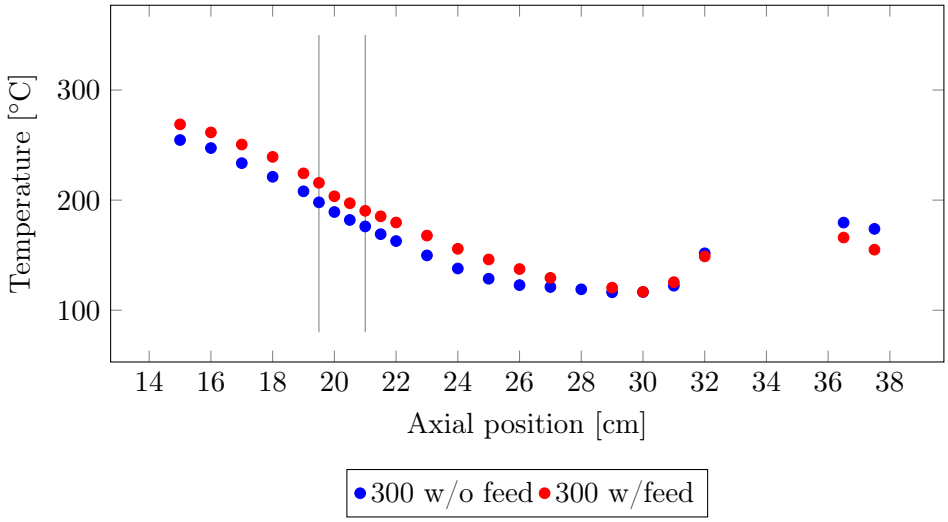

Figure G.2 – Comparison of temperature profiles for the reactor with and without (w/o) feed at 300 °C.] The total flow of the feed is at 250 NmL/ min with ordinary feed composition (8 % MeOH). The gray lines indicate the catalyst bed area.

perature profiles are presented in figure G.4.

An increase in the total flow (375 NmL/ min) was also performed during test 1, and the following temperature profiles are presented in figure G.5. For comparison is also the temperature profiles for the total flow of 250 NmL/ min at the same temperatures illustrated.

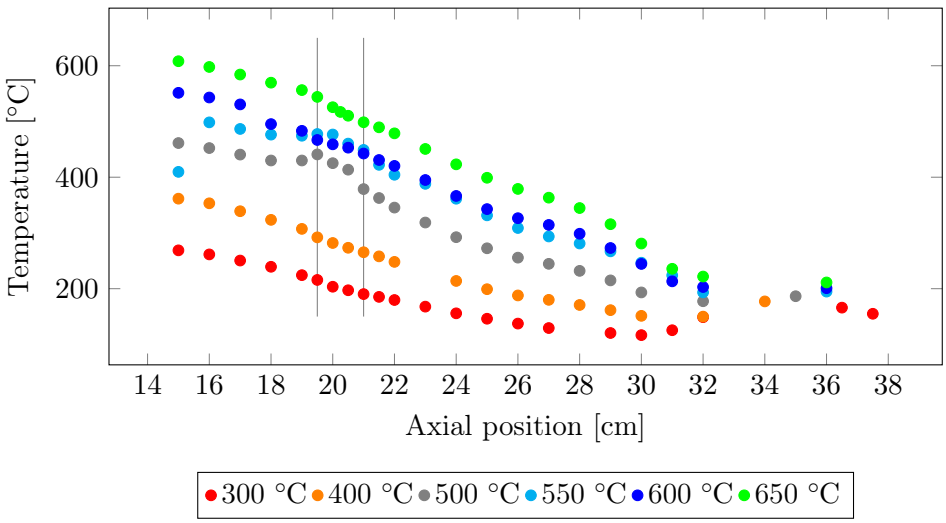

Figure G.3 – Temperature profiles obtained for different temperatures (300, 400, 500, 550, 600 and 650 °C) changes with a total flow of 250 NmL/ min with ordinary feed composition (8 % MeOH). The gray lines indicate the catalyst bed area.

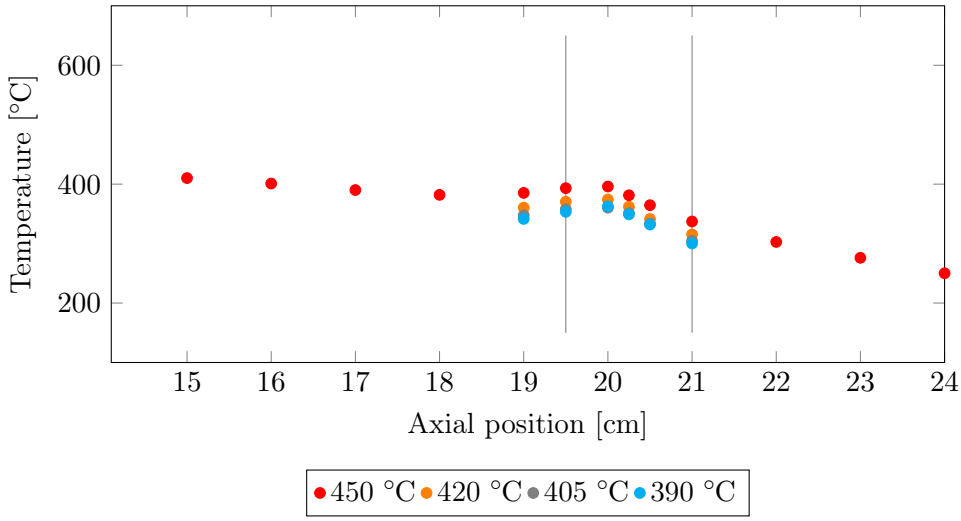

Figure G.4 – Temperature profiles for investigation of extinguish temperature for the catalyst reaction. Several temperatures around 400 °C was investigated, 390, 405, 420 and 450 °C. This was performed with ordinary feed composition (8 % MeOH) and with a total flow of 250 NmL/ min. The gray lines indicate the catalyst bed area.

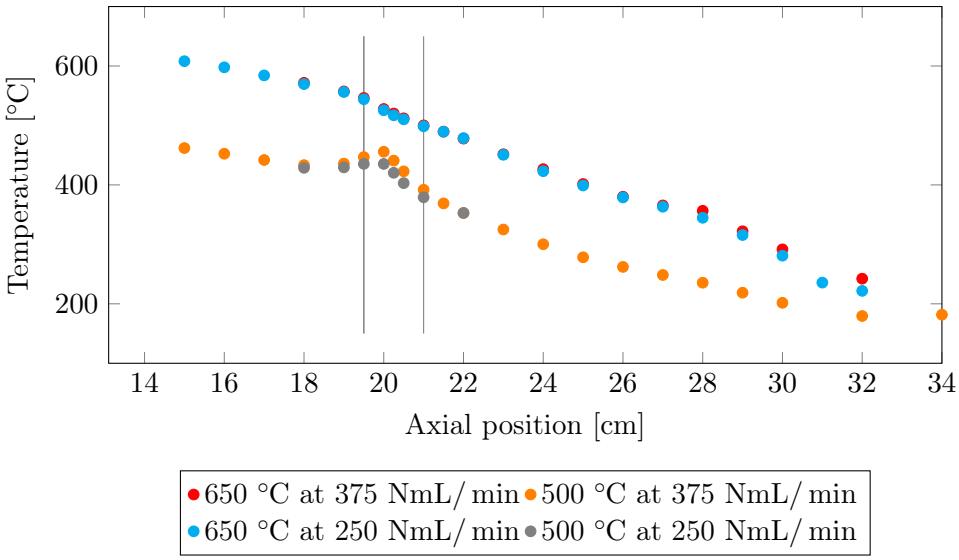

Figure G.5 – Temperature profiles for the increased total flow 375 NmL/ min, compared to the ordinary flow 250 NmL/ min, at temperature of 500 and 650 °C. Both feeds with ordinary feed composition (8 % MeOH). The gray lines indicate the catalyst bed.

G.3 Temperature profiles for test 2

Test 2 analyzed the effect of oxygen on the MTF synthesis. Test 1 showed a catalytic dominance at 550 °C, and was therefore chosen as the temperature for the analysis. Figure G.6 illustrates the temperature profile for reduced oxygen (halved amount), increased amount of oxygen (30 %) and no oxygen compared to ordinary composition of oxygen. The gray lines indicate the catalyst bed area.

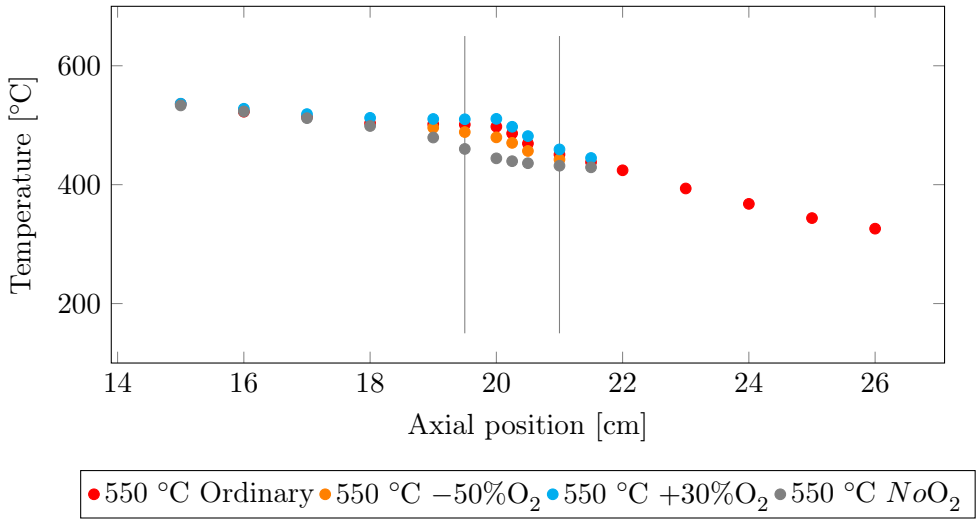

Figure G.6 – Temperature profile for the oxygen analysis. Different amounts of oxygen were analyzed, reduced (halved), increased (30 %) and no oxygen (w/o) compared to the original oxygen composition. The gray lines indicates the catalyst bed area.

Test 1 illustrated a large temperature gradient for the oven, and an air circulation was installed in the oven for test 2 to improve the gradient. Figure G.7 illustrates the air circulations effect on the temperature profile. An evident increase in the catalyst bed temperature can be observed compared to the profile for the same feed without air circulation.

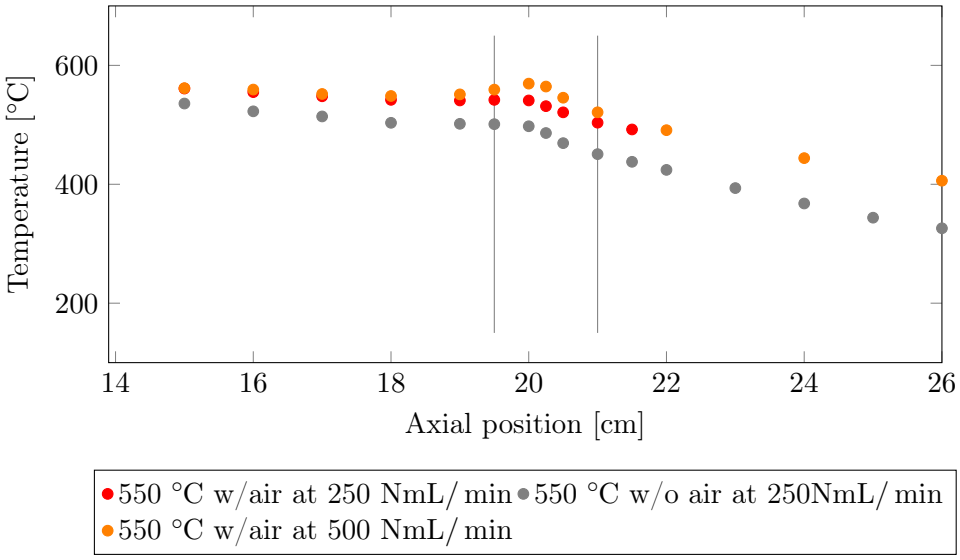

Figure G.7 – Temperature profile for analyzing the effect of the air circulation, compared to the temperature profile without air circulation. The gray lines indicate the catalyst bed area.

G.4 Temperature profiles for test 3

The reactor has a considerable volume before the catalyst bed, which gives room for homogeneous gas phase reactions to take place. This void was filled with silicon carbide (a supposed inert material) to inhibit gas phase reactions. Figure G.8 shows the resulting temperature profiles for this analysis.

The air circulation was also activated for test 3, and the temperature profiles are presented in figure G.9. By applying air circulation to the silicon carbide filled void, higher bed temperatures could be reached.

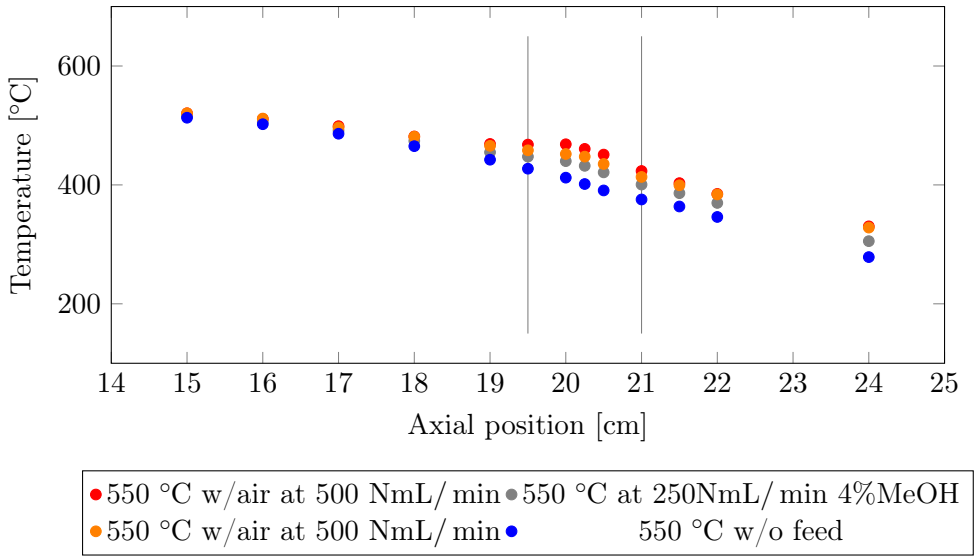

Figure G.8 – Temperature profiles for silicon carbide filled void. Analysis was performed without feed (w/o), ordinary feed composition at 250 NmL/ min, and two different compositions (4 and 8 % MeOH) at 500 NmL/ min. The gray lines indicate the catalyst bed area.

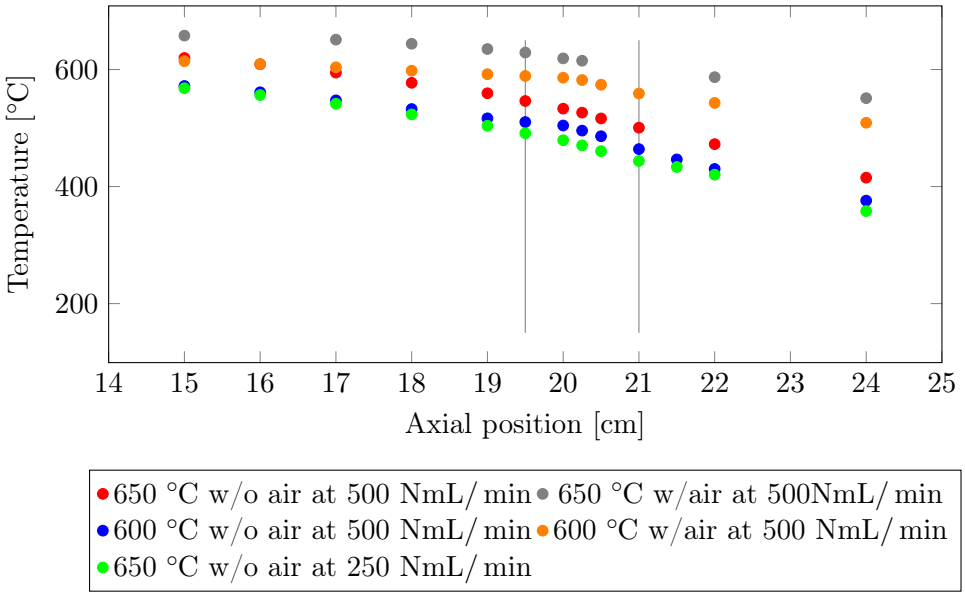

Figure G.9 – Temperature profiles for silicon carbide filled void combined with air circulation. Temperature profiles for the same temperatures without (w/o) air circulation is also presented. The gray lines indicates the catalyst bed area.

G.5 Temperature profiles for test 4

Test 4 was a reference test with an empty reactor, ran at significant temperatures from previous experiments. Figure G.10 illustrates the different temperature profiles ran at different flows (250 and 500 NmL/ min). As expected, no ignition peak is observed in the temperature profiles.

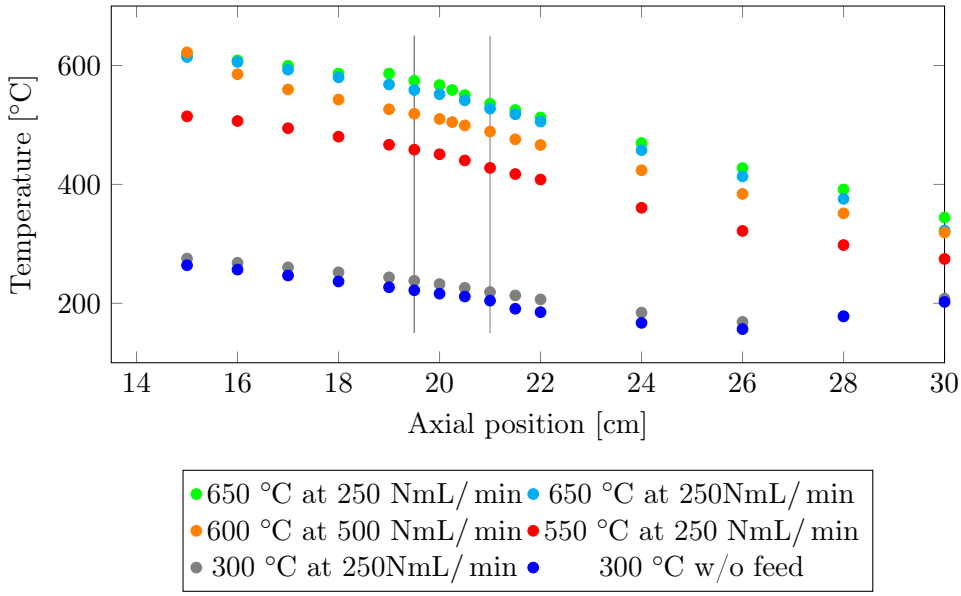

Figure G.10 – Temperature profiles obtained in the empty reactor analysis. Analysis was ran without feed (square), total flow of 250 NmL/ min and 500 NmL/ min. Both feeds with ordinary feed composition (8 % MeOH). The gray lines indicate the catalyst bed area.